THE UNIVERSITY OF ALBERTA

PETROCHEMISTRY OF THE YELLOWKNIFE GREENSTONE BELT, YELLOWKNIFE, N.W.T.

by

© Michael Patrick Cunningham

A THESIS

SUBMITTED TO THE FACULTY OF GRADUATE STUDIES AND RESEARCH

IN PARTIAL FULFILLMENT OF THE REQUIREMENTS FOR THE DEGREE

OF MASTER OF SCIENCE

DEPARTMENT OF GEOLOGY

EDMONTON, ALBERTA

FALL 1984

Energy, Mines and Resources Canada
Earth Sciences
Geological Survey of Canada
601 Booth Street
Ottawa, Ontario
K1A 0E8

Énergie, Mines et Ressources Canada
Sciences de la Terre
Commission géologique du Canada
601, rue Booth
Ottawa (Ontario)
K1A 0E8

Your file Votre référence

Our file Notre référence 116-3-6

September 26, 1984

R. St J. Lambert
Professor
Department of Geology
The University of Alberta
Edmonton, Canada
T6G 2E3

Dear Mr. R. Lambert:

Thank you for your letter of 21 September 1984 requesting permission to reproduce diagram in Figure 1-, Metamorphic map of the Slave Province, in Thompson P.H., 1978, from Geological Survey of Canada, Paper 78-10, p. 86.

Formal permission is granted to reproduce the diagram mentioned above. We do request that you acknowledge the source in the following or similar manner: "From Geological Survey of Canada, Paper 78-10, Figure 1, p. 86".

Sincerely yours,

R. G. Blackadar
Director, Geological
Information Division

dt

Canada

THE UNIVERSITY OF ALBERTA

RELEASE FORM

NAME OF AUTHOR: MICHAEL PATRICK CUNNINGHAM

TITLE OF THESIS: PETROCHEMISTRY OF THE YELLOWKNIFE GREENSTONE BELT, YELLOWKNIFE, N.W.T.

DEGREE FOR WHICH THESIS WAS PRESENTED: Master of Science

YEAR THIS DEGREE GRANTED: 1984

Permission is hereby granted to THE UNIVERSITY OF ALBERTA LIBRARY to reproduce single copies of this thesis and to lend or sell such copies for private, scholarly or scientific research purposes only.

The author reserves other publication rights, and neither the thesis nor extensive extracts from it may be printed or otherwise reproduced without the author's written permission.

Michael Patrick Cunningham
2790 Colwood Drive
North Vancouver, B.C.
Canada V7R 2R1

October 11, 1983

THE UNIVERSITY OF ALBERTA

FACULTY OF GRADUATE STUDIES AND RESEARCH

The undersigned certify that they have read, and recommend to the Faculty of Graduate Studies and Research, for acceptance, a thesis entitled

PETROCHEMISTRY OF THE YELLOWKNIFE
GREENSTONE BELT, YELLOWKNIFE, N.W.T.

submitted by MICHAEL PATRICK CUNNINGHAM, in partial fulfillment of the requirements for the degree of Master of Science.

H. Baadsgaard
.....
Chairman - Dr. H. Baadsgaard

.....
Examiner - Dr. C. Scarfe

G. L. Cumming
.....
Examiner - Dr. G. L. Cumming

R. St. J. Lambert
.....
Supervisor - Dr. R. St.J. Lambert

TO MY WIFE DOROTHY

AND OUR SON THOMAS

FOR TREMENDOUS LOVE,

PATIENCE AND SUPPORT.

ABSTRACT

Petrochemistry of the Yellowknife volcanic belt (Kam, Duck and Banting Formations) at Yellowknife, Northwest Territories, Canada, shows the suite to be more chemically complex than previously thought.

The Kam Formation is dominated by basalts and basaltic andesites, interpreted to be of mantle derivation. There exists a strong tholeiitic trend with compositions ranging from magnesian basalts to high iron tholeiitic basalts. Of much less importance, volumetrically, are the andesites and dacites considered to be partial melts of basaltic and sialic crustal material, respectively.

Andesites are the most abundant rock type of the Duck Formation, with lesser amounts of more mafic (basalt to basaltic andesite) and felsic (dacite) flows. All lavas are interpreted as partial melts of a pre-existing basaltic crust, with minor contribution from a sialic crustal source toward the felsic components.

Dacitic to andesitic flows and tuffs constitute the vast majority of the Banting Formation rock suite. Partial melting of a pre-existing tholeiitic basalt source material led to extrusion, via the same conduit system as Kam Formation volcanics, thereby intruding and overlying these older mafic flows.

Comparison of Kam versus Banting Formation volcanic rocks is characterized by their distinctly separate chemistries, with very little overlap of the two units on chemical plots. Kam Formation rocks have a definite tholeiitic trend and are analagous to geologic-

ally younger ocean floor basalts or oceanic rise tholeiitic basalts. This study indicates the Kam Formation to consist of 64% basalt, 27% basaltic andesite, 7% andesite and 2% dacite. Banting Formation rocks show a calc-alkaline trend and plot similar to geologically younger calc-alkaline basalts; the unit is composed of 14% basalt, 7% basaltic andesite, 38% andesite and 41% dacite.

Volcanics of the Duck Formation range from basalt to dacite with chemistries overlapping both Kam and Banting Formation rocks. They also have intermediate and more extreme compositions. Tholeiitic and calc-alkaline differentiation trends are indicated; low potassium and high alumina basalts have been identified. The formation contains 11% basalt, 21% basaltic andesite, 59% andesite and 9% dacite. Diverse trace element data combined with significant alkali mobility, variable carbonate contents (visible in thin section), and inconsistent Rb-Sr isotopic values suggest the Duck Formation to be distinct from the Kam and Banting Formations in petrochemistry and metamorphism.

The rubidium-strontium isotopic system has not remained closed since cessation of all volcanism prior to 2636 Ma. Continuous and episodic downdating due to thermal and dynamic events result in apparent ages of approximately 2580 Ma, 2500 Ma and 2000 Ma for the Kam Formation, Banting Formation - Giant-Yellowknife Shear Zone, and Duck Formation, respectively.

A model of ensialic development at a late stage in the evolution of the Slave Craton is consistent with all known facts.

I wish to acknowledge Dr. Richard St.J. Lambert for proposing the thesis topic and for his continued supervision. Research funds and generous field support were provided by the Department of Indian Affairs and Northern Development, through Dr. W. Padgham. Analytical work was made possible by Dr. H. Baadsgaard of the Geology Department, University of Alberta, and Dr. R. H. McNutt of McMaster University, Hamilton. Mass-spectrometer analyses were performed in facilities maintained and operated by Dr. G.L.Cumming of the Physics Department, University of Alberta.

TABLE OF CONTENTS

		Page
CHAPTER 1 -- INTRODUCTION		
1.1	LOCATION AND ACCESS	1
1.2	HISTORY	1
1.3	PHYSIOGRAPHY	3
1.4	GENERAL GEOLOGY	3
1.4.1	Overview	3
1.4.2	Boundaries	4
1.4.3	Slave Structural Province	6
1.4.4	Slave Province Geochronology	8
1.4.5	Structure and Metamorphism	9
1.4.6	Petrography	11
1.4.7	Geochemistry and Petrogenesis	13
1.5	OBJECTIVES AND FIELDWORK	14
CHAPTER 2 -- GEOLOGY AND GEOCHEMISTRY : PREVIOUS WORK		
2.1	REGIONAL GEOLOGY	16
2.2	YELLOWKNIFE VOLCANIC ROCKS	21
2.2.1	Kam Formation	21
2.2.2	Duck Formation	25
2.2.3	Banting Formation	26
2.3	YELLOWKNIFE SEDIMENTARY ROCKS	27
2.3.1	Jackson Lake Formation	27
2.3.2	Burwash Formation	29
2.3.3	Walsh Formation	30
2.4	INTRUSIVE ROCKS	31
2.4.1	Western Granodiorite	31
2.4.2	Southeast Granodiorite	32
2.4.3	Prosperous Lake Granite	33
2.5	STRUCTURE	34
2.6	MINERALIZATION	39
2.7	GEOCHEMISTRY	41
2.8	SUMMARY	44

Page

CHAPTER 3 -- GEOCHEMISTRY

3.1 INTRODUCTION 46
3.2 MAJOR ELEMENT GEOCHEMISTRY 49
3.2.1 Frequency - Silica 49
3.2.2 Total Alkalis - Silica 51
3.2.3 Total Alkalis - Alkali Ratio 53
3.2.4 Alkalis - Iron - Magnesium 59
3.2.5 Magnesium - Iron - Aluminum 61
3.2.6 Aluminum - Iron+Titanium - Magnesium ... 64
3.2.7 Summary 67
3.3 MINOR ELEMENT GEOCHEMISTRY 68
3.3.1 Silica - Zirconium/Titanium 68
3.3.2 Iron - Zirconium/Titanium 71
3.3.3 Zirconium/Titanium - Niobium/Yttrium ... 73
3.3.4 Zirconium - Titanium - Yttrium 76
3.3.5 Zirconium - Titanium - Strontium 79
3.3.6 Calcium - Yttrium 81
3.3.7 Vanadium - Nickel 83
3.4 SUMMARY OF GEOCHEMISTRY 85

CHAPTER 4 -- GEOCHRONOLOGY

4.1 INTRODUCTION 87
4.2 METHOD 87
4.3 RESULTS 90
4.3.1 Kam Formation 90
4.3.2 Duck Formation 91
4.3.3 Banting Formation 96
4.3.4 Giant Yellowknife Shear Zone 96
4.4 DISCUSSION 99
4.5 SUMMARY OF GEOCHRONOLOGY 101

Page

CHAPTER 5 -- GEOCHEMICAL COMPARISON AND PETROGENETIC MODELS

5.1	INTRODUCTION	103
5.2	FORMATION CHARACTERISTICS	110
5.2.1	Kam Formation	110
5.2.2	Duck Formation	111
5.2.3	Banting Formation	112
5.3	COMPARISON AND CLASSIFICATION	112
5.4	MODELS OF MAGMA GENESIS	115
5.4.1	Overview	115
5.4.2	Tipasjarvi, Finland	116
5.4.3	Abitibi, Canada	117
5.5	PETROGENESIS OF YELLOWKNIFE VOLCANIC ROCKS	118
5.5.1	Source Rocks and Limitations	118
5.5.2	Discussion	122

CHAPTER 6 -- CONCLUSIONS 127

BIBLIOGRAPHY 130

APPENDIX A -- GEOCHEMICAL DATA

X-ray Fluorescence	147
Atomic Absorption Spectroscopy	166

APPENDIX B -- COMPARISON STUDIES

Duplicate Analyses	174
Surface vs Drillcore	178
Variolitic vs Non-Variolitic Flows	181

APPENDIX C -- COMPARATIVE ELEMENT PLOTS 184

VITA 192

LIST OF TABLES

	Page
TABLE 1 -- Formations in the Yellowknife Bay Area	19
TABLE 2 -- Igneous Spectrum - Summary of Results	56
TABLE 3 -- Igneous Spectrum - Subdivision by Formation and Rock Type	57
TABLE 4 -- Calculated Hypothetical Alkali Mobility for Igneous Spectrum Diagram	58
TABLE 5 -- Rubidium-Strontium Geochronology Data	80
TABLE 6 -- Mean Composition by Rock Type for Yellowknife Volcanics - Major Elements	104
TABLE 7 -- Mean Composition by Rock Type for Yellowknife Volcanics - Minor Elements	105
TABLE 8 -- Mean Composition by Rock Type for Yellowknife Volcanics - Element Ratios	106
TABLE 9 -- Mean Composition by Formation - Major Elements	107
TABLE 10 -- Mean Composition by Formation - Minor Elements	108
TABLE 11 -- Discriminant Element Classification of Yellowknife Volcanic Rocks	113
TABLE 12 -- Classification of Rock Types Within Kam, Duck and Banting Formations	115

LIST OF FIGURES

	Page
FIGURE 1 -- Location Map	2
FIGURE 2 -- General Geology of Slave Province	5, 17
FIGURE 3 -- Metamorphic Map of Slave Province	18
FIGURE 4 -- Yellowknife Area : Geology	22
FIGURE 5 -- Yellowknife Area : Structure	35
FIGURE 6 -- Traverse Location Map	47
FIGURE 7 -- Silica - Frequency	50
FIGURE 8 -- Total Alkalis - Silica	52
FIGURE 9 -- Total Alkalis - Alkali Ratio	54
FIGURE 10 -- A-F-M Diagram	60
FIGURE 11 -- MgO - FeO_T - Al_2O_3	62
FIGURE 12 -- Jensen's Cation Diagram	65
FIGURE 13 -- Yellowknife Data on Figure 12	66
FIGURE 14 -- SiO_2 - Zr/TiO_2	69
FIGURE 15 -- FeO_T - Zr/TiO_2	72
FIGURE 16 -- Zr/TiO_2 - Nb/Y	74
FIGURE 17 -- Zr - Ti/100 - Yx3	77
FIGURE 18 -- Zr - Ti/100 - Sr/2	80
FIGURE 19 -- CaO - Y	82
FIGURE 20 -- V - Ni	84
FIGURE 21 -- Kam Fm. Rb/Sr Isochrons	92
FIGURE 22 -- Duck Fm. Rb/Sr Isochrons a	94
FIGURE 23 -- Duck Fm. Rb/Sr Isochrons c and d	95
FIGURE 24 -- Banting Fm. Rb/Sr Isochron	97
FIGURE 25 -- Giant-Yellowknife Shear Zone Isochron	98
FIGURE 26 -- Petrogenetic Model for Yellowknife Area ..	126

LIST OF TABLES IN APPENDICES

	Page
TABLE A1 -- Recommended Values for International Standards	148
TABLE A2 -- Data for the Yellowknife Volcanic Rocks: Elements by X-ray Fluorescence	150
TABLE A2 -- Data for the Yellowknife Volcanic Rocks: Elements by Atomic Absorption Spectroscopy.	168
TABLE B1 -- Duplicate Analyses: Major Elements	176
TABLE B2 -- Duplicate Analyses: Minor Elements	177
TABLE B3 -- Surface vs Drill Core Samples: Major Elements	179
TABLE B4 -- Surface vs Drill Core Samples: Minor Elements	180
TABLE B5 -- Variolitic vs Non-variolitic Flows: Major Elements	182
TABLE B6 -- Variolitic vs Non-variolitic Flows: Minor Elements	183

LIST OF FIGURES IN APPENDICES

	Page
FIGURE A1 -- Standards Correlation (ppm vs response): Ni, Cu, V	171
FIGURE A2 -- Standards Correlation (ppm vs response): Zn, Cr	172
FIGURE C1 -- AFM	185
FIGURE C2 -- MgO - FeO_T - Al_2O_3	186
FIGURE C3 -- Al_2O_3 - ($FeO+Fe_2O_3+TiO_2$) - MgO	187
FIGURE C4 -- SiO_2 - Zr/TiO_2	188
FIGURE C5 -- FeO_T - Zr/TiO_2	189
FIGURE C6 -- Zr - Ti/100 - Yx3	190
FIGURE C7 -- Zr - Ti/100 - Sr/2	191

CHAPTER 1

INTRODUCTION

1.1 LOCATION AND ACCESS

The Yellowknife greenstone belt crops out along the shores of Yellowknife Bay, sometimes referred to as the north arm of Great Slave Lake (Figure 1). Sample locations are within 20 km of Yellowknife, capital city of the Northwest Territories, Canada. It has a population of 9483, 1981 census, and is a major supply point for exploration and development of Canada's north.

Access is by gravel road, summer barge traffic and daily air service from Edmonton, Alberta, 1000 km south, or Churchill, Manitoba, 1150 km southeast. Scheduled wheeled aircraft serve major communities throughout the territory and charter float planes are readily available.

1.2 HISTORY

Early gold discoveries in the Yellowknife area were small, quickly exhausted deposits within the sediments. Work by the Geological Survey of Canada (Stockwell and Kidd 1932; Stockwell 1933) assisted discovery of gold in the volcanic rocks. The Con Mine began production in 1938, the Negus in 1939, and the Giant Yellowknife Mine

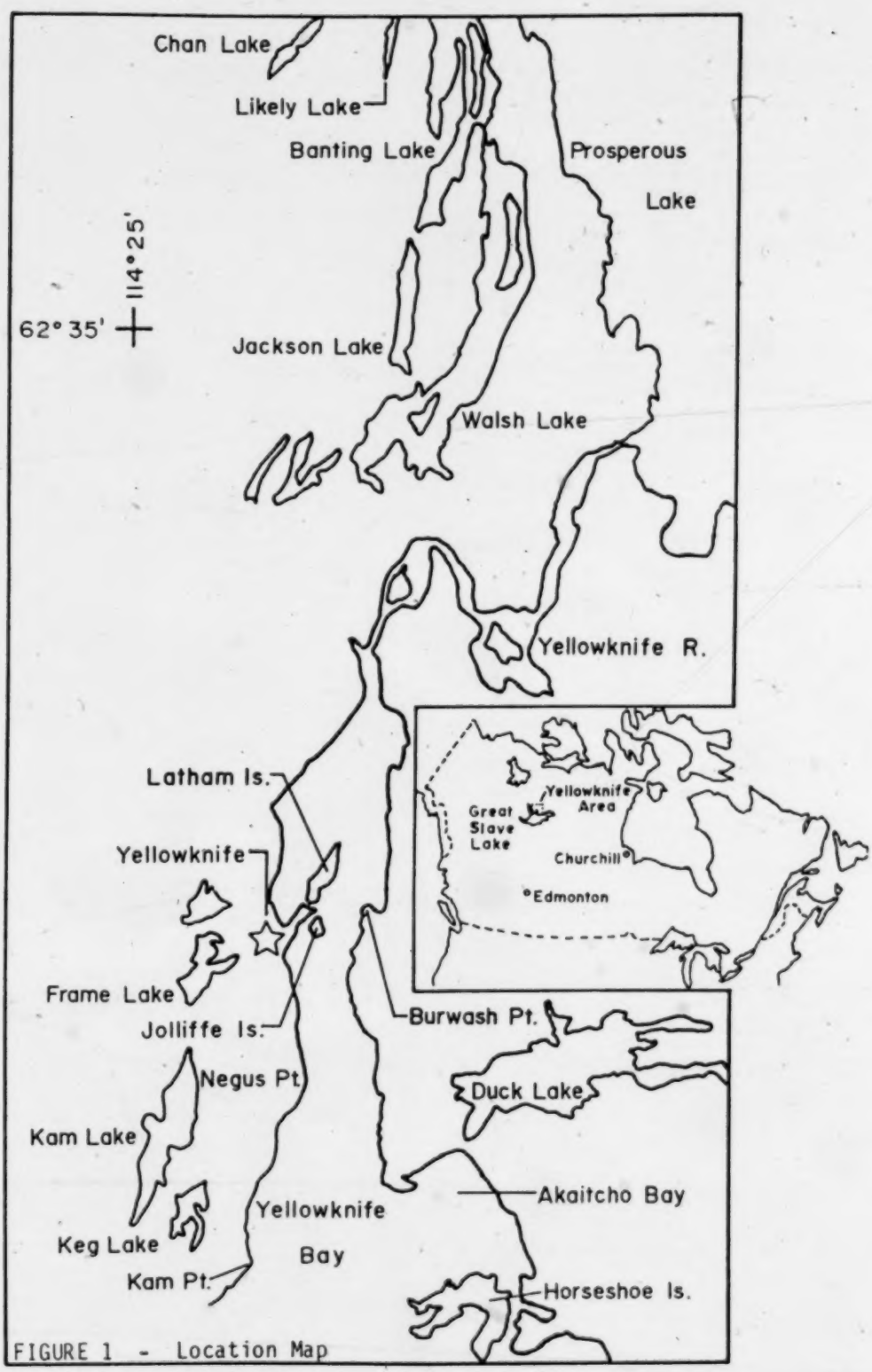

FIGURE 1 - Location Map

in 1948. Combined gold production from the mines at Yellowknife was 4.15 million grams or 133,400 ounces (1981) with a value of Can.$69.9 million (Canadian Mines Handbook 1982-1983).

1.3 PHYSIOGRAPHY

The regional physiography is typical of the Canadian Shield; flat to rolling topography is marked by lakes, muskeg and structural lineaments. Yellowknife Bay is located in the transition zone from northern coniferous forests to tundra and scattered trees. High ground is quite bare with vegetation such as mosses, lichens and low shrubs. Protected lowland contains marshes bordered by shrubs, spruce and birch trees. Exposure of the Yellowknife belt is excellent, greater than 60%, with minor moss and lichen cover. Relief can be rugged as scarps rise 30m and large blocks spall from fractured surfaces. Pleistocene glaciation retreated 10,000 to 12,000 years ago, leaving scoured and polished bedrock surfaces. Esker patterns, striae and roche moutonee suggest ice advance from the northeast (S60-65°W). Glacial deposits include erratics, outwash sand and gravel plains, and lacutrine clays.

1.4 GENERAL GEOLOGY

1.4.1 OVERVIEW

Following the work of C. H. Stockwell and D. F. Kidd, regional and detailed geology has been done by Jolliffe (1938, 1942),

Henderson and Brown (1952, 1966), and Boyle (1961). The Yellowknife greenstone belt is within the Slave Structural Province, located in the northwest part of the Canadian Shield. It has been distinguished from the Bear and Churchill Structural Provinces by trend, style and relative age of tectonism (Price and Douglas 1972). Rocks of the Slave Province are of Archean age, and have undergone little or no subsequent metamorphism. Geologic boundaries to this province, a 190,000 square kilometre rectangular block, are unconformities, metamorphic fronts and/or faults (Figure 2).

1.4.2 BOUNDARIES

To the west, the boundary with the Bear Province is an unconformity; Aphebian sediments unconformably overlie Yellowknife Supergroup metasediments and metavolcanics, and locally Kenoran intrusive rocks. Where no Aphebian strata are preserved the boundary has been placed between the little modified Archean basement and Archean ortho-/paragneisses remobilized as late as 1735 Ma, or retaining Archean ages as old as 2712 Ma (Frith et al 1974). The Aphebian stratigraphic succession suggests miogeosynclinal and eugeosynclinal sedimentation at the margin of a stable Archean platform, the Slave Structural Province (Fraser et al 1972; Neilsen 1978).

The eastern boundary, with the Churchill Province, is marked by an abrupt increase in metamorphic grade (the Thelon Front) due to the rapid uplift and erosion of Archean Slave Province material and/or equivalents. Variations in the rate and magnitude of uplift have

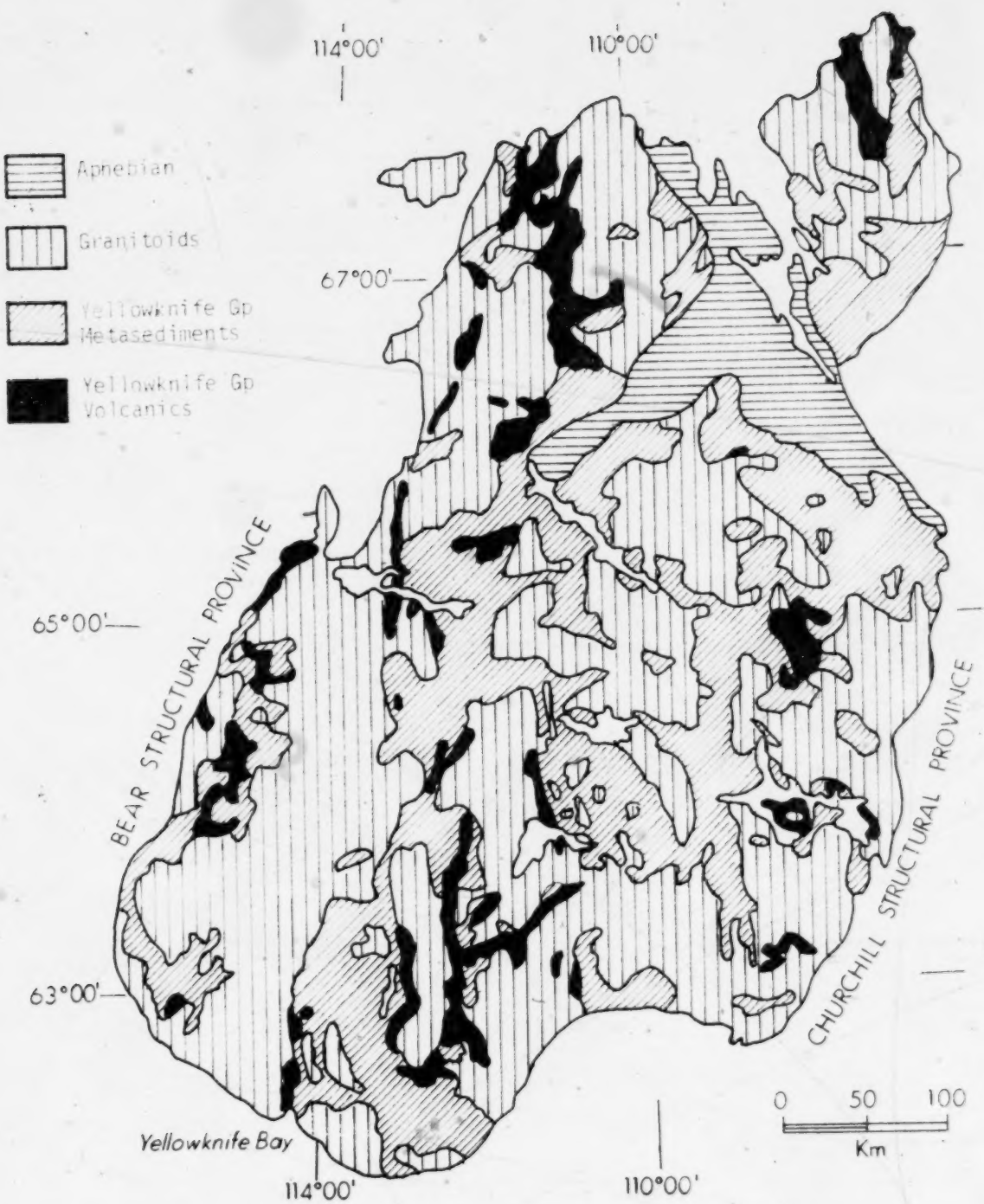

Figure 2 - General geology of Slave Province

caused an erratic distribution of metamorphic assemblages, both prograde and retrograde, and also therefore, of K-Ar ages (Fraser 1978). Uplift and metamorphism resulted in medium pressure kyanite bearing assemblages along the Thelon Front, probably during the Aphebian era. Prior interpretation for the Thelon Front considered it the western limit of Hudsonian (1735 Ma) metamorphism, separating low grade metamorphic terrane of the Slave Province and medium grade metamorphic terrane of the northwest Churchill Province (Wright 1967; McGlynn and Henderson 1972). Fraser (1978) interprets the Thelon Front as a narrow, 5-10 km wide, zone of flexure resulting from differential uplift. This caused exposure of deeper crustal levels, material of higher metamorphic grade, followed by greater erosion which reduced the preservation of supracrustal material. The Thelon Front has been offset by the Bathurst Trench and terminated by the McDonald Fault; both structures locally define the Slace-Churchill boundary. Hudsonian orogenic events are evident throughout the Churchill Province.

To the north and south, Paleozoic sediments unconformably overlie rocks of the Slave Province.

1.4.3 SLAVE STRUCTURAL PROVINCE

The Slave Structural Province is underlain by about twenty deformed and variably metamorphosed north trending belts of Archean supracrustal material, separated by granitic material of plutonic and anatectic origin. Approximately one half of the granite rock is highly metamorphosed; it may be granitized equivalents of the Yellowknife Supergroup.

Two thirds of the province is granitic rock; one third is Yellowknife Supergroup material of which five percent is extrusive volcanic rock and twenty-eight percent is sedimentary and metasedimentary rock. The lavas usually occur as 1500 to 3000 metre thick sequences, with a maximum of 10,000 metres. The sedimentary strata are typically less than 4500 metres thick. (Hoffman and Henderson 1972; McGlynn and Henderson, 1972). The predominance of sediments in the Slave Province (80-85%) is in contrast with the Superior Structural Province where sedimentary rock comprise 8-16 percent and volcanics 40-50 percent of the greenstone belts (McGlynn and Henderson 1972; Goodwin 1972). It also contrasts with other Archean terranes in its paucity of iron formations and ultramafic rocks (Hoffman and Henderson 1972; Windley 1977).

The Yellowknife Supergroup is better preserved in the west half of the province (Figure 2); the general succession being subaquaeously extruded basaltic flows (commonly pillowed and sometimes variolitic), andesitic to dacitic flows, felsic flows and pyroclastics interbedded with, and overlain by, greywacke-mudstone turbidites (Henderson 1970, 1972, 1975; McGlynn and Henderson 1972). Typically the conformable contact between the volcanic pile and sediments is marked by deposition of thin discontinuous conglomerate wedges. These conglomerates contain angular volcanic clasts and locally granitic boulders, volcanogenic lithic wackes, quartzites and exhalite deposits (McGlynn and Henderson 1972; Baragar and McGlynn 1976).

In the west half of the province, where greenstone belts and suspected ancient basement material preservation is high, fold axes trend north-south. In the east, where young syntectonic plutons are more abundant and supracrustal material less abundant, fold axes are variable to east-west (Stockwell et al 1970; McGlynn and Henderson 1972).

1.4.4 SLAVE PROVINCE GEOCHRONOLOGY

Detailed geochronology studies have been done in the Yellowknife Bay and Indin Lake areas. Stockwell (1963, 1964) defined the Kenoran orogeny based upon normal distribution of mica K-Ar age dates with a mean of 2480 Ma, confirmed at 2463 Ma by Green and Baadsgaard (1971).

The authors also estimated extrusion of the metavolcanics at 2625 $\pm$ 160 Ma ($\lambda^{87}Rb = 1.39 \times 10^{-11}/Yr$) or 2569 $\pm$ 157 Ma ($\lambda^{87}Rb = 1.42 \times 10^{-11}/Yr$); the U-Pb system for a zircon from the Brock or Townsite dacitic flows gave a range of ages from 2195 Ma ($^{206}Pb - ^{238}U$) through 2440 Ma ($^{207}Pb - ^{235}U$) up to 2650 Ma ($^{207}Pb - ^{206}Pb$). Rubidium-strontium ages for batholiths in the Yellowknife region, recalculated to $\lambda^{87}Rb = 1.42 \times 10^{-11}/Yr$, are as follows: Western Granodiorite 2555 $\pm$ 58 Ma, Southeast Granodiorite 2584 $\pm$ 37 Ma, and the Prosperous Lake Granite 2520 $\pm$ 25 Ma. The Western and Southeast Granodiorites yield $^{207}Pb - ^{206}Pb$ ages of 2575 and 2640 Ma, respectively.

A model lead age from sulfide mineralization in Kam Formation metavolcanics has been calculated at 2820 Ma by Robertson and Cumming (1968). Cumming and Tsong (1975) date the Western Granodiorite at 2675 ± 15 Ma and the Southeast Granodiorite at 2665 ± 40 Ma using a Pb-Pb two stage model; following recalculation the Western Granodiorite is dated at 2636 ± 10 Ma with mineral ages extending down to 2430 ± 45 Ma, and one Stock Lake sample giving 1850 ± 80 Ma. Nikic et al (1975, 1980) used zircon Pb-Pb methods to date presumed pre-existing basement material, from a diatreme intersected in the Con Mine, at 3030 Ma.

R. A. Frith et al (1974), R. Frith et at (1977), and R. A. Frith (1978) outline geology and geochronolgy for the Indin Lake region of the Slave - Bear Province boundary, north-northwest of Yellowknife. Rubidium-strontium studies on tonalitic basement gneiss suggests an age of 2940 Ma, this may be a potash metasomatism age as zircons from the same rocks yield an age of 3100 Ma. Yellowknife Supergroup metavolcanics and metasediments are about 2700 Ma old, granitic and migmatitic rocks are dated at about 2500 Ma, and minor intrusive phases (diabase dikes, granodiorite rocks, granitic pegmatites) are about 1960 Ma old (λ 87 Rb = $1.39 \times 10^{-11} yr^{-1}$).

1.4.5 STRUCTURE AND METAMORPHISM

Across the Slave Province, remnant Archean supracrustal material occurs in three separate, discontinuous, north trending zones intruded by, and in part underlain by, granitic rock. Thick sequences

of mafic volcanics form margins to sedimentary basins, the volcanic succession is in part younger and in part contemporaneous with greywacke-mudstone turbidites.

Sedimentary strata, with interbedded thin volcanic units, are typically isoclinally folded. Axial planes dip steeply with moderate plunges, features which are often modified by steeply plunging cross folds at high angles to older structures (Fyson 1975; Drury 1977). In contrast, thick competent volcanic units form steeply dipping monoclinal successions away from bounding granitic rocks, or occur as broad open folds.

An ancient basement to the supracrustal succession has been interpreted from field interpretation of basal unconformities and pre-Kenoran radiometric ages.

Regional metamorphism ranges from lower greenschist to upper amphibolite grade under a low pressure - high thermal gradient regime (McGlynn and Henderson 1972; Nielsen 1978). Early batholiths of granodiorite and diorite developed narrow thermal aureoles, however the younger pegmatitic muscovite granite batholiths resulted in large areas of cordierite porphyroblastic rocks and the development of a broad zonation (10-15 km) of prograde index mineral isograds in the meta-pelitic or metagreywacke rock types (Ramsay and Kamineni 1977). The cordierite-biotite-andalusite-sillimamite-(staurolite) assemblages are typical of low pressure regional metamorphism of the Pyreneean type (Thompson 1978).

Near the younger granitic batholiths regional metamorphism (M_2) accompanied deformation (D_2) and thermal doming under conditions of moderate pressures and temperatures, 3.0-4.5 kb and 500°C. Later stage metamorphism (M_3) developed the index mineral sequence chlorite, biotite, cordierite, gedrite, andalusite and sillimanite under low confining pressures and higher temperatures, 2.5-3.5 kb and 550-700°C (Ramsay and Kamineni 1977).

Archean rocks were eroded, overlain by Aphebian sediments locally deformed, and overlain by Helikian sediments. Diabase dike swarms and faults, which cut much of the Slave Province, may be related to the formation and deformation of younger Proterozoic basins and geosynclines.

1.4.6 PETROGRAPHY

The Yellowknife volcanic belt exhibits mineral assemblages common to many greenstone belts, i.e. upper greenschist to lower amphibolite facies mineralogy, based upon examination of 160 thin sections.

Most Kam Formation mafic volcanics, the predominant rock type, are composed of hornblende, plagioclase (An 42-48), chlorite, epidote, cummingtonite, plus variable amounts of opaques, quartz, actinolite and biotite, typical of amphibolite grade metamorphism. Other samples are in greenschist facies metamorphic grade, containing significant actinolite (+/- hornblende), chlorite/penninite, plagio-

clase and epidote. Within these samples, plagioclase phenocrysts (1 mm) are ragged and altered to secondary feldspar, epidote, zoisite/clinozoisite and white mica. Rarely possible relict clinopyroxene phenocrysts are noted, now altered to hornblende, actinolite, chlorite, epidote, opaques and/or carbonate.

Felsic volcanic samples, e.g. the Brock-townsite Flow, contain plagioclase and quartz phenocrysts 3-5 mm in size. The plagioclase is usually embayed, sericitized, saussuritized, and rimmed with iron oxides. Quartz is fractured and annealed with recrystallized quartz grains. Matrix material is very fine grained quartz, feldspar, chlorite, sericite and iron oxides.

Mineralogy of the Duck Formation samples is similar to that of Kam Formation rocks, however a few differences are noted. The greater abundance of intermediate volcanics increases observation of samples with pilotaxitic (trachytic) texture, and vesicules now elongated and filled with recrystallized quartz. Also of note is the increased carbonate, intersertal, in veins, and as replacement of plagioclase phenocrysts.

Mafic to intermediate phases of the Banting Formation are similar to Kam and Duck Formation samples, but with generally lower carbonate contents. A few highly altered phenocrysts (clinopyroxene?) were observed. Thin sections give evidence of variability from one sample to another along traverses, across strike: samples blackened by high iron oxide content, vesicules with pressure shadow trails of

recrystallized quartz; plagioclase phenocrysts altered totally, or selectively along alternate lamellae; biotite in quartz-muscovite veinlets discordant to schistosity, or segregated into biotite rich (40%) and biotite poor (10%) zones.

1.4.7 GEOCHEMISTRY AND PETROGENESIS

Baragar (1966) described the Yellowknife succession as two volcanic cycles, each becoming more felsic up section. Both tholeiitic and calc-alkaline differentiation trends are recognized, the low K content of some tholeiites is noted. The tholeiitic trend is attributed to fractional crystallization, while the calc-alkaline trend is attributed to contamination by sialic material.

Folinsbee et al (1968) refer to the greenstone belt as a very ancient island arc and make comparison with a similar thickness of Miocene mafic volcanic-turbidite rocks in the Fossa Magna of Japan. This sequence developed over approximately 12 Ma, and a similar time frame is considered reasonable for the Yellowknife sequence.

Green and Baadsgaard (1971) found no isotopic evidence for contamination of a tholeiitic magma to produce volcanics of calc-alkaline affinity, hence the trend is primary, and 13,000 m of marine volcanics were extruded approximately 2650 Ma ago (U-Pb zircon data).

Pillowed low K tholeiites compose most of the Kam Formation lower and upper cycles, with andesites and dacites becoming propor-

tionally more abundant towards the top of each division (Condie and Baragar 1974). Lower cycle mafic volcanics have a flat to slightly LREE enriched pattern, while a dacite shows a negative Eu anomaly and no HREE depletion. Upper cycle mafic volcanics are LREE enriched, andesites range from slight LREE enrichment to HREE depletion.

Jenner et al (1981) also ran REE patterns for Kam, Duck and Banting Formation samples, concluding that "the complex nature of the Yellowknife volcanics and their altered nature suggest characterization of these volcanics as calc-alkaline....should be viewed with caution."

1.5 OBJECTIVES AND FIELDWORK

The research program was designed to follow upon the work of Boyle (1961), Baragar (1966) and Henderson and Brown (1966) which was concerned primarily with the volcanic rocks of the Kam Formation, Yellowknife Supergroup. The objectives of this study are:

1) to present the major and trace element chemistry of the Yellowknife volcanic belt, as no comprehensive analyses for all volcanic formations are currently available;

2) to date the volcanic formations by rubidium-strontium methods, as a continuation of regional Rb-Sr, Pb-Pb and U-Pb isotopic studies;

3) to compare analytical results from this study with data available for other Archean volcanic belts;

4) to compare these data with those used to support petro genetic models for other greenstone belts, and thus to propose a model for the Yellowknife volcanic belt.

This study is important locally as it will address the petrologic questions of, a) initial magma type, i.e. Komatiite, Mg-tholeiite, tholeiite, contaminated tholeiite or calc-alkaline, and b) pre-existing sialic crust as possible basement to the Archean volcanic sequence. It is a base study, necessary for continued study and analysis of volcanic sequences in the Slave Province.

Three months were spent in the Yellowknife region during summers 1978 and 1979 running traverses and collecting samples to give a complete suite of least visibly altered lavas from all three volcanic formations. Detailed geological maps were available for the Kam Formation (Henderson and Brown 1966) and in progress for the Banting Formation (Hauer 1979; Helmstaedt et al 1980; Easton and Jackson 1981). Mapping subsequently included the Duck Formation (Easton et al 1982).

CHAPTER 2

GEOLOGY AND GEOCHEMISTRY : PREVIOUS WORK

2.1 REGIONAL GEOLOGY

The supracrustal rocks bordering Yellowknife Bay are at the western edge of the large well preserved Yellowknife-Cameron River Archean volcano-sedimentary basin (Hoffman and Henderson 1972). Sediments of the basin are similar to those across the province; great thicknesses of greywacke and mudstone exhibiting all the features characteristic of turbidites, minor lithic wackes and conglomerates. Significant thicknesses of volcanic rock occur along the east and west contacts of the basin with granitic rocks. The mafic lavas are dark green to dark grey amphibolites, less frequently true greenschist facies metamorphic rocks, and locally may show contact metamorphism overprint. Metamorphic grade of the sediments is greenschist facies in the east and west, cordierite-amphibolite facies in the center (Duncan Lake - Prelude Lake), and gneissic to migmatitic in the north (Figure 2 and 3).

Stratigraphy of the Yellowknife Supergroup, for the Yellowknife Bay area, is summarized in Table 1 (Jolliffe 1942; Boyle 1961; Henderson and Brown 1966; Henderson 1970; Helmstaedt et al 1980; Easton et al 1981, 1982). Seven formations are recognized: the Jackson Lake, Walsh and Burwash Formations of the Duncan Lake Group; the Kam and Duck Formations of the Beaulieu Group; the Banting Forma-

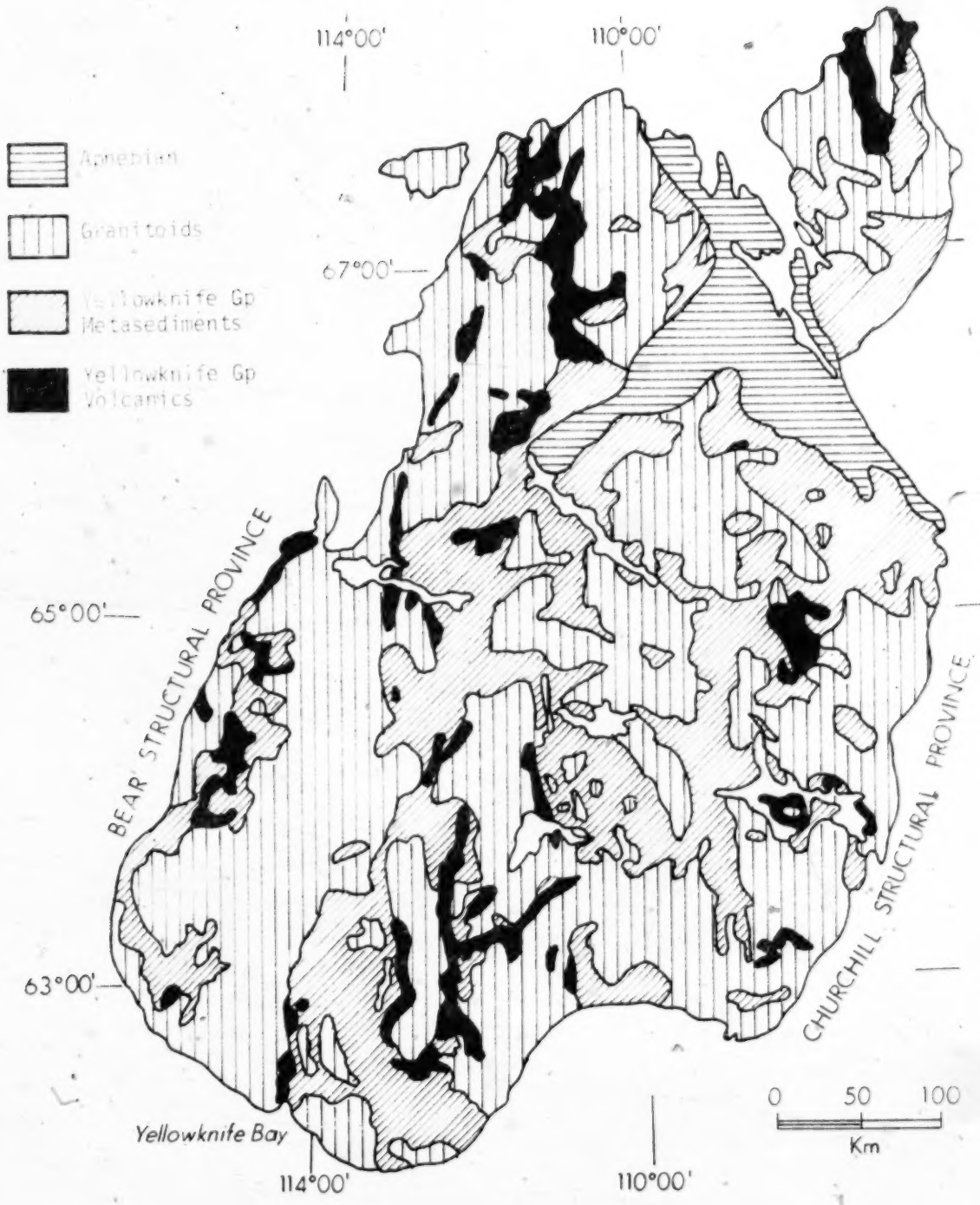

Figure 2 - General geology of Slave Province

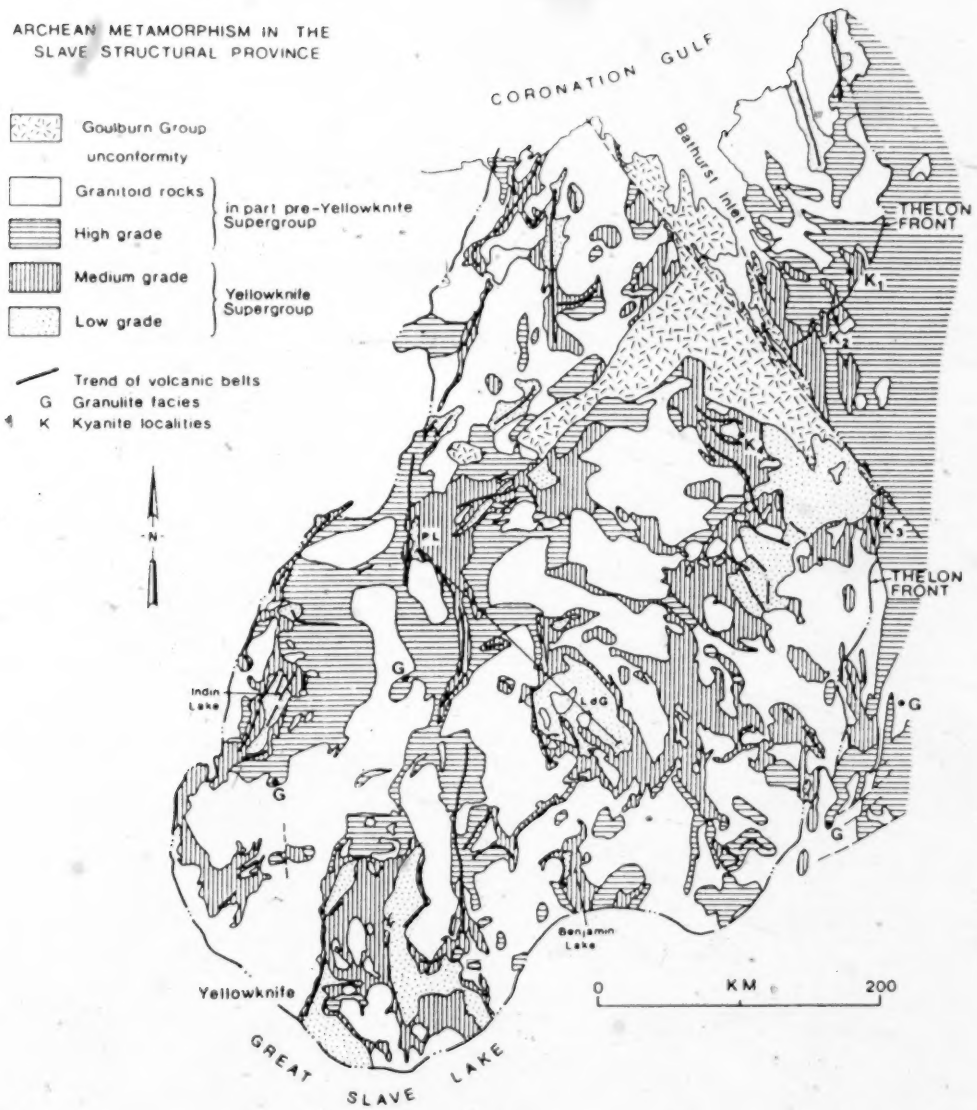

Figure 3 - Metamorphic Map of Slave Province
(From Thompson 1978)

TABLE 1 - Formations in the Yellowknife Bay Area

ERA	SUPER-GROUP	GROUP	West Side Yellowknife Bay FORMATION & LITHOLOGY	East Side Yellowknife Bay FORMATION & LITHOLOGY	West Side DIV. & LITH.		Both Sides DIV. & LITH.	
CENOZOIC			Pleistocene glacial deposits	Pleistocene glacial deposits				
			Unconformity					
PROTERO-ZOIC			Diabase Gabbro	Diabase Gabbro				
			Intrusive	Contact				
ARCHEAN			Western Granodiorite Quartz-Feldspar Porphyry (QFP) Gabbro Diorite	Prosperous Lake Granite Southeast Granodiorite QFP, Gabbro Diorite	ss., conglom.		C	grywcke, slate
					grywcke. slate	B	B	slate, grywcke. fel. volc.
			Intrusive	Contact				
	YELLOW-KNIFE	DUNCAN LAKE	JACKSON LAKE volc. lithic ss. & conglom.	BURWASH greywacke, thin slate interbeds	fel. volc.			ss., conglom.
			Unconformity	BANTING fel. volc., agglom., tuff				
			Diorite Gabbro					
			Intrusive Contact	WALSH slate, siltst.				
		BEAU-LIEU	pillowed and massive mafic to intermed. lava	pillowed and massive intermediate volcanics	mafic volcanics	A	A	mafic volcanics
			KAM ? ? OCTOPUS	DUCK ? ?				
Henderson (1970)			Helmstaedt et al (1980)	Easton et al (1981, 1982)	Boyle (1961) Henderson & Brown (1966)		Jolliffe (1946)	

tion which has not been assigned to a group; the Octopus Formation, consisting of basic and felsic volcanics, and sediments stratigraphically below the Kam Formation, is not well defined (Helmstaedt et al 1982).

Structural features in the Yellowknife Bay area include:

a) some slump structures are disharmonic folds with no flattening of fabric and are related to either formation of early isoclinal folds or syndepositional deformation of wet sediments in an unstable sedimentary basin (Drury 1977);

b) isoclinal syncline, horizontal to gently canoe shaped and slightly overturned to the west, extending north, through Yellowknife Bay, immediately east of Yellowknife River and east of Banting Formation rocks (Henderson 1972; Easton and Jackson 1981);

c) deformation of the sediments on the east limb, of the syncline, into steeply plunging to overturned cross folds related to intrusions (Drury 1977);

d) deformation of the volcanics on the east limb, of the syncline into a variably plunging subsidiary anticline, (Henderson 1972);

e) steep to vertical strike slip sinistral faults affecting volcanic rocks, sediments and intrusives (Jolliffe 1942; Henderson and Brown 1966);

f) diabase dyke and irregular gabbroic bodies intrude all rock units, offset by the late faults (Boyle 1961).

2.2 YELLOWKNIFE VOLCANIC ROCKS - BEAULIEU GROUP

Large segments of the volcanic rocks have been assigned to the Beaulieu Group of the Yellowknife Supergroup. This predominantly volcanic group consists of the Kam Formation, west side Yellowknife Bay, and the Duck Formation, east side (Henderson 1970). The Banting Formation has not been assigned to either the Beaulieu or the sediment dominated Duncan Lake Group. Formation names are restricted to the Yellowknife Bay area, while other formations of similar lithologies occur throughout the Slave Province.

2.2.1 KAM FORMATION

The Kam Formation (Figure 4) consists of approximately 9,200 metres of basaltic to andesitic lava flows. Detailed investigations (Boyle 1961, Henderson and Brown 1952, 1966; Baragar 1966) indicate the volcanic pile forms a northeasterly striking homoclinal succession containing massive and pillowed flows, variolitic flows, diabase dykes, gabbroic sills and irregular intrusives, minor tuffs and cherty tuffs.

Flows are of variable lateral extent, thicknesses range from a few metres up to 150 metres, and some show massive - pillow - pillow breccia sequence. Contacts are best defined by flow top breccia and tuffaceous material. Pillows vary in size, from 0.15 metres to 1.5 metres averaging 0.5 metres, and in shape, from almost circular through 'bun', 'pillow' and 'mattress'.

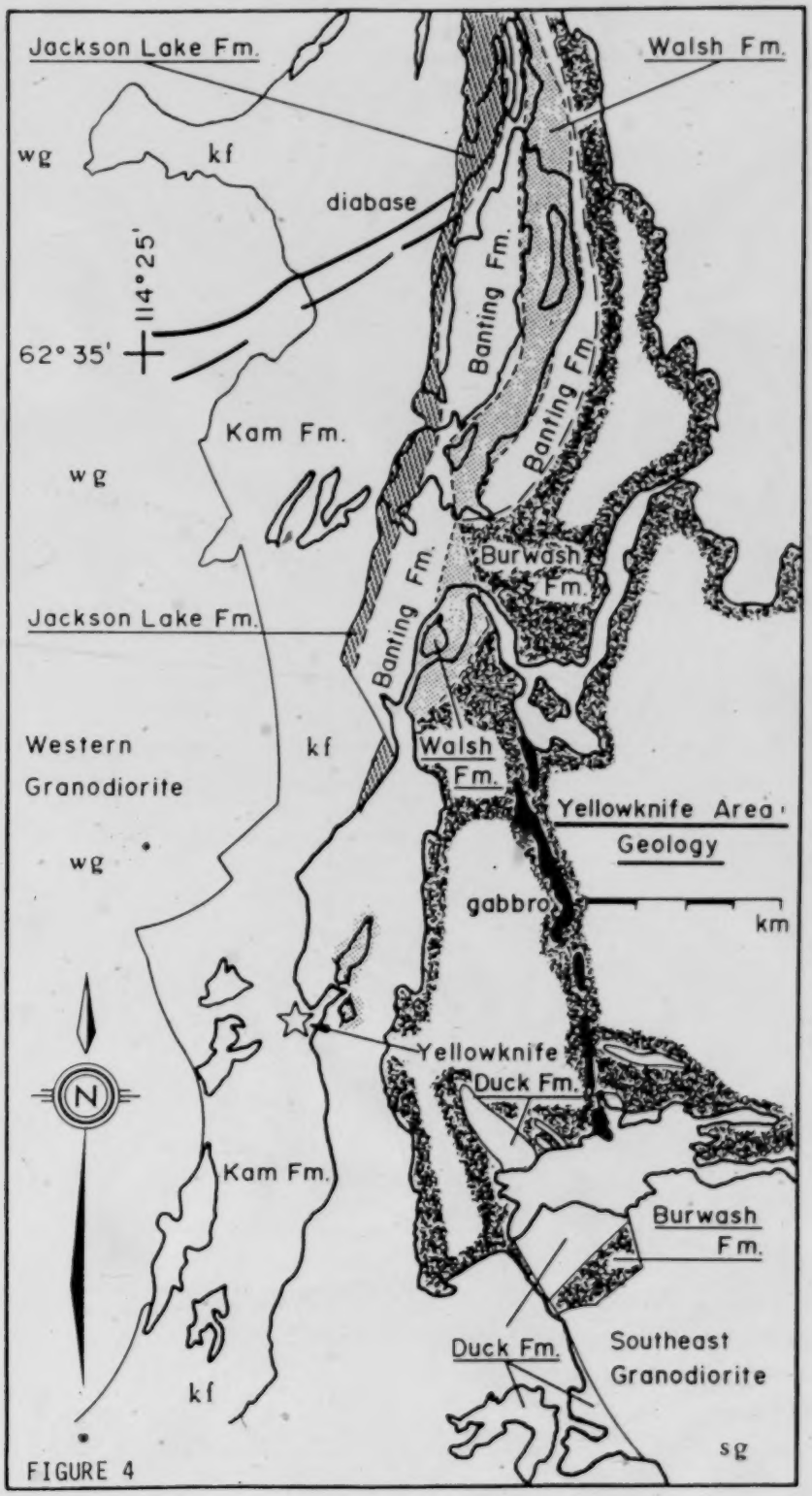
Jackson Lake Fm.
Walsh Fm.
wg
kf
diabase
114° 25'
62° 35'
Banting Fm.
Banting Fm.
Kam Fm.
wg
Banting Fm.
Burwash Fm.
Jackson Lake Fm.
Western Granodiorite
kf
Walsh Fm.
Yellowknife Area Geology
wg
gabbro
km
N
Yellowknife
Duck Fm.
Kam Fm.
Burwash Fm.
Duck Fm.
Southeast Granodiorite
kf
sg

FIGURE 4

Massive flows are coarser grained than pillowed flows and are distinguished from compositionally identical sills by the presence of amygdules, ropy to rubbly flows tops and more irregular contacts with interflow sediments.

Eight groups of variolitic flows have been identified, typically pillowed. Varioles are light coloured, 5 to 10mm in diameter and locally appear to have coalesced into larger masses. They consist of epidote, hornblende and oligoclase, the feldspar content being greater than the rock as a whole (Henderson and Brown 1966). Use of variolitic and porphyritic units as a stratigraphic marker horizons has allowed pre-faulting reconstruction of the Kam Formation (Henderson 1978).

Lavas are extensively intruded by compositionally similar gabbroic sills and irregular bodies, and by late diabase dykes. The dykes may be feeder conduits to lava flows, and it is thought they are closely related in time and origin to the flows.

Located in the central part of the volcanic pile is a 350 metre thick felsic volcanic unit, primarily dacitic in composition. Much of the unit contains quartz and feldspar phenocrysts; basic members exhibit pillow structure while more felsic portions are coarsely fragmented with discontinuous bands of breccia and agglomerate. This distinctive unit, light coloured on weathered surface, has been called both the Brock and the Townsite flows, and is located in the north part of the city of Yellowknife (Traill 1950; Henderson and Brown 1966; Baragar 1966).

An upper acidic member was said by Baragar (1966) to unconformably overly the Kam Formation. It has since been named the Banting Formation, which may locally lie on and be intrusive into the Kam Formation (Easton and Jackson 1981).

Regional metamorphism of the mafic volcanics within the Kam Formation is of low pressure type, upper greenschist to lower amphibolite facies leaving no primary minerals preserved. Very little of the metavolcanic sequence falls in the lower greenschist facies.

Boyle (1961) defined three metamorphic facies across the Kam Formation relating them to the intrusive Western Granodiorite:

a) contact amphibolite facies - recognized in thin section by presence of brown to green pleochroic hornblende, andesine plagioclase, epidote, quartz, magnetite, ilmenite, sphene, carbonate, sulfide;

b) intermediate epidote amphibolite facies - fibrous actinolite, oligoclase plagioclase, epidote (+/- zoisite +/- clinozoisite), quartz, magnetite, chlorite, leucoxene, carbonate;

c) greenschist facies - green chlorite, albite plagioclase, epidote (+/- zoisite +/- clinozoisite), carbonate, quartz, leucoxene, sulfides.

Green and Baadsgaard (1971) noted transition of the amphibole in the metavolcanics from the intrusive contact to Yellowknife Bay as blue green hornblende replaced by actinolite and finally chlorite. The authors note that epidote does not persist into the

hornblende-hornfels facies and therefore the assemblage andesine - epidote - horneblende, in Boyle's (1961) contact amphibolite facies, is typical of regional rather than contact metamorphism.

Froese (1973) defines the transition from greenschist to amphibolite facies by the reactions:

a) high pressure - epidote + almandine = anorthite + hornblende, the assemblage plagioclase - hornblende - almandine is stable throughout the amphibolite facies;

b) low pressure - hornblende + chlorite = anorthite + cummingtonite, the assemblage plagioclase - hornblende - cummingtonite is stable throughout the amphibolite facies.

A white amphibole coexisting with blue-green hornblende may often be cummingtonite, rather than tremolite, thus signifying the transition from upper greenschist to lower amphibolite facies.

2.2.2 DUCK FORMATION

The Duck Formation consists of mafic to intermediate flows exposed along the east side of Yellowknife Bay. The succession is broken by major faults and Quaternary sediments. Outcrops are dark to light greyish green, massive and pillowed, often appearing more siliceous than Kam Formation mafic volcanics. There are few sills, irregular intrusive mafic bodies or variolitic flows. Transitions from massive to pillow to pillow breccia are common, as is hyaloclastic interflow material. Pillows tend to be compact 'bud' like in

nature with less frequent 'tops' determinations. These volcanics are on the east limb of the major syncline down Yellowknife Bay that has been refolded into a subsidiary anticline of variable plunge and axial direction. Through Horseshoe Island, west of the Akaitcho Fault, the axis of the anticline plunges southwest, however, south of Duck Lake and east of the Akaitcho Fault it plunges east-northeast.

Metamorphism within the Duck Formation straddles the greenschist - amphibolite border as shown by the assemblages:

a) albite/oligoclase - zoisite - actinolite/hornblende - chlorite, and

b) oligoclase/andesine - zoisite - hornblende - almandine - cummingtonite.

Felsic samples generally have an albite - chlorite/penninite - epidote/clinozoisite assemblage with feldspar phenocrysts and quartz blebs indicative of lower greenschist facies; FeO + MgO components are lacking to produce actinolite, hornblende or cummingtonite. Easton et al (1982) have mapped a northeast trending greenschist - amphibolite boundary south of Horseshoe Island and east of Akaitcho Bay as far as Duck Lake; the Akaitcho Fault accounts for the sinistral offset.

2.2.3 BANTING FORMATION

The Banting Formation consists of felsic volcanic flows, tuffs, agglomerates and interbedded sediments outcropping for 25 km in a linear trend north from the mouth of Yellowknife River. It is

conformable with the underlying Jackson Lake Formation, the overlying Burwash Formation and the intervening Walsh Formation. Generally in fault contact with the Kam Formation, one location indicates Banting Formation rocks both intrude and overlie Kam Formation pillow lava. Younger plutons or batholiths have intrusive, shear or fault contacts. The formation is a homoclinal succession facing east; metamorphism is more pronounced east of Walsh Lake (amphibolite grade) than west of the lake (greenschist facies). Variable in composition, the Banting Formation consists of mafic to intermediate massive and pillowed flows, porphyritic intermediate and felsic lavas, agglomerate, bedded and crystal tuffs, ash flows, and interflow sediments (argillite, sandstone, conglomerate). Within this unit strike lengths are short, shearing common and overburden extensive. Whole rock samples for chemical analyses were selected from flows which appeared least altered and least sheared.

2.3 YELLOWKNIFE SEDIMENTARY ROCKS - DUNCAN LAKE GROUP

Three formation names designate Yellowknife Supergroup sediments placed in one group for the Yellowknife Bay map area by Henderson (1970). A fourth, the Octopus Formation, has not been fully described and assigned (Helmstaedt et al 1980, 1982).

2.3.1 JACKSON LAKE FORMATION

The Jackson Lake Formation unconformably overlies the Kam Formation mafic volcanics with a sharp locally irregular contact that generally strikes north. A sinstral offset of the formation, near the

head of Yellowknife Bay, is due to the Akaitcho Fault. To the north it either pinches out, or has been faulted between the Kam and Banting Formations, while in the south it crops out on Jolliffe Island and on the Sub Islands (Figure 4).

A basal conglomerate lies with angular unconformity on the Kam Formation, apparently in-filling up to 250 metres of topography, the top of the formation is either under water or faulted against the Banting Formation. The conglomerate is composed predominantly of angular mafic volcanic blocks (less than one metre) with fewer, and smaller, felsic cobbles. Examples of well rounded granitic cobbles are located on the Giant-Yellowknife Mine property and on Jolliffe Island. Stratigraphically higher in the unit clasts become smaller and more rounded; the frequency of mafic clasts decreases, felsic clasts increases, and small quartz cobbles and scattered chert pebbles appear.

Conformably overlying the conglomerate layers are variably thick to thin bedded sandstones. Weathering light brown to light green they are often cross bedded and contain thin interbeds of dark siltstone or black shale. The beds range from medium grained and massive through fine sand and silt laminations to extensively scoured gravels. Almost all coarse clasts are felsic volcanic pebbles (Henderson 1970). The light green to grey matrix is observed in thin section to be deformed volcanic rock fragments which have lost original outlines due to shearing.

Low grade regional metamorphism is indicated by the development of chloritoid, chlorite and muscovite in the matrix material.

2.3.2 BURWASH FORMATION

Burwash Formation turbidites comprise the most extensive supracrustal rock in the Yellowknife Bay - Cameron River basin. Equivalent rocks are found as far east as the East Arm of Great Slave Lake (110 km) and as far north as Fishing Lake - Gordon Lake (95 km). Within much of this area rocks are of low to medium grade regional metamorphism, locally reaching high grade (Thompson 1978). Along Yellowknife Bay, metamorphism has been below the biotite isograde and primary sedimentary structures are well preserved (Henderson 1970).

The formation consists of interbedded greywackes and slates exhibiting all the features of turbidites, with an estimated thickness of 4572 metres (Henderson 1972). Individual greywacke beds are laterally continuous with sharp bases and commonly show most or part of the Bouma cycle. Beds range in thickness from thin rippled units, less than two centimetres, to massive three metre units but average 30 centimetres. Typically greywacke predominates over shale horizons, usually less than five centimetres thick. Higher in the section beds become thinner, shale more abundant, and deformation more frequent.

The Burwash Formation conformably overlies the Duck Formation, as shown by flows and tuffaceous beds in the contact area north of Duck Lake (Henderson 1972; Easton 1982). Stratigraphic relation-

ships redefined by Helmstaedt et al (1980) and Easton (1982) indicate the Burwash Formation to conformably overlie not only the Duck Formation but also the Banting and Walsh Formations. A north trending synclinal axis, previously positioned through Walsh Lake, has been relocated 0.5 to 1.0 km east of the Banting-Burwash Formation contact, coincident with a band of argillacious material.

2.3.3 WALSH FORMATION

The Walsh Formation occurs along the Yellowknife River west of the Hay-Duck Fault, and along the shores of Walsh Lake east of the Hay-Duck Fault where it is intercalated with two divisions of the Banting Formation. It is thought that the Walsh Formation grades upward into the Burwash Formation, on the penninsula in the Yellowknife River. Here, contacts are covered by sand plains and no evidence for Banting Formation rocks has been found.

The formation consists of turbidites, similar in structure but different in composition compared with those in the Burwash Formation. There is a greater proportion of shale to greywacke, the greywackes being thin bedded and fine grained. Deformation is due to an argillacious composition and relative proximity to the fold axis. Estimates of formation thickness have not been made.

2.4 INTRUSIVES

The Slave Province is an Archean granite-greenstone terrain, large batholiths deform and separate volcano-sedimentary sequences. At Yellowknife, the supracrustal succession has been affected by three large intrusive bodies: the Western Granodiorite, the Southeast Granodiorite and the Prosperous Lake Granite.

2.4.1 WESTERN GRANODIORITE

The Western Granodiorite is a large granitic batholith extending 70 kilometres westward from its contact with the Kam Formation metavolcanics. Compositional phases vary from diorite to syenite, including quartz diorite, granodiorite and quartz monzonite. It is a heterogeneous batholith locally porphyritic and sometimes pegmatitic. Contacts against Yellowknife Supergroup rocks are sharp ranging from a few metres to a kilometre wide, but may be masked by angular blocks of assimilated metavolcanics up to 800 metres in diameter. West of Kam Lake these xenolithic blocks show no evidence of reaction however, indications of assimilation reactions do occur on the shore of the west arm of Long Lake and around Ryan Lake. Along the southwest shore of the small lake 900 metres west of Frame Lake (south half) there developed a hybrid rock of granitized amphibolite (Henderson and Brown 1966).

Medium to coarse grained, with mottled texture the hybrid is composed of 50-60 percent feldspar (less than 0.6 centimetres), 30-40

percent hornblende crystals (2.5 centimetres), 5-10 percent quartz; subangular to rounded fragments (seven centimetres) of dark greenstone are enclosed by a light coloured, fine grained chill envelope or corona of feldspar and hornblende 0.6-1.2 centimetres wide. These hybrid rocks cut the main greenstone belt with sharp contact and are in turn cut by the main mass granodiorite with sharp contacts.

Radiometric methods (Green and Baadsgaard 1971) have dated the Western Granodiorite at 2610 $\pm$ 58 Ma by Rb-Sr whole rock isochron (I.R. = 0.7035 $\pm$ .0027), by zircon concordia plot at 2596 $\pm$ 16 m.y. and K-Ar (hornblende) age maximum at 2540 $\pm$ 56 Ma. A recalculation using $\lambda^{87}Rb = 1.42 \times 10^{-11}/Yr$ yields a Rb-Sr age of 2555 Ma.

2.4.2 SOUTHEAST GRANODIORITE

The Southeast Granodiorite occurs on the east side of Yellowknife Bay, extending some 65 kilometres south southeast. The main body has a biotite granodiorite composition, but the western segment is quartz diorite in composition, with numerous metavolcanic xenoliths.

Green and Baadsgaard (1971) have dated the Southeast Granodiorite resulting in a range of ages: zircon Pb-Pb dates average 2611 Ma, hornblende K-Ar dates average 2580 Ma, and the Rb-Sr whole rock age is 2640 $\pm$ 37 Ma ($^{87}Sr/^{86}Sr$ I.R. = 0.7011 $\pm$ 0.0008). Zircons from diorite boulders in Jackson Lake Formation conglomerates, on the Sub Islands and Garbage Island in Yellowknife Bay have been dated by

207Pb-206Pb methods at 2595 Ma and 2575 Ma supporting the theory that the Southeast Granodiorite predates at least part of the Yellowknife Supergroup. The apparent intrusive relationships on its north and eastern margins may be due to late Archean remobilization. The Rb-Sr whole rock data may be recalculated, using $\lambda^{87}Rb = 1.42 \times 10^{-11}/Yr$, to 2584 Ma.

2.4.3 PROSPEROUS LAKE GRANITE

The Prosperous Lake Granite occurs northeast of Yellowknife Bay forming the east shore of Prosperous Lake. Half the granite mass is composed of pegmatites, concentrated near the margin, having dyke like form and sharp contacts with the main body. Simple pegmatites predominate, containing quartz, microcline, cleavlandite, muscovite, tourmaline and garnet, but a few complex pegmatites occur just outside the margin of the granitic body and contain beryl, spodumene, amblygonite, scheelite and columbo-tantalites. It is the youngest plutonic body in the map area and may be an anatectic melt of rocks similar to the surrounding metasediments; for $\lambda^{87}Rb = 1.42 \times 10^{-10}/Yr$, the Rb-Sr mineral isochron is calculated at 2520 Ma.

Emplacement under conditions of low pressure (Folinsbee 1942; Green and Baadsgaard 1971) is suggested by knotted schists and metavolcanics in the sillimanite-cordierite-muscovite-almandine facies. The stable occurrence of staurolite-cordierite suggests hydrous fluid pressure of 1.5 - 3.5 kb and a temperature range of 530-685° (Green and Baadsgaard 1971). Oxygen isotope studies have shown

high $\delta^{18}O$ values for the Prosperous Lake Granite (Drury 1979) indicating the pervasive influence of meteroic water during its evolution, and may indicate possible metasediment-altered silicic volcanic source material, or total contamination of magma by meteoric waters.

A retrogressive hydrothermal episode has been cited as the cause for chloritization of biotite and the reduction of porphyroblasts (andalusite, garnet, poikiloblastic cordierite, staurolite and sillimanite) to micaceous pseudomorphs.

2.5 STRUCTURE

A pre-greenstone belt basement of silicic material, postulated on geological grounds (McGlynn and Henderson 1972), has been supported by seismic methods indicating both volcanics and granites to be underlain by a higher velocity sialic material to a depth of 32 kilometres (Clee et al 1974), and dated by Niekic et al (1975, 1980) from a tonalitic gneiss boulder contained in a diatreme.

Mafic to intermediate volcanics and sediments have been folded into a north trending isoclinal syncline, the axis being through Yellowknife Bay and immediately east of Walsh Lake (Figure 5). The east limb has been refolded into a subsidiary anticline with a northeast axis. Units have been offset by high angle left lateral wrench faults (strike slip faults) after the close of the Archean. Well documented by Campbell (1948) the West Bay Fault has displacements of 4900 metres horizontal and 480 metres vertical.

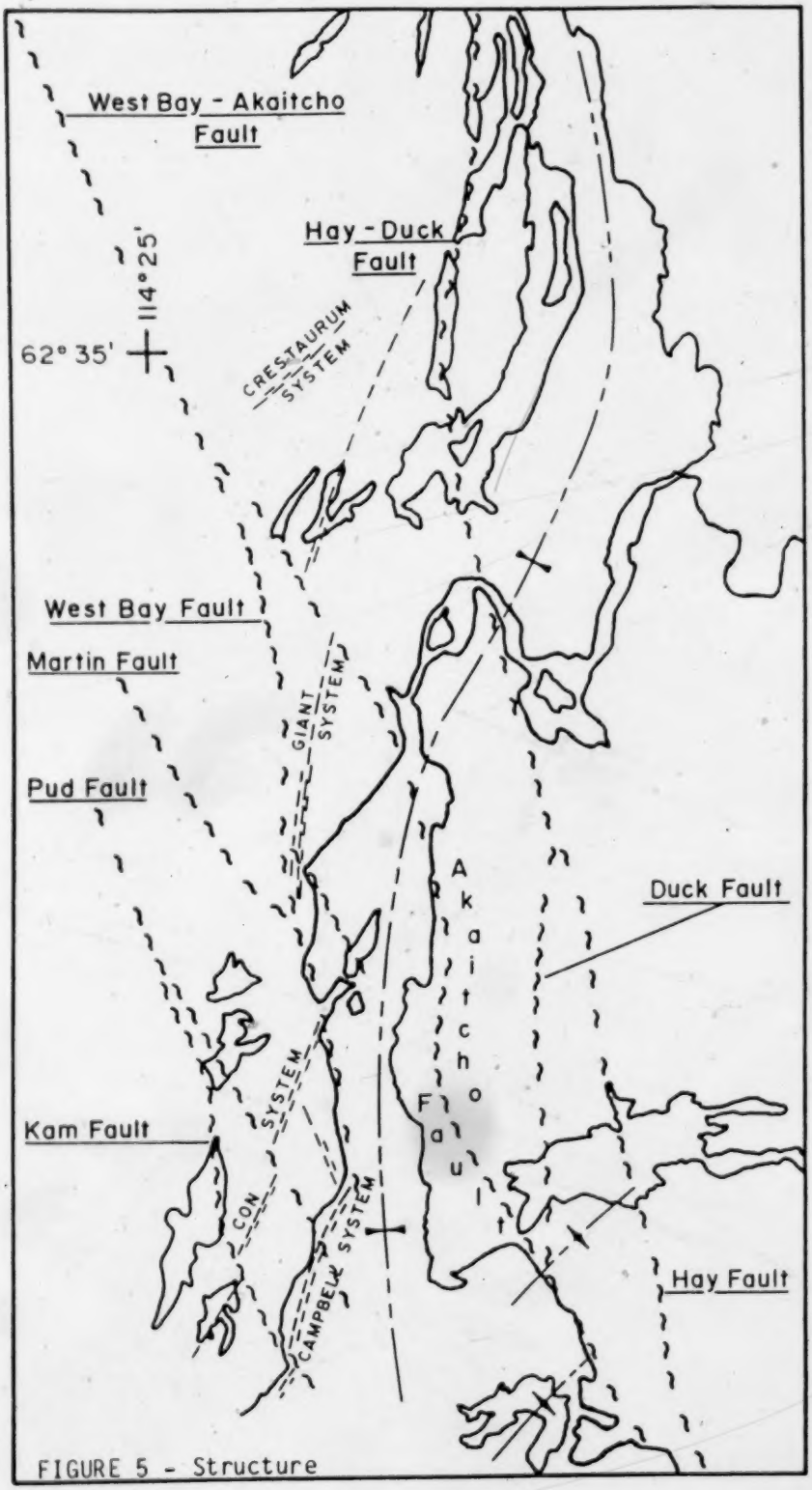

FIGURE 5 - Structure

Contact of the Western Granodiorite with the Kam Formation is generally faulted; however, where unfaulted, the boundary varies from steep and parallel to the strike of the volcanics to highly discordant north of Ryan Lake (Drury 1977).

Main phase folding is variable, the tightness of folds and density of axial traces decreases eastwards away from the Western Granodiorite, hence in the east section of the map area there are few folds of this generation. To the north, where only 100 metres of volcanics separate the granodiorite from the sediments, main phase folds approach upright isoclinal form. A similar correlation of fold style around an early granodiorite complex has been made near Ross Lake (Fyson 1975).

The west and north margins of the Southeast Granodiorite are lobate, with narrow folded screens of sediments and volcanics caught between masses of granitic material. Supracrustal material usually strikes parallel the roughly east-west margin of the granitic mass due to refolding of the west southwest - east northeast trend of main phase axial traces. These late phase folds and the thrusting of volcanic rocks upon metasediments have been attributed to remobilization of the Southeast Granodiorite (Drury 1977).

Early phase deformation is recognized as long limbed isoclinal folds in the sediments resulting in 1) overturned strata in areas void of main phase deformation and far from areas of late phase

deformation, 2) overturned asymmetrical main phase folds exhibiting inverted and right-way-up bedding suggest prior strata inversion, 3) aerial photograph interpretation, of structurally complex zones between areas of right way up and inverted strata, as axial zones of major early phase long limbed isoclinal folds refolded by main phase and possibly late phase deformation, 4) axial surface disclocation of minor isoclinal folds transgressed by main phase cleavage.

More competent volcanic strata has been affected by shearing and faulting, but are free of intergranular and penetrative deformation. Shear zones are of two types: 1) simple, narrow zones parallel the attitude of the flows, usually localized along tuffaceous horizons or flow contacts (e.g., Kam Point shear zones, A.E.S. shear zones, Ranney shear zone system), and 2) larger discordant zones dipping 50-70° northwest, 10-150 metres wide formed by a network of high deformation surrounding blocks (horses) of relatively undeformed greenstone, (Giant Campbell System, Con System, Bow Lake System, Negus-Rycon System). Shear zones parallel to flow contacts have proven of little economic value compared to the larger discordant zones.

Investigation of these cross cutting shear zones indicate overall dips of 40°-60° west, but internal shear planes dip more steeply. Movement is west side up (reverse faults) with displacements of 200 metres to 450 metres. Most authors have viewed these structures as thrust fault systems related to the folding of supracrustal material and intrusion of the Western Granodiorite (Campbell 1949; Brown and Dodson 1953; Boyle 1961; Henderson 1978). Conditions

resulted in recrystalization and rock flowage at depth under high pressure and elevated temperatures (Henderson and Brown 1966). Henderson argues for consideration of the suggestion that initial movement was prefolding along concordant zones associated with near horizontal water saturated tuffaceous horizons in a normal manner (Henderson 1970). Later movement was discordant, along the now west dipping surfaces, as well as the concordant tuffaceous horizons. Kerrich and Allison (1978) suggest that during folding flexural slip was accommodated parallel to interflow horizons generating minor shear zones with discontinuous displacement between the boundaries but a mechanism for formation of these discordant shear zones was not made.

Contrary to the views mentioned above, Drury (1977) doubts that the shear belts are thrusts predating the formation of steep dips, due to the variety of angles at which they cut the originally horizontal flows.

The Yellowknife area is cut by numerous major north-north west trending faults (West Bay, Kam-Pud, Hay-Duck) and cross-over faults (Akaitcho, Martin, Townsite, Aye), most evident on the west limb of the syncline. These major faults have displacements measured in tens of kilometres; the zone of disruption is usually less than one metre wide, having formed by brittle fracture, mechanical grinding and brecciation along planar zones. They strike north to N25°W, dip nearly vertically and have left lateral strike slip. They extend 200 kilometres north-northwest across the Western Granodiorite and associated intrusives to the Indin Lake volcano-sedimentary belt where the

single fault splays into several smaller left lateral faults, with cross-over faults, similar to the system at Yellowknife (Henderson and Brown 1966).

2.6 MINERALIZATION

Economic deposits of gold occur in quartz and quartz-carbonate veins associated with major shear zones transecting volcanic and sedimentary rocks of the Yellowknife greenstone belt. Ductile shear zones are 10-150 metres wide, dip northwest at 50°-70°, and cut the stratigraphy at angles of 20°-70° in the vertical plane. Past producers (Rycon, Negus, Akaitcho, Crestaurum) and currently operating mines (Giant, Con) are hosted principally by mafic flows of the Kam Formation; gold has also been extracted from tuff and sediment hosted shear zones at the Consolidated Discovery, Thompson-Ludmark and Ptarmigan mines, now closed.

Ore zone mineralogy is quartz, carbonate, pyrite, arsenopyrite, pyrrhotite, stibnite, sulphosalts, gold and aurostibnite. Wall rock amphibolite and epidote-amphibolite mineralogy has been replaced in shear zones by a weakly schistose chlorite-albite-sericite -leucoxene assemblage. Alteration zones around gold veins are due to carbon dioxide, water, sulfur and arsenic (Boyle 1979).

Development of the large shear zones is generally attributed to main phase deformation of the volcano-sedimentary package during continued intrusion of the Western and Southeast Granodiorites (Drury

1977; Kerrich et al 1977). However, Henderson (1978) suggests the faults started much earlier, possibly as gravitational slides initiated along planes of weakness or concordant zones associated with water saturated interflow tuff beds.

Major gold bearing quartz veins parallel schistosity and, together with veins along interflow horizons, must postdate early horizontal and vertical displacement across the shear zone. Relationships describe the stress state for hydraulic fracturing under conditions of abnormally high fluid pressure and represent a rotation of the principal stress direction 75° away from the orientation prevailing during formation of the shear zone. The fluid source may have been metamorphic dehydration reactions at the greenschist-amphibolite transition (Kerrich et al 1977; Kerrich and Allison 1978). Shear zones acted as permeable conduits to focus convective fluid flow driven by energy from the adjacent batholith.

A 25 percent decrease in FeO_T and a 20 percent increase in $Fe^{+2}/\Sigma Fe$ is noted when comparing 'background' metabasalts (FeO_T = 10%; $Fe^{+2}/\Sigma Fe$ = 0.75) with ore grade schists (FeO_T = 7.5%; $Fe^{+2}/\Sigma Fe$ = 0.95). Kerrich et al (1977) argue for a massive flux of hydrothermal solutions through the shear zone system; iron reduction suggests a water/rock ratio of 3:1 while iron dilution yields a ratio of 150:1. Lateral diffusion of material from surrounding schists into dilatent low pressure openings (Boyle 1961) is considered an inadequate method of ore formation based upon expected diffusion rates and required gold enrichment.

2.7 PREVIOUS GEOCHEMICAL WORK ON THE YELLOWKNIFE GREENSTONE BELT

Previous geochemical workers on the volcanic rocks of the Yellowknife Supergroup have studied the Kam Formation, Yellowknife Bay area (Boyle 1961; Baragar 1966; Green and Baadsgaard 1971) and portions of other greenstone volcanic belts. The Cameron River region has been studied by Lambert (1977), the Indin Lake - Arseno Lake region by Frith (1973, 1978), Frith and Leatherbarrow (1975), and the Hackett River area by Frith and Hill (1975), Frith et al (1977) and Ewing (1979). The mafic volcanic Kam Formation, host to the gold deposits, has been most extensively analyzed (Baragar 1966; Condie and Baragar 1974). Limited minor and rare earth element data is available for the Duck and Banting Formations (Jenner et al 1981). Brown (1949) gave the make-up of the Yellowknife greenstone belt (Kam Formation), excluding the upper acidic member (Banting Formation), as: massive andesitic flows 43%, pillowed andesite flows 42%, variolite andesite flows 11%, dacite flows 3%, tuff and cherty tuff 1%. Based upon normative mineralogy (Brown 1952), Baragar (1966) revised this to: basalt 49%, quartz basalt 6%, andesite 27%, latite 3%, dacite 8%, quartz dacite 7%. Henderson and Brown (1966) state that about 50 percent of the flows are massive, the remainder have well developed pillow structure.

The major geochemical contribution is that of Baragar (1966) dealing with major element analyses of the Yellowknife volcanic rocks, on the west side of Yellowknife Bay and a Cameron River section.

General chemical variation and petrographic indicator diagrams of data vs. stratigraphic position gave these results:

1) acidic members show an abrupt change in composition from preceeding basic and intermediate lavas, for all major element analyses except Na_2O and Al_2O_3;

2) the CaO content of basic and intermediate lavas decreases upward from the base of the volcanic sequence to the Brock (Townsite) flows; and from the immediately overlying mafic lavas to the upper acidic member;

3) the lavas west of the Sub Islands are more felsic than preceeding extrusives;

4) FeO and MgO show short range systematic variations;

5) the volcanic rocks show cyclic increases in acidity, capped by acidic volcanism;

6) MgO/FeO (total) shows no overall variation but rather short range trends of iron enrichment, and

7) a similar trend for the Solidification Index is shown.

Baragar's AFM diagram shows two trends for the Yellowknife volcanics:

1) sub-parallel to the FeO-MgO join (FeO > 50%) grouped about the Kam point gabbro sill trend, suggesting Fe-Mg exchange; and

2) a diagonal trend suggesting alkali enrichment with no iron peak, from about 15-35-30 (AFM) to 60-35-5 percent.

These trends are explained as follows, respectively:

1) Fe-Mg variation due to crystal fractionation a common trend of tholeiitic magmas; and

2) alkali-silica enrichment, without iron peak, is theoretically possible, but it is more likely to be due to contamination of basaltic magmas by granitoid country rocks.

Bulk composition of the Yellowknife volcanic rocks (Kam Formation) was compared by Baragar (1966) with data for circum-oceanic basalts and oceanic basalts (Chayes 1964). Frequency diagrams suggested mixed affinities, being similar to circum-oceanic basalts in TiO_2, MgO and CaO content but similar to oceanic basalt in Al_2O_3, FeO content (but more reduced), and the distribution pattern of the Differentiation Index; Baragar did not carry the tectonic implications further. Regarding the mixed affinities he stated: "possibly this will prove to be characteristic of continental geosynclinal environments." Final conclusions favour original tholeiitic magmas with crystal fractionation in high level chambers and sialic crustal contamination imposing a calc-alkaline trend.

Green and Baadsgaard (1971) note that the Yellowknife volcanic rocks meet the definition of spilite (Cann 1969); i.e., rocks of basaltic texture in which greenschist facies mineralogy is completely or almost completely developed. The authors conclude that the Yellowknife volcanic rocks show a calc-alkaline trend arguing there is little evidence for an overall iron enrichment in the metavolcanics, and no evidence for contamination of the volcanics by sialic crustal

material. Relatively high SiO_2 and lime/alkali ratio suggest calc-alkaline magmatism comparable to some younger examples of island arc volcanism.

Condie and Baragar (1974) describe two cycles of low potassium tholeites, each increasing in andesite and dacite upward in the section. Rare earth element data show these tholeiites to have a flat to very slightly enriched light rare earth element (LREE) pattern, similar to oceanic rise and west Pacific arc tholeiites. Comparison within the sequence shows the upper cycle tholeiites to be LREE enriched, especially in La and Ce, similar to some tholeiites from Iceland and Hawaii. The Yellowknife volcanic rocks are variable but often show moderate negative Eu anomalies and differ slightly from the neutral to slightly positive Eu values for most young andesites of calc-alkaline and arc tholeiite series. Condie and Baragar conclude from REE data that the Yellowknife belt is an example of an arc-type Archean greenstone belt characterized by flat (tholeiites) to enriched REE pattern and negligible to moderate negative Eu anomalies. However, the whole question of using REE patterns to characterize ancient greenstone belts in terms of modern tectonic setting is beset with difficulties (Condie 1980).

2.8 SUMMARY

A homoclinal succession of volcanic and sedimentary rocks have been subdivided into seven formations (Octopus, Kam, Duck, Banting, Jackson Lake, Walsh, Burwash). Detailed geological mapping

(1:10,000) of the Kam Formation has recently been expanded to include all but the Burwash Formation. Changes to the stratigraphic column have occurred at each phase of the mapping program, resulting in a better understanding of the volcano-sedimentary relationships, and continue to be made with each year's mapping.

Radiometric age dating, of the Kam Formation and major intrusive phases, has given a range of values indicating continuous geological events (extrusion, deposition, intrusion, erosion) over a short period of geologic time, once the various analytical methods and decay constants employed have been rationalized. Geochemical investigations have centred on Kam Formation metavolcanics and the shear zone hosted gold mineralization. Kam Formation major element, and limited rare earth element analyses of all volcanic formations, indicate a complex character to the source magma(s).

Previous work does not contain samples from all volcanic formations. Analyses for major and trace elements have not been in sufficient number to characterize the diversity of rock types within the sequence.

CHAPTER 3

GEOCHEMISTRY

3.1 INTRODUCTION

One hundred and fifty-six (156) samples of the Yellowknife greenstone belt have been analyzed by x-ray fluorescence for 17 elements; eighty (80) have also been analyzed for five elements by atomic absorption spectroscopy (Appendix A). Sample distribution for the three defined formations is: Kam Formation (lower unit) 52, Kam Formation (upper unit) 31, Duck Formation 44, and Banting Formation 29. Duplicate samples were taken at eight lower Kam Formation sites; surface grab samples and 1/2" drill core samples (Appendix B).

Traverses were made up section with samples taken at regular intervals to obtain a representative population for each formation (Figure 6). Samples are of massive and pillowed lavas; obvious intrusive phases were avoided, as were severely altered zones and variolitic flows. Usual sample weight was about two kilograms (4.5 pounds) taken as one piece, or several pieces in close proximity (3 metres). Prior to analysis, samples were further screened to minimize the effects of weathering, alteration and fracturing.

The Kam Formation has been split into lower and upper units at the top of the Brock or Townsite dacitic flows; traverses upsection in the Kam Formation closely parallel those by Baragar (1966). The

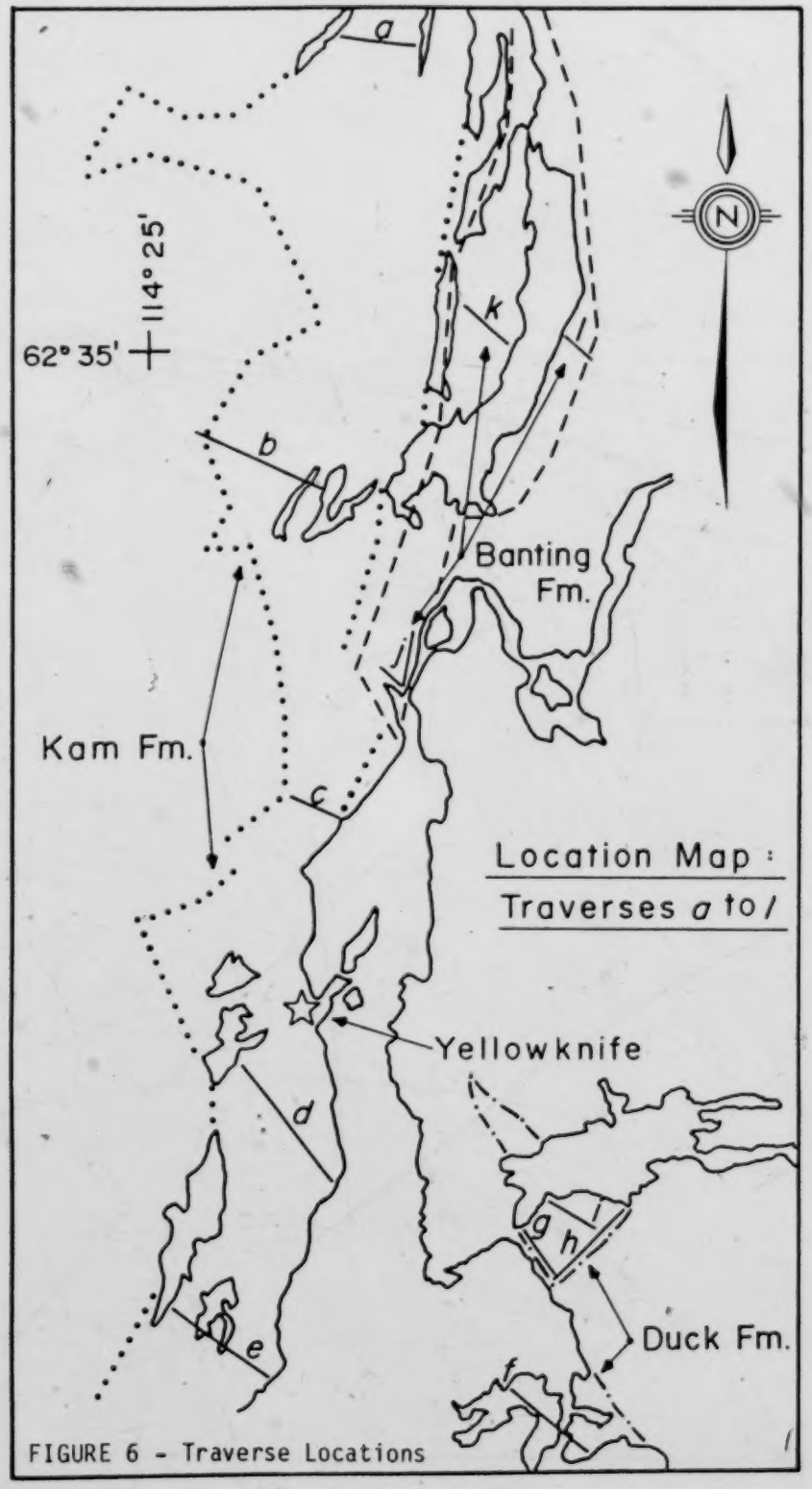

FIGURE 6 - Traverse Locations

division was used initially for ease of reference, however geochemcial differences have become evident. Major and minor element geochemistry of the lower Kam, upper Kam, Duck and Banting Formations will be discussed and compared with other greenstone belts, including the average compostions of Archean rocks by Condie (1976, 1979, 1981).

Discrimination diagrams have been used in this study to interpret the Yellowknife volcanic rocks. From the major element binary and ternary plots, Section 3.2, the samples can be divided by:

1) rock type - basalt to rhyolite;
2) character - alkaline or subalkaline;
3) alkali mobility - igneous to metasomatic values;
4) differentiation - komatiitic, tholeiitic, or calc-alkaline; and
5) tectonic affinity - within plate or plate margin.

Elements and element ratios considered relatively immobile, during alteration of volcanic rocks, have been used in the literature to generate a series of plots. When those employed by this study, Section 3.3, are compared with the major element plots of Section 3.2 they are seen to define the data coherently and with less scatter. Numerous other diagrams were plotted during the course of this study, however Section 3.2 is restricted to those relationships which have the greatest clarity.

The volcanic formations show a consistent range of compositions internally and retain consistent relationships between them.

Where the data are inconsistent, or not coherent, interpretation becomes difficult and highly speculative.

3.2 MAJOR ELEMENT GEOCHEMISTRY

Major element data has been plotted on binary and ternary diagrams to describe the volcanic suite and assist in later interpretations.

3.2.1 FREQUENCY-SILICA (Frequency Percent vs SiO_2)

The silica frequency diagram (Figure 7) is multi-modal, containing three relative abundance peaks, decreasing in height with increasing silica. Basaltic rocks (less than 54% SiO_2) constitute 52 percent of the samples; andesites (54-62% SiO_2) 35 percent, dacites (62-72% SiO_2) 11 percent, and rhyolites (SiO_2 greater than 70%) 2 percent. Trace element geochemistry has defined basaltic andesites (52-56% SiO_2) as a distinct and significant group for the Yellowknife volcanic rocks, therefore based upon silica content this suite of samples is classified as follows: basalts 31 percent, basaltic andesites 34 percent, andesites 22 percent, dacites 11 percent, and rhyolites 2 percent.

Basaltic andesites (53%) and basalts (35%) dominate the Kam Formation lower unit having a normal distribution about 53% SiO_2; the upper unit consists of basalts (67%) and basaltic andesites (33%)

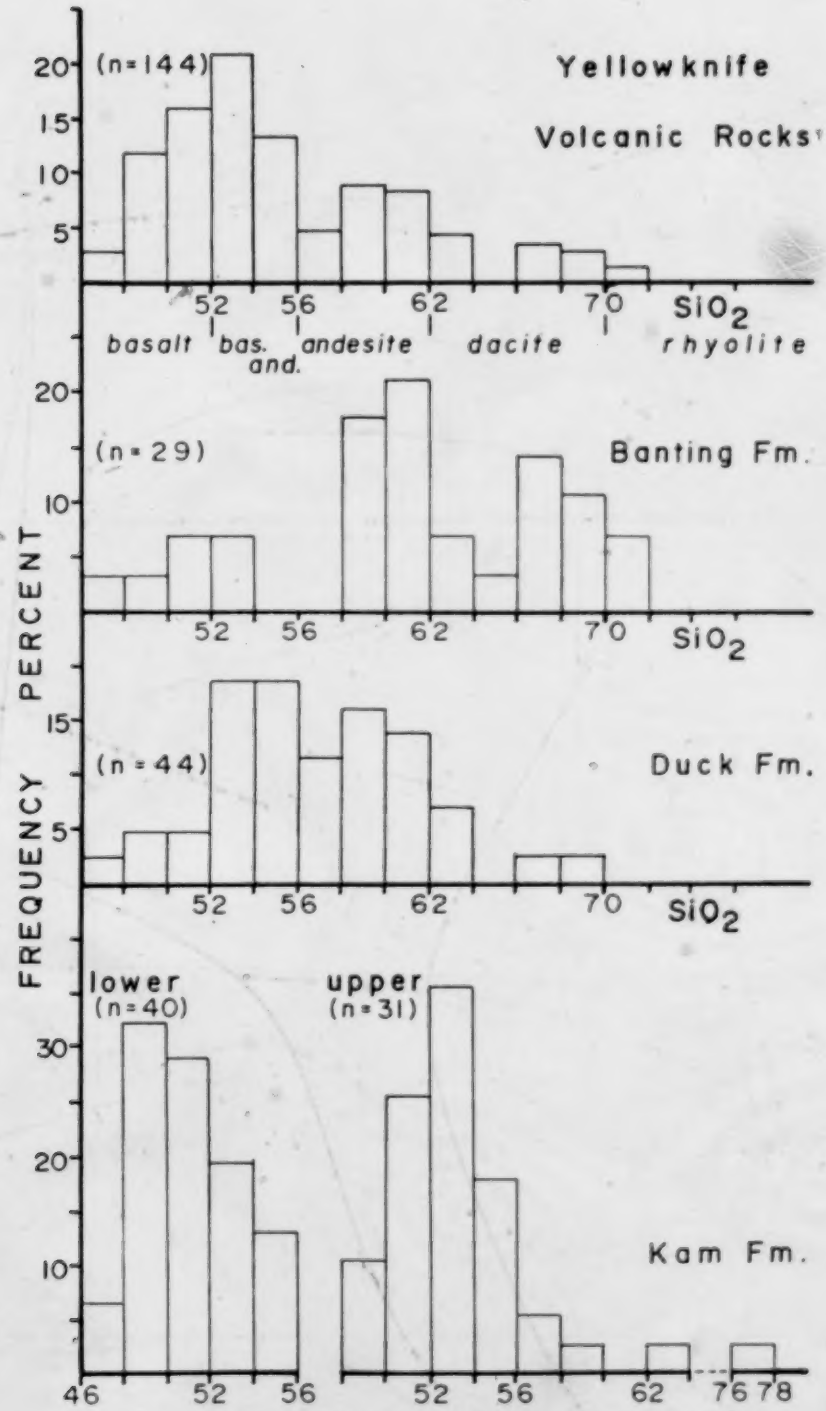

FIGURE 7 - FREQUENCY – SILICA DIAGRAM

clustered about 51% SiO_2. Duck Formation samples range in silica content from 46 to 70 percent and show near normal distribution around 56% SiO_2; the majority of samples are andesites (41%) or basaltic andesites (36%). A lack of samples between 54 and 58 percent silica yields a bimodal appearance to the Banting Formation. Andesites (38%), dacites (34%) and rhyolites (7%) are above the silica gap; basalts (21%) are below the gap. The six basaltic samples, all from the same traverse section, are consistently distinct from other Banting Formation rocks. Three of the six are from outcrops near the mouth of the Yellowknife River and are samples of a mafic intrusive phase (Easton and Jackson 1981) having major and minor element chemistry identical to that of Kam Formation basalts.

3.2.2 TOTAL ALKALIS-SILICA ($K_2O + Na_2O$ vs SiO_2)

Total alkalis vs silica diagrams show the Yellowknife volcanics to be sub-alkaline (Schwarzer and Rogers 1974) and tholeiitic (MacDonald and Katsura 1964) in character. Banting and Duck Formation samples (Figure 8, A and B) range in silica content from 50 to 70 percent, total alkalis range from 1 to 7 percent; three samples plot in the alkali basalt field. Banting samples have an extremely broad scatter with no pattern evident, however, the Duck samples show a weak positive correlation of total alkalis with silica in the sub-alkaline tholeiite field. Kam Formation samples (Figure 8, C) have a restricted range of silica content (46%-56%) and total alkalis vary from 1 to 6 percent. The upper Kam unit is tightly grouped in the

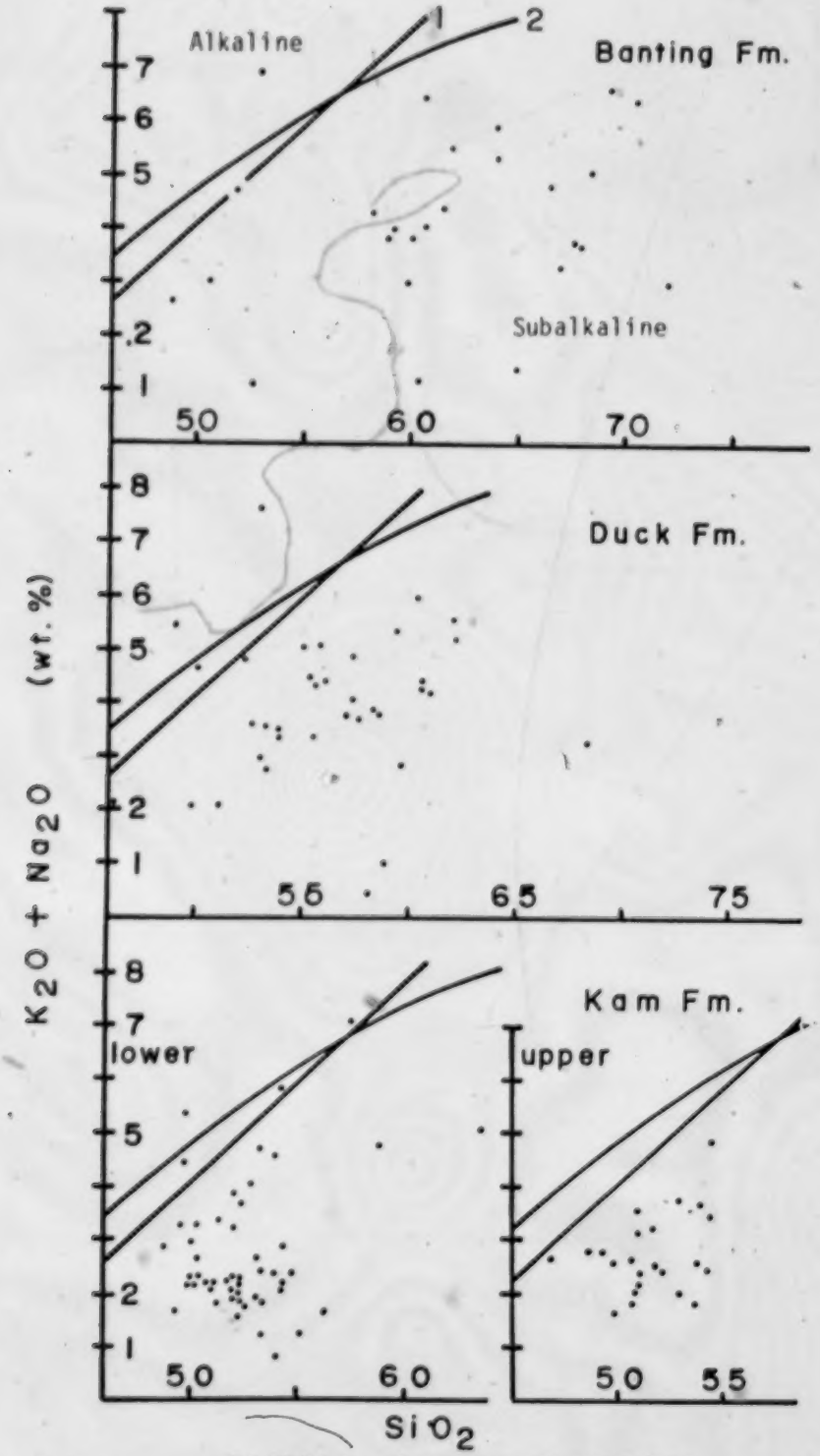

ALKALI–SILICA DIAGRAM

FIGURE 8 - Total Alkalis vs Silica
1 - MacDonald and Katsura (1964)
2 - Schwarzer and Rogers (1974)

tholeiitic basalt field, approximately 51% SiO_2 and 2.5% Na_2O+K_2O; the lower Kam is more diffuse, a few samples plot in the alkaline field.

3.2.3 TOTAL ALKALIS-ALKALI RATIO (K_2O+Na_2O vs $[K_2O/(K_2O+Na_2O)]100$)

Hughes (1973) defined an igneous spectrum binary plot of Na_2O+K_2O vs $[K_2O/(Na_2O+K_2O)]100$ to separate samples having undergone alkali metasomatism and spilitization from those having igneous alkali contents or a lesser degree of alkali mobility (Figure 9). Conclusions drawn from his work include: 1) igneous rocks having compositions which lie outside the igneous spectrum are metasomatic; 2) petrographic interpretations of rocks with spilitic or keratophyric mineralogy based solely on chemical compositions are dangerous; 3) rubidium-strontium isotope studies of spilites and keratophyres may yield diffuse isochrons and anomalous ages, as the system may not have been closed with respect to rubidium and strontium.

Boundaries for the igneous spectrum alkali diagram are somewhat subjective and arbitrary. A small change in boundary position can greaty affect the number of samples classified as metasomatic, e.g., if the current boundary of the spilitic field is increased or decreased +/-3% along X axis and +/-0.5% along Y axis the number of enclosed data points changes from 47 to 16; i.e., from 32 percent to 11 percent of the population. The spilite field as defined by Hughes (1973) encloses 35 samples, 24 percent of the total.

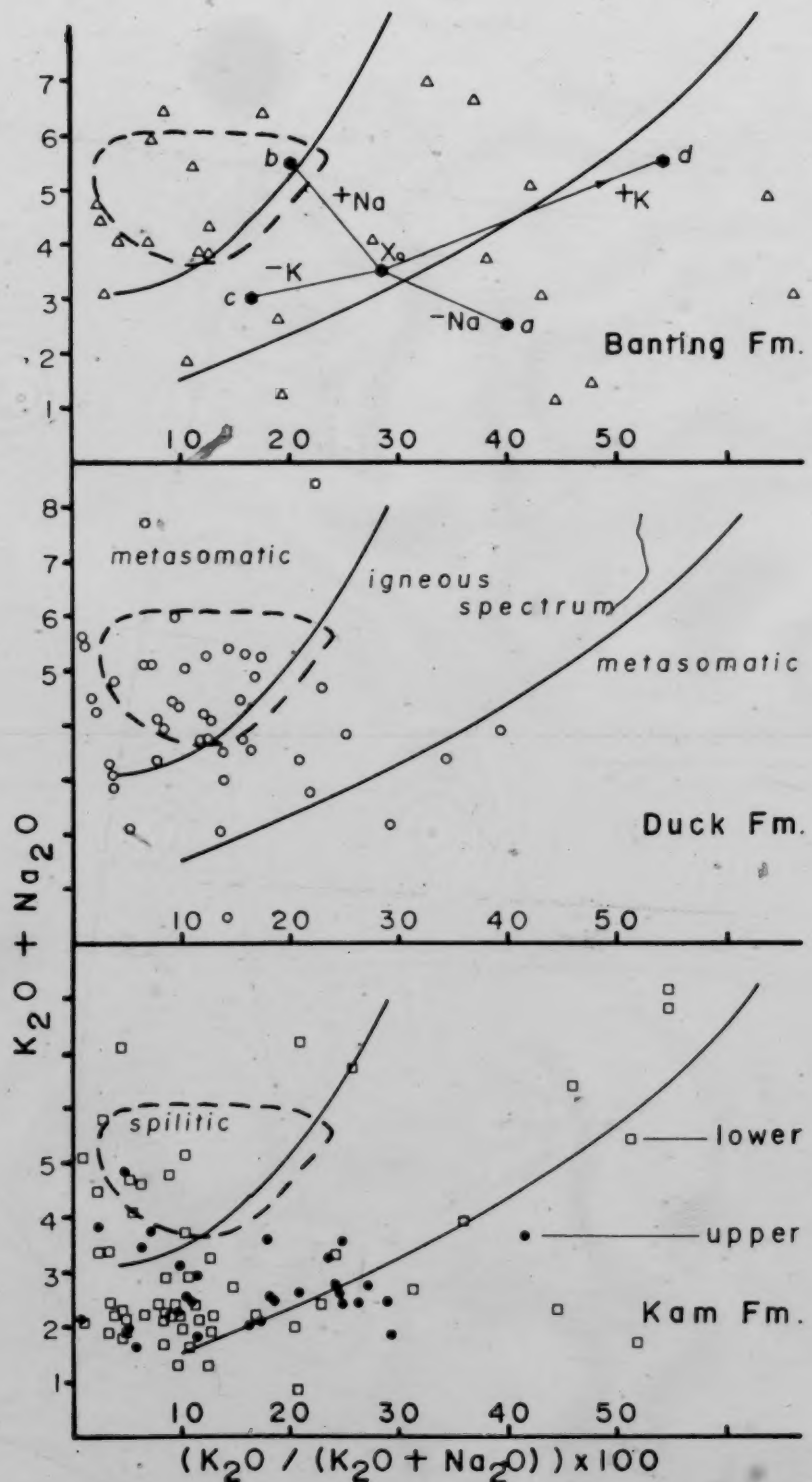

FIGURE 9 - Total Alkalies - Alkali Ratio

Table 2 summarizes the distribution of points by formation into the various fields on the diagram and Table 3 breaks down the distribution by rock type within each formation. General results include:

1) 52 percent of samples from the upper and lower Kam Formation plot within the spectrum, 30 percent of Duck Formation samples and 31 percent of Banting Formation analyses also plot inside the spectrum, i.e., have 'igneous' values;

2) only 8 percent of Kam Formation samples are spilitic, whereas 47 percent of Duck and 28 percent of Banting Formation rocks plot as spilites;

3) metasomatic values plot above (50 of 82, 61%) and below (39%) the igneous spectrum, signifying relative increase in sodium and potassium respectively;

4) andesites and dacites of the Duck and Banting Formations constitute 69 percent of the spilitic samples (24 of 35);

5) 58 percent of all basalts and basaltic andesites (51 of 87 samples) are within the igneous spectrum and are considered to represent original composition, 6 percent are spilitic and 36 percent (31 samples) are otherwise metasomatic;

6) less than 23 percent of all andesites and dacites plot within the spectrum (13 of 59), the remainder (77%) are metasomatic.

The field of spilites overlaps slightly into the igneous spectrum resulting in 8 analyses (23%) being spilitic and within the spectrum; 27 of 35 analyses (77%) are contained in the spilite field but outside the igneous spectrum. Of 59 andesite-dacite samples 44 percent are spilitic and 41 percent metasomatic.

TABLE 2: Summary of Yellowknife Volcanic Belt data plotted on Igneous Spectrum Diagram

FORMATION		IGNEOUS	(spilitic)	METASOMATIC (spilitic)	(below) +K	(above) +Na	(N)
BANTING	SAMPLES(N)	7	2	6	9	5	29
	PERCENT(%)	24.2	6.9	20.7	31.0	17.2	100
DUCK	(N)	11	6	15	5	7	44
	(%)	25.0	13.6	34.1	11.4	15.9	100
KAM (UPPER)	(N)	17	0	1	9	3	30
	(%)	56.7	0.0	3.3	17.0	10.0	100
KAM (LOWER)	(N)	21	0	5	9	8	43
	(%)	48.9	0.0	11.6	20.9	18.6	100
TOTAL	(N)	56	8	27	32	23	146
	(%)	38.4	5.5	18.5	21.9	15.7	100

IGNEOUS	(spilitic)	METASOMATIC
64/146	(35/146)	82/146
43.8%	(24%)	56.2%

IGNEOUS SPECTRUM after C. J. Hughes (1973)

TABLE 3: Igneous Spectrum - Subdivision of Yellowknife Data by Formation and Rock Type

	IGNEOUS SPECTRUM					
	In	In (Spilitic)	Out	(+K) Out (Metasomatic)	(+Na)	N
BANTING FM						
dacite	2	1	2	6	1	12
andesite	1	1	4	2	3	11
bas. and.	1	0	0	1	0	2
basalt	3	0	0	0	1	4
Total	7	2	6	9	5	29
DUCK FM						
dacite	1	0	1	0	2	4
andesite	4	2	13	3	4	26
bas. and.	3	4	1	1	0	9
basalt	3	0	0	1	1	5
Total	11	6	15	5	7	44
UPPER KAM FM						
dacite	0	0	0	0	0	0
andesite	0	0	0	0	0	0
bas. and.	3	0	1	1	1	6
basalt	14	0	0	8	2	24
Total	17	0	1	9	3	30
LOWER KAM FM						
dacite	1	0	0	0	0	1
andesite	0	0	2	1	2	5
bas. and.	8	0	1	3	2	14
basalt	12	0	2	5	4	23
Total	21	0	5	9	8	43

Note: In - data plots within the Igneous Spectrum
Out- data plots outside the Igneous Spectrum

Figure 9 and Table 2 clearly show alkali mobility in volcanic rocks of the Yellowknife greenstone belt, however, it is inconsistent in severity and type. Scatter on the Igneous Spectrum Diagram is in part a function of initial rock composition, as well as type and degree of metasomatism. Mobility relative to a hypothetical original composition (X)o is shown as a, b, c, d on Figure 9 with the values given in Table 4.

Table 4: Calculated Hypothetical Alkali Mobility for the Igneous Spectrum Diagram

	K_2O^*	Na_2O^*	x	y
(X)o	1.0	2.5	28.5	3.5
a	1.0	1.5	40.0	2.5
b	1.0	4.5	20.2	5.5
c	0.5	2.5	16.6	3.0
d	3.0	2.5	54.5	5.5

where:

* = data in weight percent

x = $[K_2O/(K_2O + Na_2O)]100$

y = $K_2O + Na_2O$ (percent)

(X)o = initial data (hypothetical)

Prior to application and interpretation of data sensitive to alkali mobility, the AFM diagram for example, use of Hughes' igneous spectrum screen will help to identify metasomatic samples and avoid

possibly confusing results. Further caution should be exercised for samples having greater than 3 percent volatile content; some Yellowknife volcanics have high loss on ignition (L.O.I.) values of 4.73-8.56 weight percent (Appendix A).

3.2.4 ALKALIS-IRON-MAGNESIUM ($[Na_2O+K_2O]$-FeO_T-MgO)

Analyses with limited alkali mobility as indicated on Hughes igneous spectrum diagram have been plotted on AFM diagrams ($[Na_2O+K_2O]$-FeO_T-MgO). Kam Formation iron enrichment from 45 to 70 percent is matched by magnesium decrease from 45 to 20 percent, at a relatively constant total alkali content of 10 percent*, resulting in a tholeiitic trend. Duck Formation data scatters across the TH-CA boundary curve; while there is no evidence for an iron enrichment trend, three samples are iron enriched relative to a calc-alkaline trend line from apex A (Na_2O+K_2O) to 62% FeO_T along the F-M join. A calc-alkaline trend is suggested by the Banting Formation samples (Figure 10).

Baragar (1966) outlined tholeiitic and calc-alkaline trends for Yellowknife volcanics on an AFM diagram. This earlier work did not screen out samples with alkali metasomatism, resulting in somewhat enlarged calc-alkaline trend lines, nor did it recognize and treat 'Segment F' as a distinct geologic formation, now referred to as the Banting Formation.

* Diagram percent, not weight percent.

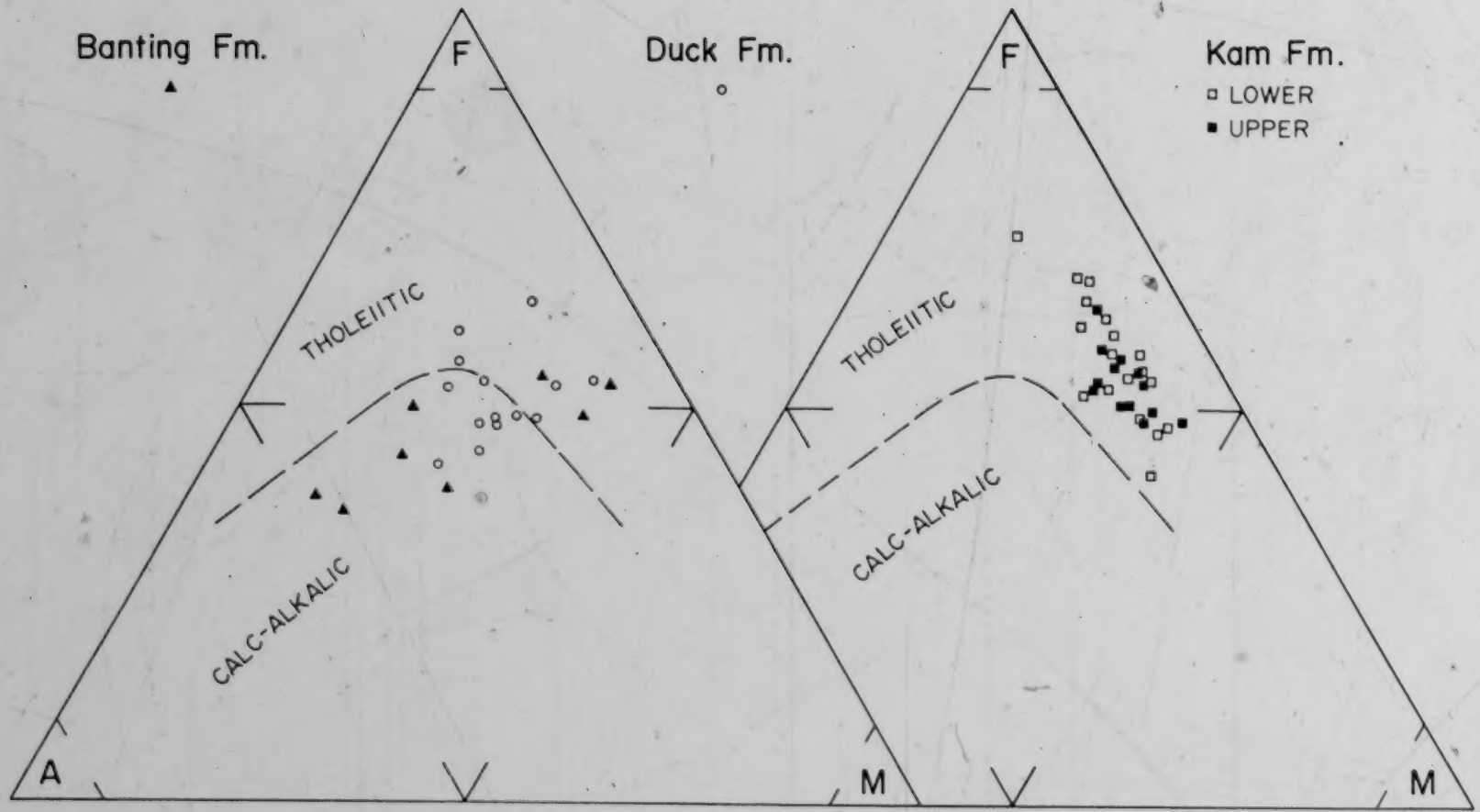

FIGURE 10 - A-F-M Diagram

Recent work by Jolly (1977, 1980), Jahn et al (1980) and Condie (1981) illustrate the variability of magmatic trends throughout greenstone stratigraphy. Jolly (1980) cites four fractionated lava suites in the Abitibi area, grading up section from magnesium through magnesium-tholeiite and tholeiite to calc-alkaline. Tholeiitic and calc-alkaline trends for Yellowknife volcanics are not unique, and may in fact be quite poorly developed when compared with other Archean greenstone belts.

3.2.5 MAGNESIUM-IRON-ALUMINUM (MgO-FeO_T-Al_2O_3)

A major element tectonic discriminant diagram has been developed by Pearce, Gorman and Birkett (1977) using magnesium, iron and aluminum. It was designed for Cenozoic volcanic rocks with silica contents of 51 to 56 percent and total iron expressed as FeO_T, thereby limiting use to basaltic andesites and some basalts.

Yellowknife rocks meeting the silica requirement are predominantly from the Kam Formation. Samples are enclosed by fields outlining 50, 70 and 90 percent of the population which is centred in the 'oceanic island' field close to the triple junction with 'continental' and 'ocean ridge and floor' (Figure 11). A plot of average values shows the Kam Formation in the ocean island field near the border with the continental field; Duck and Banting Formations mean values are just within the orogenic field, bordering the continental field.

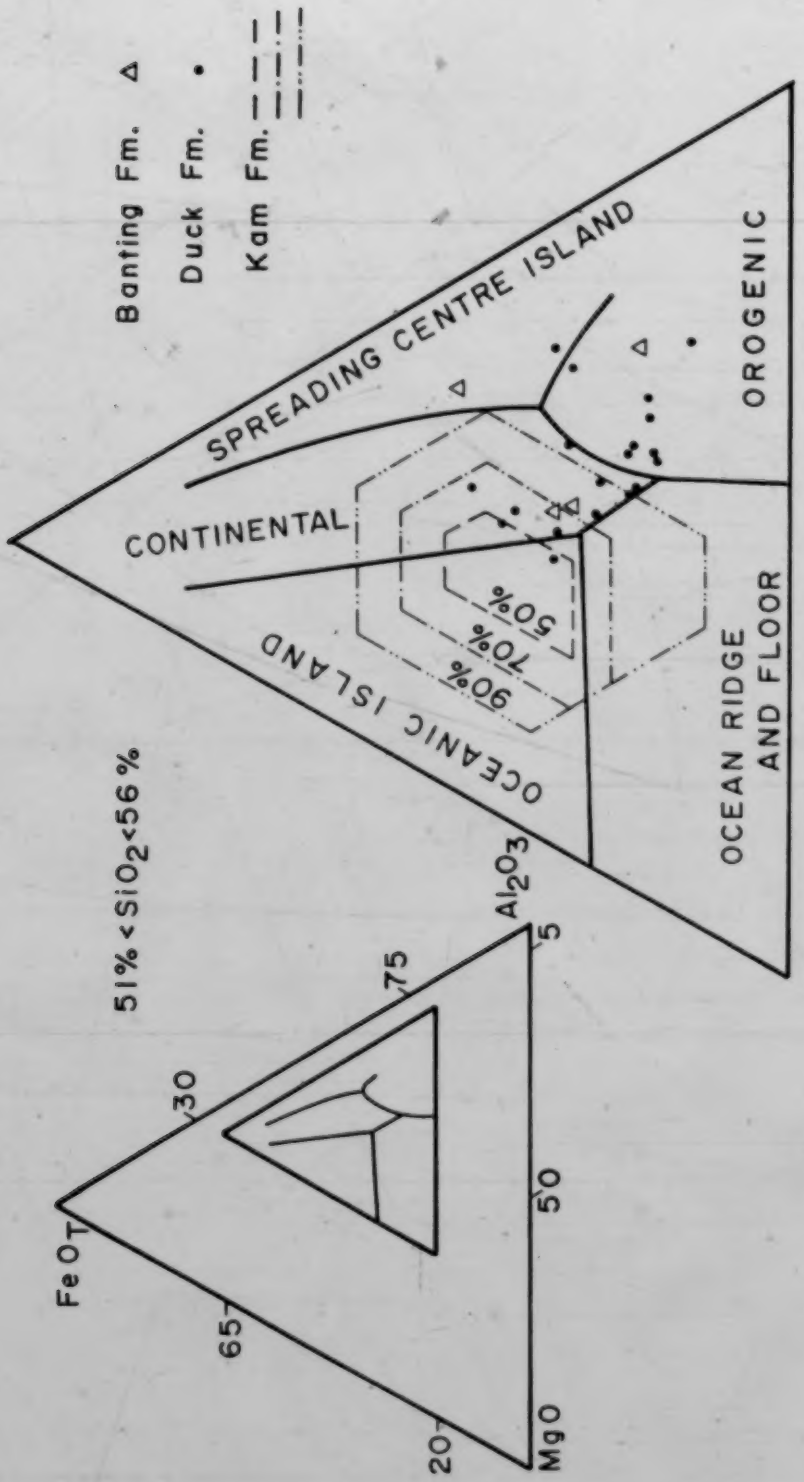

FIGURE 11 - MgO - FeO_T - Al_2O_3

The MgO-FeO_T-Al_2O_3 diagram has been subdivided by Pearce, Gorman and Birkett into: a) oceanic and continental within plate volcanics (Oceanic Island and Continental fields) represented by Hawaii and the African Rift; b) Spreading Centre Island or interplate volcanics, Iceland or Galapagos for example; and c) convergent and divergent plate margins, i.e., the Orogenic and the Ocean Ridge and Floor fields.

Thirty-six (36) of fifty-three (53) lower Kam Formation samples have 51-56 percent silica, with the following tectonic field distribution: ocean island (n=15), continental (n=13), ocean ridge and floor (n=7), and spreading centre island (n=2). The upper Kam Formation, 20 of 31 samples with 51-56 percent silica, is more restricted in its distribution: oceanic island (n=15), continental (n=1), ocean ridge and floor (n=3) and orogenic (n=1).

The Duck Formation (n=44) has 19 samples with 51-56 percent silica; they scatter across the continental (n=9) and orogenic (n=8) fields, with few in the spreading centre island (n=1) and the ocean island (n=1). Only 4 of 29 Banting Formation rocks meet the silica requirement; two plot in the continental field, one each in the orogenic and the spreading centre island fields. The Banting Formation mean value is on the continental-orogenic fields boundary curve close to the triple junction with the spreading centre island field. Two samples from the Yellowknife River traverse plot in the continental field near the oceanic island-ocean ridge and floor junction next to the 70 percent enclosure of Kam Formation samples.

The Kam Formation may be analogous with Cenozoic to more recent Within Oceanic Plate island volcanism. A continental-orogenic field trend by the Duck Formation samples may indicate a change in magma mode of formation, however, not a change in the tectonic setting. Unknown variables hindering the application of this diagram to Archean rocks include the existence and properties of Archean Plates, geothermal gradients affecting pressure temperature conditions of magma generation and rates of activity, and composition of the Archean mantle and mechanisms of eruption.

3.2.6 ALUMINUM-IRON+TITANIUM-MAGNESIUM (Al_2O_3-[FeO+Fe_2O_3+TiO_2]-MgO)

Jensen's cation diagram (Jensen 1976) was developed from data on the Archean greenstones of the Abitibi belt; komatiitic, Mg-tholeiitic, tholeiitic and calc-alkaline trends can all be plotted. It has been used to check for komatiitic affinity in the Yellowknife volcanic suite (Figure 12), the initial requirements being TiO_2 less than 1 percent and MgO greater than 9 percent. One sample from the Banting and five from the Kam Formation met these criteria. The sole Banting Formation sample is considered a mafic intrusive phase, chemically equivalent to many Kam Formation basalts.

These six plot in a small area (Figure 13) of the high magnesium tholeiitic basalt field, adjacent to the basaltic komatiitic line defined by MgO/Al_2O_3 equals 1.0 (cation proportions) or 1.275 (weight percent ratio). A Penrose Conference Report (Arndt and

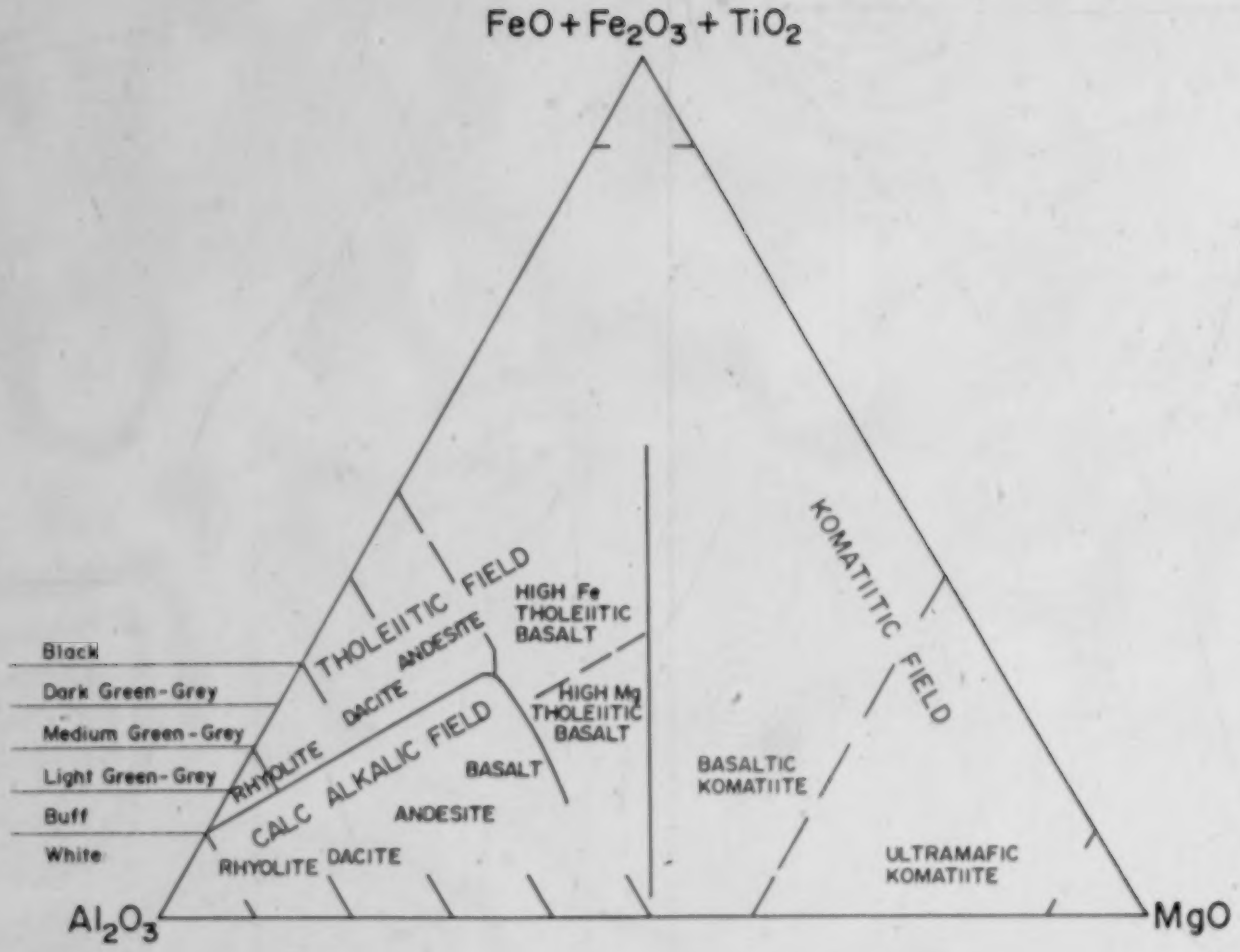

FIGURE 12 - Jensen's Cation Diagram

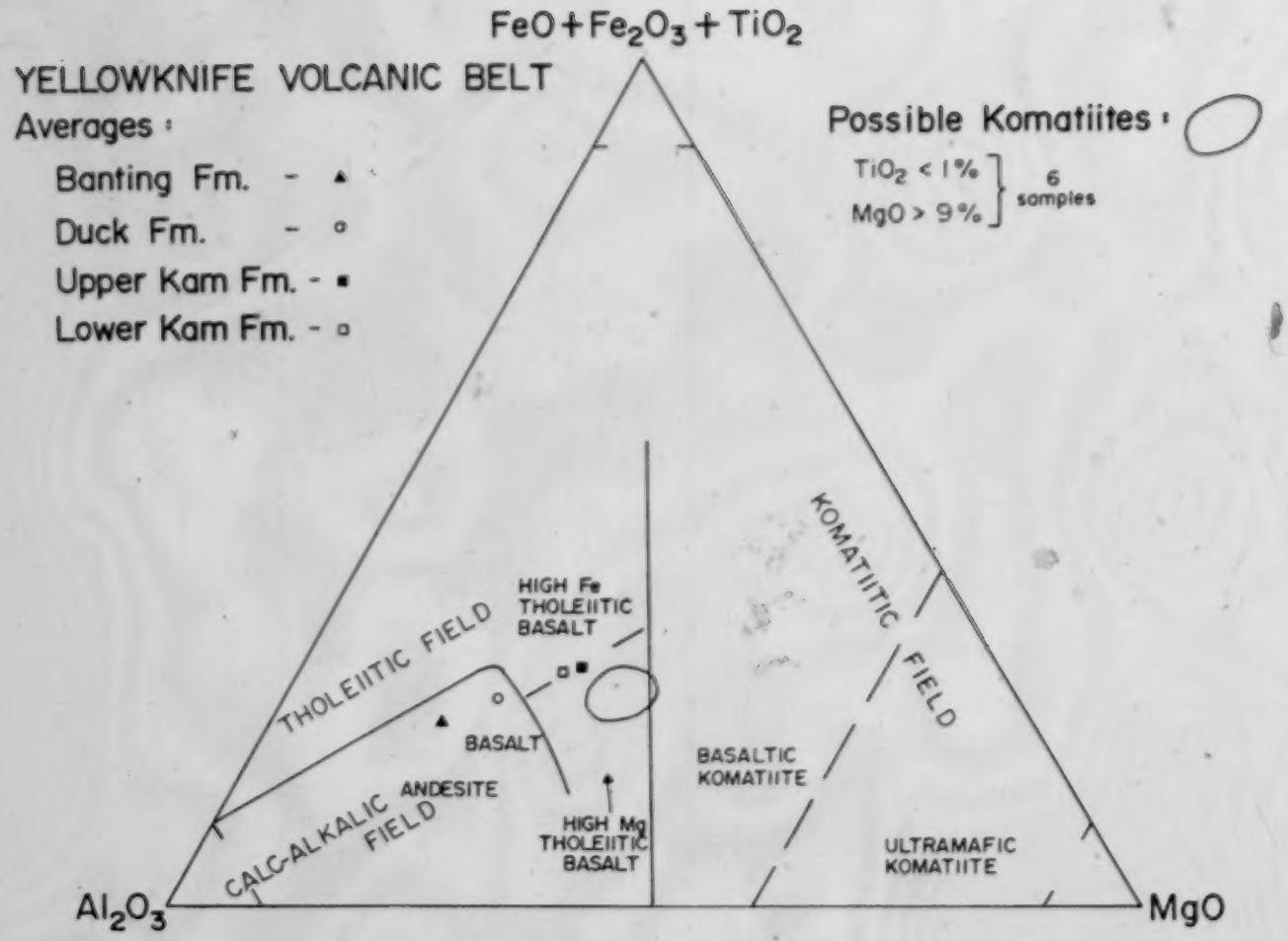

FIGURE 13 - Yellowknife Data on Figure 12

Brooks 1980) suggests reserving the term komatiite for volcanic rocks with MgO greater than or equal to 18 percent. The selected Yellowknife volcanic rocks could not be classed as komatiites under this scheme (maximum MgO 9.73%), however alternative classification methods discussed at the same conference suggest usage of the terms komatiitic basalt and magnesium basalt for rocks of decreasing komatiitic character.

Average values for the upper and lower units of the Kam Formation plot along the high iron - high magnesium tholeiitic basalt line; the magnesium rich to iron rich range of basalt composition indicates a tholeiitic trend. Duck and Banting Formation averages plot as calc-alkaline basalt and andesite respectively.

3.2.7 SUMMARY

Major element geochemistry indicates the Yellowknife volcanic belt to consist of sub-alkaline rocks having a mafic tholeiitic trend and an intermediate to felsic calc-alkaline trend. Silica content has frequency peaks at 53, 59 and 67 percent, each progressively diminishing in height. Approximately 32 percent of basalts (19 of 59) contain greater than 2.5 percent Na_2O, an amount used by Gunn (1976) to suggest that 40 percent of Archean lavas may have been partially spilitized. From the Hughes' Igneous Spectrum diagram for the Yellowknife rocks, it is concluded that 43 percent of basalts are 'metasomatic' but only 5 percent are 'spilitic'. Interpretation of the MgO-FeO_T-Al_2O_3 tectonic descriminant diagram is severely limited

by the scatter of Duck Formation data, very few data points for the Banting Formation, and the problems of applying the results of Cenozoic tectonics to Archean data. High magnesium - low titanium samples, selected as possible komatiitic rocks, have been defined as high magnesium tholeiitic basalts using major element (Al, Fe, Ti, Mg) content. Jensen's cation diagram indicates a transition from average tholeiitic basalts to calc-alkaline basalts and andesites, up section, corresponding the Kam, Duck and Banting Formations respectively.

3.3 MINOR ELEMENT GEOCHEMISTRY

Trace element data for the Yellowknife volcanic rocks helps to describe and characterize the formations utilizing comparative diagrams: major vs minor element, major vs minor element ratio, minor element ratio vs minor element ratio, minor element vs minor element.

3.3.1 SILICA-ZIRCONIUM/TITANIUM (SiO_2 vs Zr/TiO_2)

Winchester and Floyd (1977) defined 10 compositional divisions on a plot of SiO_2 vs Zr/TiO_2 (Figure 14). Silica is used as an historically recognized measure for rock classification and relative immobility, at least comparable to aluminum (Davies, Grant and Whitehead 1979). Zirconium and titanium are considered quite stable (Humphries and Thompson 1978), with stable correlations between them (Cann 1970; Winchester and Floyd 1976; Coish 1977). The ratio Zr/TiO_2 has shown good coherence with SiO_2. Division between rocks of alkaline and sub-alkaline character is a line of decreasing positive

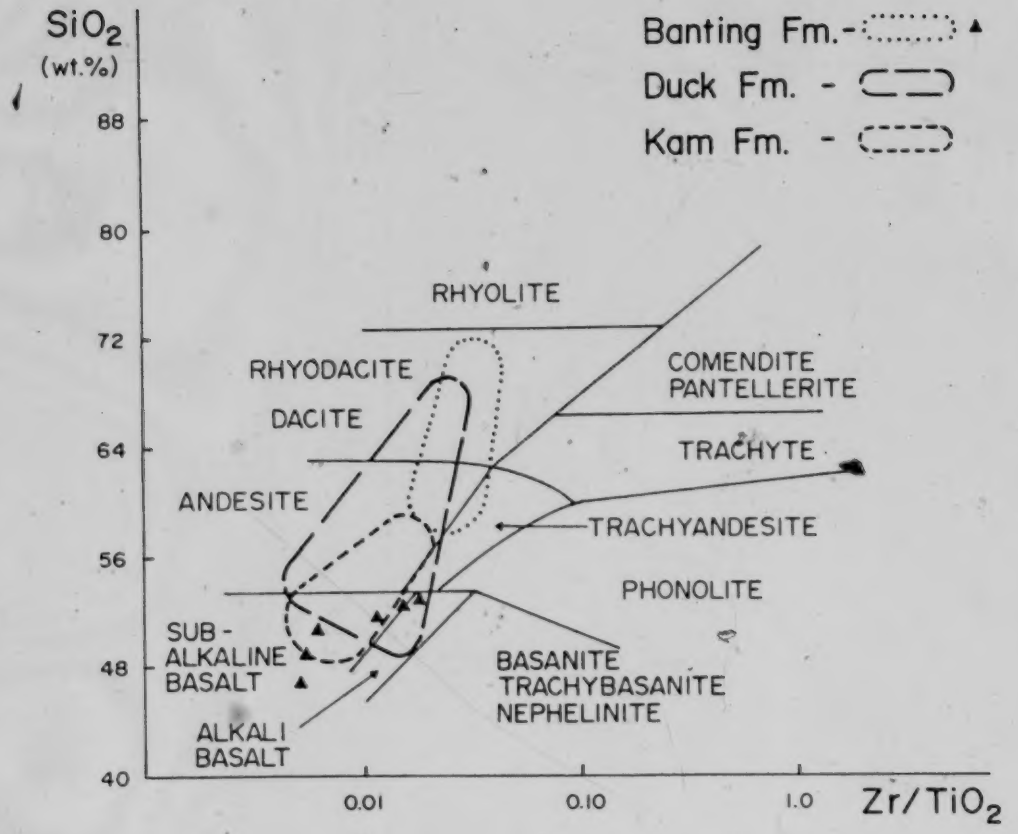

FIGURE 14 - SiO_2 - Zr/TiO_2

slope, Zr/TiO_2 increasing with SiO_2; alkaline rocks plot on the high Zr/TiO_2 side.

Kam Formation volcanic rocks, upper and lower units, plot in the sub-alkaline field straddling the basalt-andesite boundary. Enclosed by an elliptical field increasing in Zr/TiO_2 (0.005 to 0.01) and silica (48% to 56%) are 77 of 83 samples (93%). Four samples are more siliceous, andesite to rhyodacite, and two show an alkaline affinity.

Duck Formation analyses scatter widely, in the sub-alkaline field, as intermediate volcanics; 42 of 44 samples (95%) are sub-alkaline and two (5%) are alkali basalts. Thirty samples (68%) are dacites.

Banting Formation rock samples show a composition gap from 54 to 58 percent SiO_2. Below the gap, four basaltic samples are from the same Yellowknife River mouth traverse while the other two show slight alkaline affinity. Three analyses, low SiO_2 and low Zr/TiO_2, are considered mafic intrusive phases. Above the gap there is a slight Zr/TiO_2 increase (0.02 to 0.035) with increasing silica as rocks vary from andesite to rhyodacite; two plot as trachyandesites.

This differentiation - alkalinity plot indicates a sub-alkaline basalt-andesite-dacite sequence. Slight overlap in the alkaline field is due to geochemical continuum, inconsistencies and problems related to definition in terms.

3.3.2 IRON-ZIRCONIUM/TITANIUM (FeO_T vs Zr/TiO_2)

Using a measure of tholeiitic magmatism, iron enrichment expressed as FeO_T, plotted against Zr/TiO_2, a measure of fractionation shown to increase markedly with silica content, Scarfe and Goff (pers. comm. 1981) have devised a method to recognize tholeiitic and calc-alkaline trends (Figure 15).

Kam Formation analyses (n=64) plot 78 percent (n=50) as ocean floor basalts on this diagram, 14 percent (n=9) within the high FeO_T tholeiites field (FeO_T greater than 13.5%), 5 percent (n=3) within the high Zr/TiO_2 tholeiites field (Zr/TiO_2 greater than .015), and 3 percent (n=2) within the field of calc-alkaline basalts. These calc-alkaline 'basalts' are actually rhyodacitic to rhyolitic in composition.

Thirty four analyses of the Duck Formation indicate 15 samples (44%) to be ocean floor basalts; 8 (24%) plot in the tholeiite and low-K tholeiite field, and 11 (32%) lie within the CAB field. Data appears scattered on the FeO_T vs Zr/TiO_2 diagram, however 80 percent of samples are within a narrow envelope. Its trend line has a positive slope, or tholeiitic character, with increasing fractionation, i.e., increasing Zr/TiO_2. Peak iron content corresponds closely with the Zr/TiO_2=0.0064 discrimination line, above which the trend shows a negative slope, calc-alkaline character. As fractionation continues the envelope moves from the tholeiitic to the calc-alkaline field.

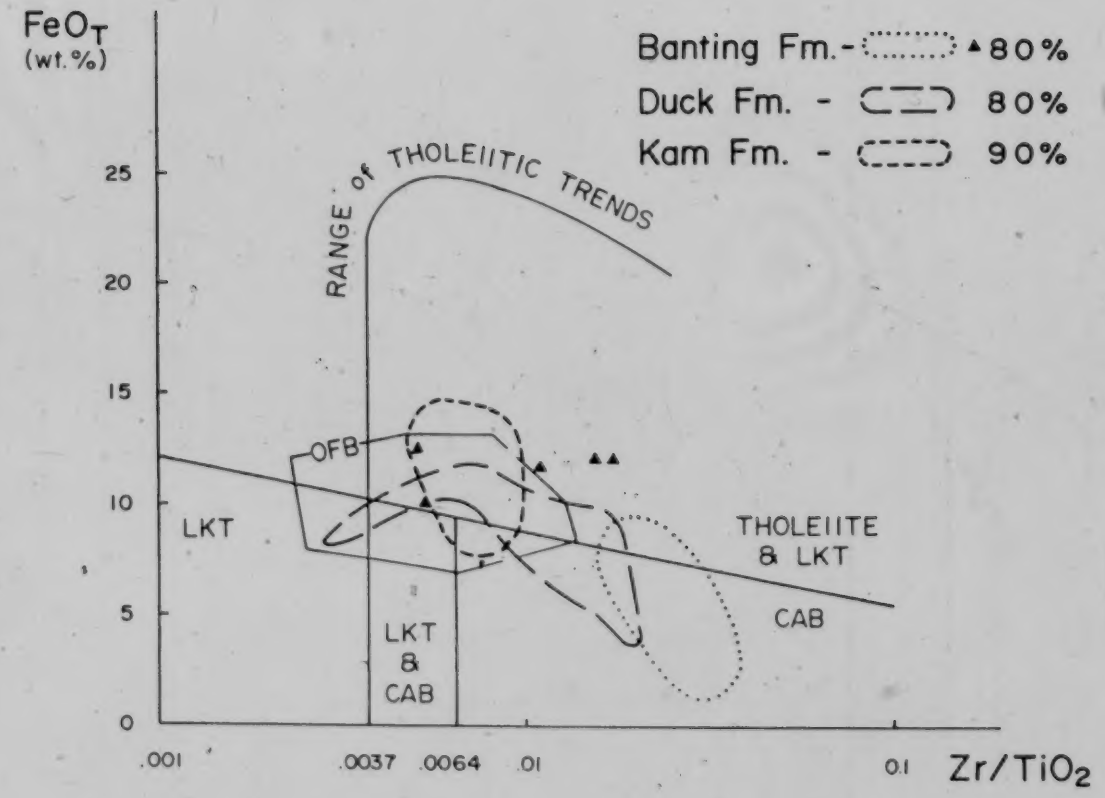

FIGURE 15 - FeO_T - Zr/TiO_2

Banting Formation samples (n=23) plot along a calc-alkaline trend, negative slope, with a few samples plotting in the tholeiitic field. This zone includes 17 of 23 analyses (74%), the remaining 6 plot in two groups within the tholeiitic field. Three have low Zr/TiO_2 (0.005), plot along the Kam Formation field line and are considered mafic phases intrusive into the Banting Formation. Interpolation suggests a general Banting Formation trend similar to the Duck Formation.

FeO_T vs Zr/TiO_2 indicates ocean floor basaltic magmatism, followed by a sequence of mixed tholeiite and calc-alkaline lavas, and finally definite calc-alkaline volcanism with minor tholeiitic basalts.

3.3.3 ZIRCONIUM/TITANIUM-NIOBIUM/YTTRIUM (Zr/TiO_2 vs Nb/Y)

Differentiation indicies, based upon ratios of immobile elements, result in a diagram analogous to the silica-total alkalis plot (Figure 8) but with greater definition of the mafic to felsic volcanic fields (Figure 16).

Volcanic rocks have been divided into ten classes using ratios of immobile elements in the Zr/TiO_2 vs Nb/Y diagram of Winchester and Floyd (1977). The Zr/TiO_2 ratio increases coherently with silica while Nb/Y remains constant or increases only slightly for subalkaline rock suites. The alkaline - subalkaline boundary has been placed at Nb/Y = 0.67, however data suggests a zone of tholeiite

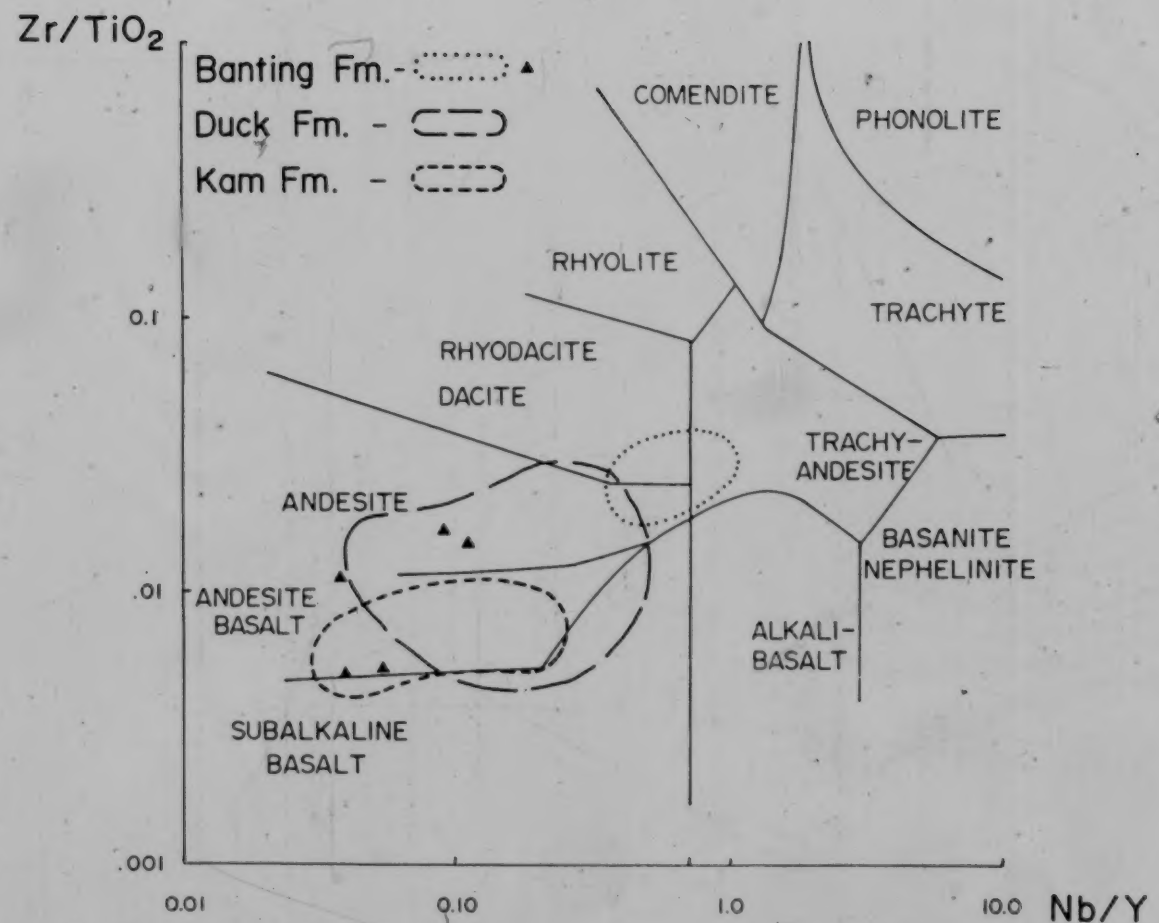

FIGURE 16 - Zr/TiO_2 - Nb/Y

overlap into the alkaline volcanic field up to Nb/Y = 1.2 (Floyd and Winchester 1975). Compositions with Nb/Y greater than 1 are nepheline normative. This overlap may be due to yttrium mobility related to the solubility of Ca-silicates during hydrothermal alteration; Ti, Zr and Nb will be less affected.

Kam Formation samples lie on the subalkaline side of the line with 55 of 61 (90%) situated in the andesite-basalt field; there are four subalkaline basalts, three andesites and one dacite. Twenty-three samples were reported as containing zero parts per million niobium, by X.R.F. analysis.

Duck Formation results scatter across the subalkaline field: subalkaline basalt (7), andesite-basalt (14); andesite (20) and dacite (2). The Nb/Y ratio shows an order of magnitude range (0.04 to 0.4), as does the Zr/TiO_2 ratio (0.003 to 0.03). Three traverse groups were made: 727 is the Horseshoe Island traverse; 720, 721, 722 is the Akaitcho Fault traverse; and 726 is more along strike than across strike from Duck Lake to Akaitcho Bay. Horseshoe Island data, west of the Akaitcho Fault, shows a consistent Zr/TiO_2 ratio of approximately 0.01 (0.009 to 0.016) over the whole range of Nb/Y (0.04 to 0.4). The down limb traverse, 726 series samples, similarly shows a narrow Zr/TiO_2 range (0.0I5 to 0.02), over a moderate Nb/Y range (0.12 to 0.4) within the field of subalkaline andesites. Samples taken north-west-southwest parallel to, but away from, the Akaitcho Fault yield the greatest range in Zr/TiO_2 (0.003 to 0.026).

Banting Formation analyses group about the andesite-dacite-trachyandesite junction. Six samples suggest alkaline character, Nb/Y greater than 0.67, but lie within the demonstrated field of tholeiite-alkaline overlap up to 1.1 (Pearce and Cann 1973) or 1.2 (Floyd and Winchester 1975). One sample from the Yellowknife River mouth traverse plots on the andesite-basalt line, two analyses of mafic intrusive phases lie on the subalkaline basalt line in the Kam Formation field; two samples, located east of Walsh Lake, lie in the andesite zone.

3.3.4 ZIRCONIUM-TITANIUM-YTTRIUM (Zr-Ti/100-Yx3)

A tectonic discriminant diagram by Pearce and Cann (1973) was developed using data from Cenozoic basaltic rocks meeting one criteria: CaO+MgO greater than 12 percent and less than 20 percent. The diagram has been split into Within Plate Basalts (WPB) and Volcanic Arc Basalts (VAB), the latter being further sub-divided into Low Potassium Tholeiites (LKT), Ocean Floor Basalts (OFB), and Calc-Alkaline Basalts (CAB) (Figure 17).

Seventy-seven (77) of eighty-three (83) Kam Formation samples meet the CaO+MgO requirement; seventy lie within the Ocean Floor Basalts field, four in the Calc-Alkaline Basalts field, one in the Low Potassium Tholeiite field, and two plot as Within Plate Basalts.

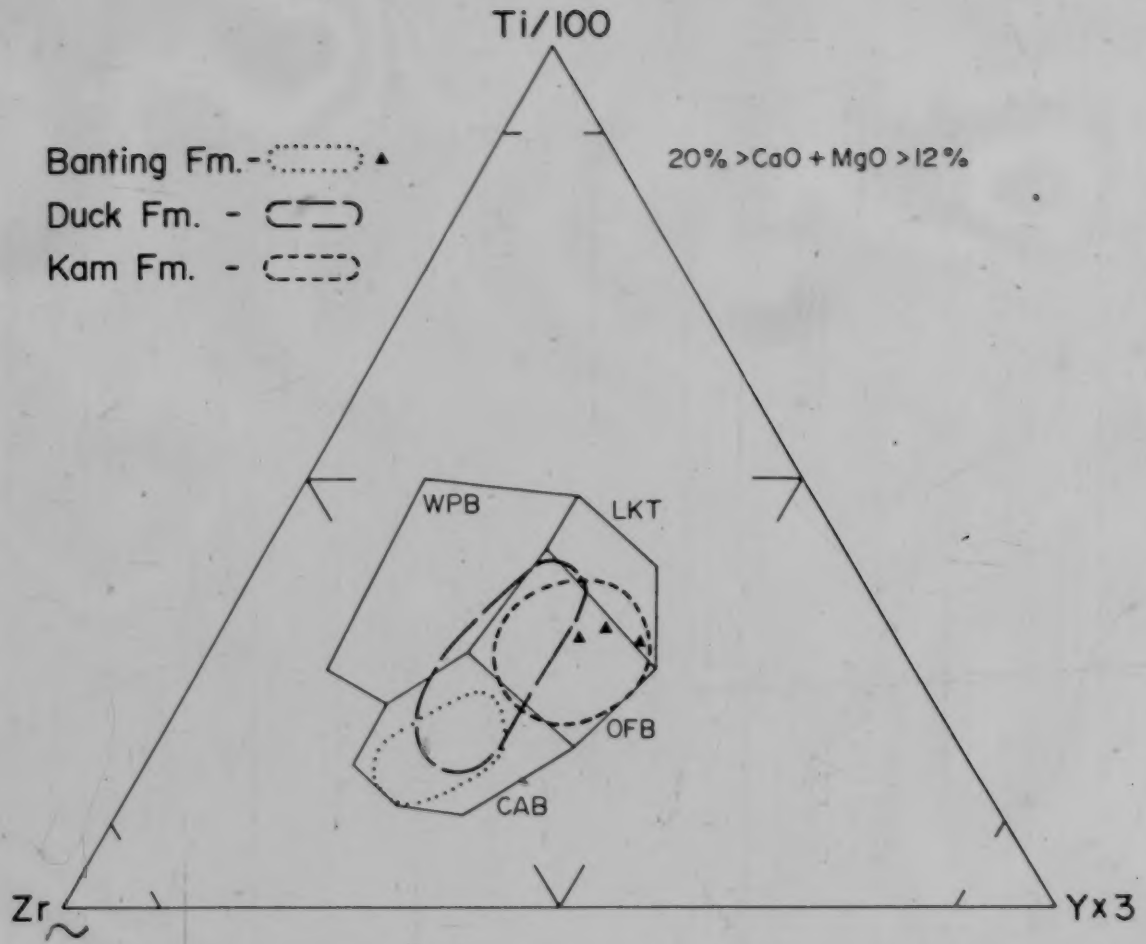

FIGURE 17 - Zr - Ti/100 - Yx3

Of forty-four (44) Duck Formation analyses, twenty-three (23), 52 percent, meet the requirement. Samples show a wide range in the proportions of zirconium and titanium, but relatively consistent yttrium values. The 90 percent envelope overlaps both Ocean Floor and Calc-Alkaline Basalt fields, in addition to overlapping the Kam and Banting Formation zones.

Only ten (10) of twenty-nine (29) Banting Formation analyses met the CaO+MgO criteria with the three (3) mafic intrusive phase samples, from the Yellowknife River mouth traverse, plotting in the OFB field. The remaining seven plot within the CAB field; more differentiated samples plot toward the zirconium apex.

The Yellowknife volcanic suite plots as a Plate Margin or Volcanic Arc Basalt (VAB) sequence with characteristics of both diverging (OFB) and converging (CAB) margins. Very few samples lie in the Within Plate Basalt (WPB) field encompassing both oceanic islands (Hawaii, Iceland, Galapagos, Tristan da Cunha, Gough) and continental basalts (African Rift Valley, Deccan, Karoo, Afar). This is in contrast with Figure 11, MgO-FeO_T-Al_2O_3 (Pearce, Gorman and Birkett 1977), wherein a significant number plot as oceanic island and continental WPB. The fact that major and minor element diagrams do not agree should emphasize the problems of Archean tectonics.

As a first attempt to resolve the problem, an assumption is made that either Figure 11 or Figure 17 is correct, and therefore either iron or yttrium may be too high for the plot to be applied to

Yellowknife volcanics. On Figure 15 (FeO_T vs Zr/TiO_2) titanium, zirconium (also in Figure 17) and iron (also in Figure 11) show the Yellowknife samples to be largely ocean floor basalts (OFB), in support of Figure 17 (Zr - Ti/100 - Yx3).

Archean tholeiites differ from modern volcanic rocks by their high FeO_T, high FeO/Fe_2O_3 and low Al_2O_3; their FeO_T/MgO ratio is greater than Modern Ocean Floor Basalts (MORB) but less than modern arc tholeiites. From these considerations it is concluded that Figure 11 (MgO - FeO_T 0 Al_2O_3) is not applicable to Yellowknife volcanic rocks, and may be inappropriate for all Archean basalts. Trace element plot Figure 17 assists in differentiating Kam vs Banting Formation rock suites and clearly shows the broad overlapping character of Duck Formation volcanics.

3.3.5 ZIRCONIUM-TITANIUM-STRONTIUM (Zr-Ti/100-Sr/2)

A diagram similar to Zr-Ti/100-Yx3 utilizes strontium (Sr/2), rather than yttrium, to assist classification of Plate Margin volcanic rocks (Pearce and Cann 1973). Kam Formation data (Figure 18) indicates a relatively constant Zr-Ti/100 relationship over a wide range in strontium; overwhelmingly OFB (rise tholeiites) and a few LKT. The Duck Formation indicates a relatively constant Ti/100-Sr/2 relationship over a wide range of zirconium content, including Zr rich samples; primarily OFB or rise tholeiites of high Zr. Banting Formation samples (10) are low Ti; compositionally they range from low potassium tholeiite (high Sr/2), through calc-alkaline, to high Zr

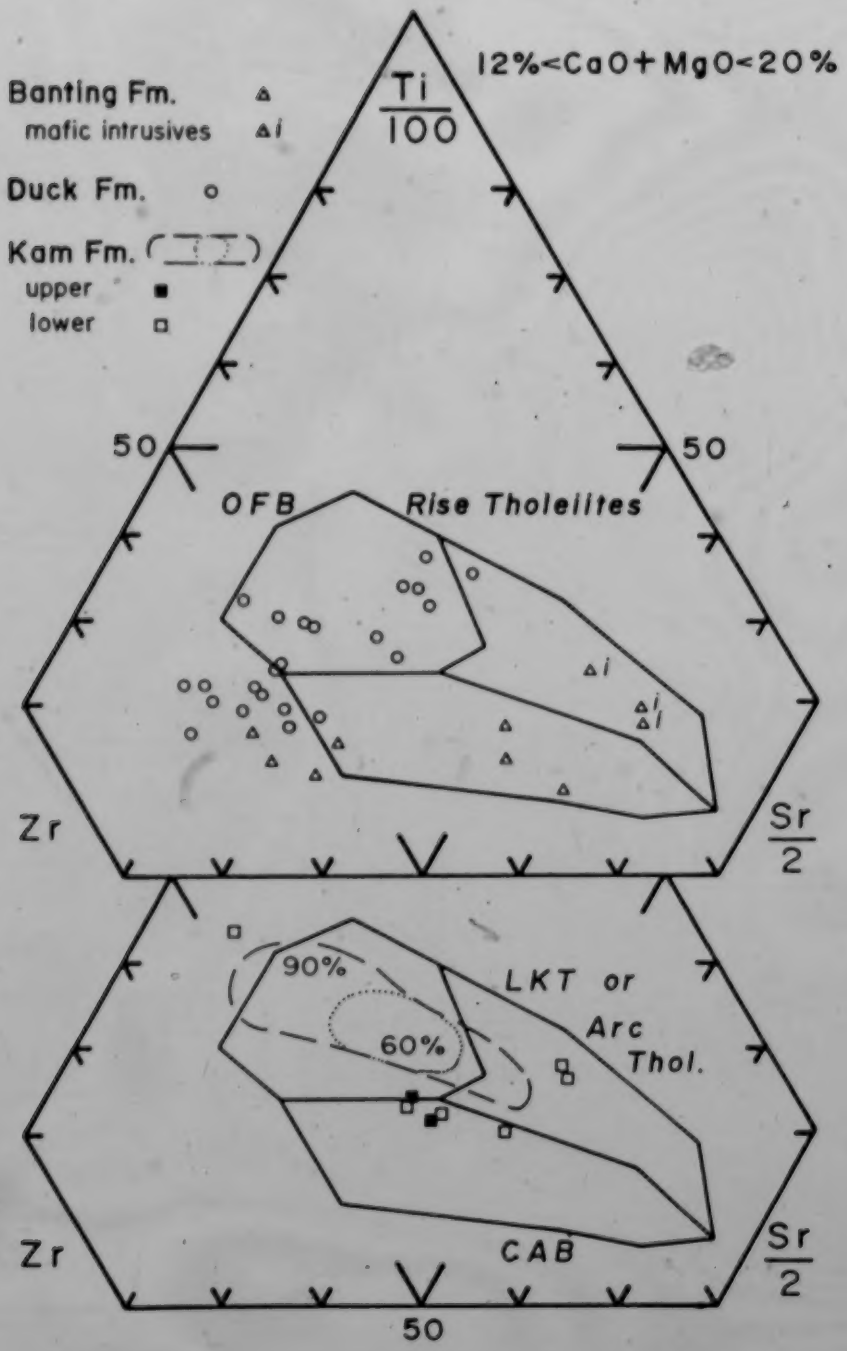

FIGURE 18 - Zr - Ti/100 - Sr/2

basalts. The three LKT or Arc Tholeiites are mafic intrusive samples from the Yellowknife River traverse.

Pearce and Cann (1973) suggests using Ti vs Zr as a check to the Zr-Ti/100-Sr/2 diagram for altered samples with similar results: Kam Formation ocean floor basalts; Ti and Zr rich Duck Formation plotting as OFB and CAB with many situated outside the defined fields; Banting samples plot as LKT-OFB, CAB and Zr rich CAB. The high Ti and Zr contents are consistent with oceanic island basalts, as noted by Floyd and Winchester (1975).

Condie (1981) plots average tholeiites from Archean greenstone belts; his Yellowknife value shows greater Ti and less Zr than the majority of Kam Formation samples from this study.

3.3.6 CALCIUM-YTTRIUM (CaO vs Y)

Lambert and Holland (1974) have used CaO (wt%) vs Y (ppm) to define J and L type trends for yttrium enriched and deficient rocks, relative to a calc-alkaline series standard. The J and L trends correspond to hornblendic and pyroxenic controlled differentiation trends, respectively. Rock samples from the Yellowknife greenstone belt have been classified as basalt, basaltic andesite, andesite and dacite for each of three formations: Kam, Duck and Banting. These values have been plotted, from Tables 6 and 7, on Figure 19.

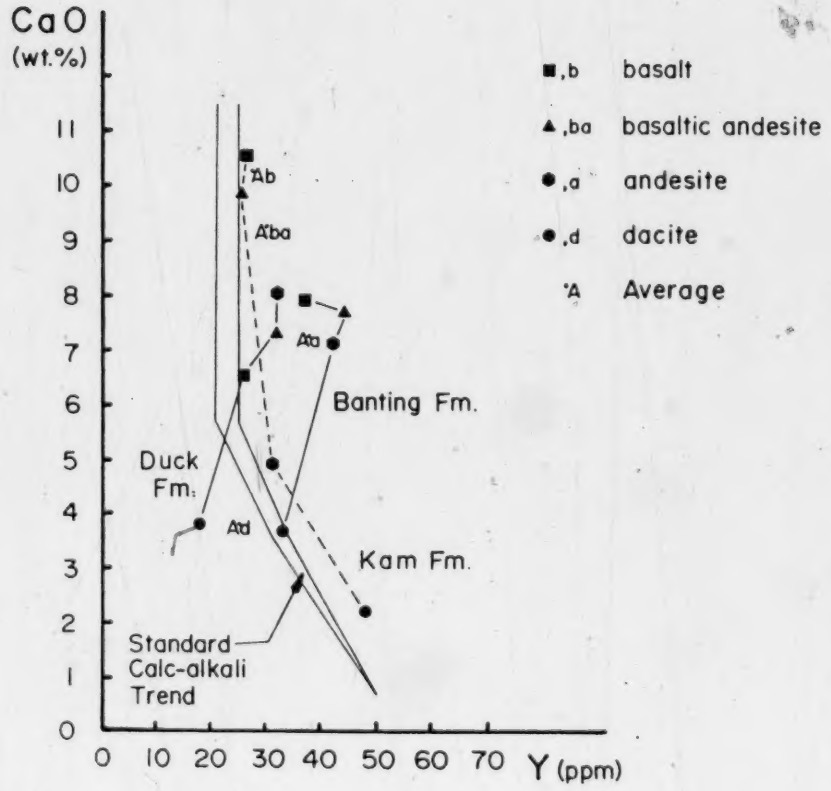

FIGURE 19 - CaO - Y

Yellowknife rocks are slightly yttrium enriched, 25-50 ppm relative to the standard calc-alkali trend developed from more recent volcanism. The Kam Formation trend is poorly defined due to a lack of andesitic and dacitic material. The Duck and Banting Formations define similar J-type trends, belonging to the proposed hornblendic differentiation series.

A weighted average plot using all data yields a definite J-type hornblendic differentiation trend. The pattern suggests hornblende-plagioclase fractionation in an intracontinental, and/or above a subduction, zone at time of formation. This discussion assumes common magma source material and petrogenetic history.

3.3.7 VANADIUM-NICKEL (V vs Ni)

On log-log plots of vanadium versus nickel, Kam Formation data plots almost exclusively in the OFB field and above the tholeiite line, Duck Formation data extends from OFB through a broad zone of overlap between the tholeiitic and calc-alkaline lines, Banting Formation rocks trend from definitely calc-alkaline to transitional with the same set of Yellowknife River mouth traverse samples sitting in the OFB field. The Archean andesite rock designations of Condie (1981) lack vandium content, however the Kam-Duck-Banting Formation trend is consistent with a TH1-F1 progression.

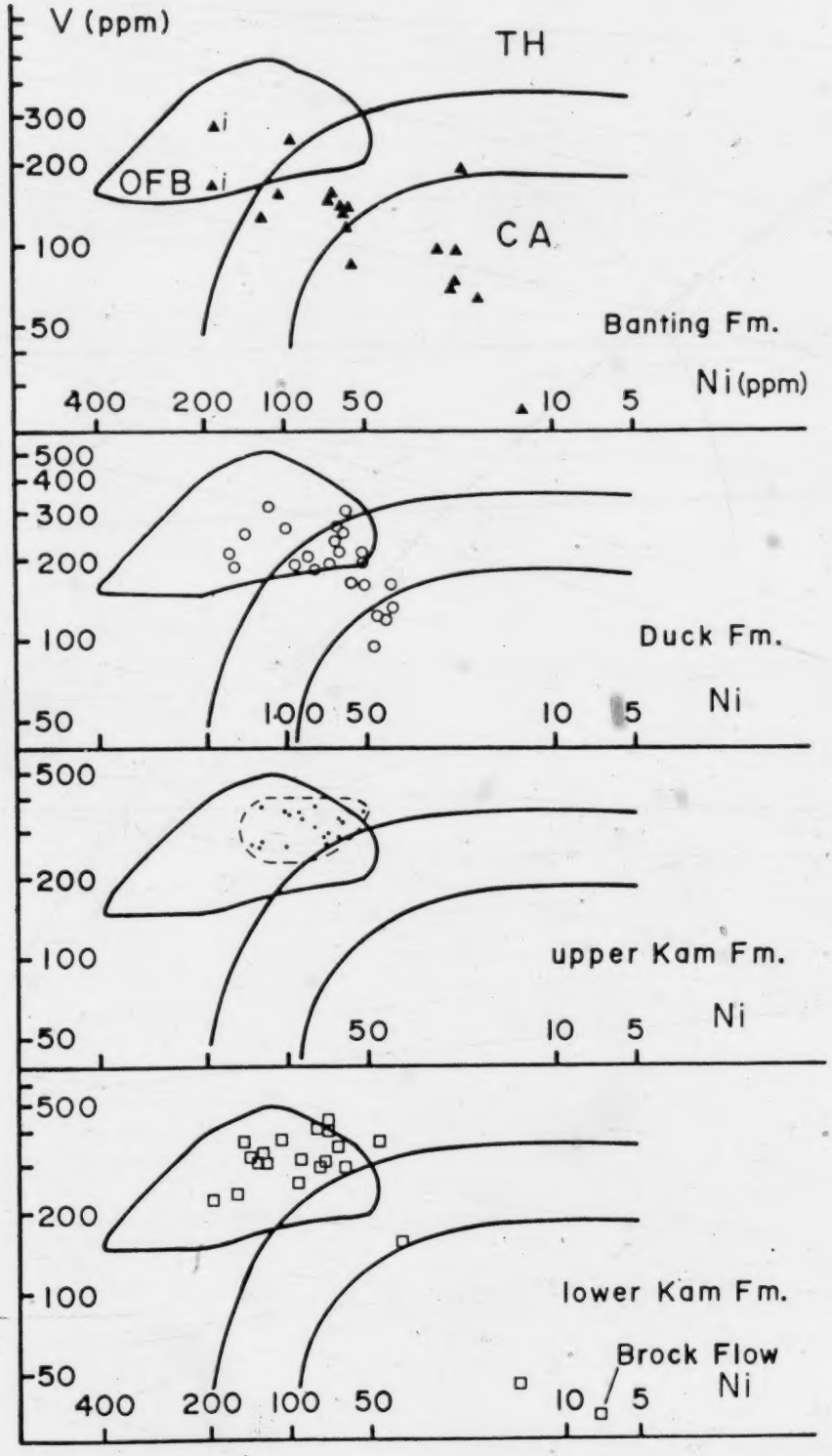

FIGURE 20 - V - Ni

3.4 SUMMARY OF GEOCHEMISTRY

Interpretation of Yellowknife data plotted on various geochemical plots, show the Yellowknife volcanic belt to be a subalkaline sequence consisting of 31% basalt, 34% basaltic andesite, 23% andesite, 11% dacite and 1% rhyolite. The predominant rock types within each formation change from basalt - basaltic andesite in the Kam Formation to basaltic andesite - andesite in the Duck Formation and andesite - dacite in the Banting Formation.

Alkali mobility is seen to be of concern, especially for the Duck and Banting Formations. Significant numbers of samples have metasomatic values, on the Hughes igneous spectrum diagram. These metasomatic samples were not used for the AFM diagram (Figure 10). Samples of limited alkali mobility indicate an iron enrichment tholeiitic differentiation trend for Kam Formation samples, a variable trend for Duck Formation data, and a calc-alkaline trend to the Banting Formation on the AFM diagram. Trace element diagrams support these findings, e.g. Figure 15 - FeO_T vs Zr/TiO_2. A test for komatiitic affinity shows there to be none, Section 3.2.6., but six samples do group in the high Mg-tholeiitic basalt field, adjacent to the basaltic komatiite line.

Figure 11 (MgO-FeO_T-Al_2O_3), a major element tectonic discrimination diagram, indicates the basaltic rocks to be of Within Plate tectonic origin. However, Figure 17 (Zr-Ti/100-Yx3), a trace element

tectonic discrimination diagram, suggests these rocks to be of Plate Margin tectonic origin. Interpretation concludes that the major element plot (Figure 11) is inappropriate for Yellowknife rocks, and possibly for Archean volcanic rocks in general.

Strict application of models and diagrams, derived from Cenozoic and younger volcanism, to Archean rocks should be avoided. However, petrogenetic models for the volcanics at Yellowknife should be consistent with extrusion of tholeiitic ocean floor basalts and calc-alkaline basalts which are related today to a plate margin setting.

CHAPTER 4

GEOCHRONOLOGY

4.1 INTRODUCTION

Rubidium - strontium whole rock studies were made on the Kam, Duck and Banting Formations, together with the Giant-Yellowknife Shear Zone of the Yellowknife volcanic belt. Sample selection followed examination of X.R.F. data for rubidium and strontium to obtain samples with a range of Rb/Sr ratios, and thin section work to avoid highly altered or carbonate rich samples (Table 5).

Data plotted on the igneous spectrum diagram (Figure 9) shows severe alkali movement suggesting the system was not closed with respect to rubidium and strontium. Awareness of this is pertinent in the case of the Duck Formation, for which the most discordant results were obtained; it has the highest percentage of analyses plotting as spilites (45%) and the lowest percentage plotting as igneous values (30%).

4.2 METHOD

For those samples in which rubidium and strontium were determined by isotope dilution methods (Table 9), approximately 100 mg of powdered sample was used for analysis on a MicroMass 30 mass spectrometer. Analytical error for $^{87}Rb/^{86}Sr$ is 1% or less, based on

TABLE 5: Rubidium - Strontium Geochronology Data

	$(^{87}Sr/^{86}Sr)$	± .0000x	$(^{87}Rb/^{86}Sr)$	Rb	*	Sr	*	(Rb/Sr)
BANTING FM.								
707-2AB	.72474	3	.636	34	b	155	b	.2194
707-6B	.70295	5	.027	2.3	b	250	b	.0092
708-2AB	.73585	3	.930	84	b	262	b	.3206
708-4C	.77919	3	2.143	75	b	102	b	.7353
718-7CD	.74128	4	1.136	70	a	179	a	.3911
705-1C	.70673	4	.076	4.9	b	187	b	.0262
DUCK FM.								
720-11	.70324	3	.052	2	b	112	b	.0179
722-7B	.71346	4	.336	19	a	164	a	.1159
726-2B	.72041	4	.582	40	a	199	a	.2010
720-7A	.72096	3	.601	22	ab	106	b	.2075
722-3A	.71989	3	.516	13	b	73	b	.1781
726-1BC	.74355	5	1.402	28	b	58	b	.4828
720-8A	.71841	3	.523	26	ab	144	b	.1806
726-8A	.70307	3	.020	1	a	146	ab	.0068

	$(^{87}Sr/^{86}Sr)$	$\pm$ .0000x	$(^{87}Rb/^{86}Sr)$	Rb	*	Sr	*	(Rb/Sr)
KAM FM.								
725-6A	.76917	3	1.813	66	b	106	b	.6226
725-1A	.70456	5	.081	5	b	179	b	.0279
620-20	.70182	3	.011	0.7	b	187	b	.0037
620-55	.70249	3	.018	1	a	160	a	.0062
803-1	.70213	3	.022	1	a	130	a	.0077
803-5	.70355		.011	1	a	87	a	.0015
710-12AB	.70202	3	.011	0.4	b	109	b	.0037
712-1B	.72425	4	.788	25	a	92	a	.2717
714-1B	.72657	6	.777	30	a	112	a	.2679
714-4A	.73435	5	.977	34	a	101	a	.3366
716-1A	.71711	4	.483	18	a	108	a	.1667
620-30	.72864	3	.774	28	a	105	a	.2667
710-4A	.72862	3	.774	24	a	90	a	.2667
710-7A	.73152	3	.934	28	a	87	a	.3218
710-1A	.74816	5	1.578	44	a	81	a	.5432
620-33	.72577	3	.710	24	a	98	a	.2449
GIANT_YK CORE								
0.76m	.70290	2	.099	9	a	264	a	.0341
30.12	.86321	4	4.501	121	a	79	a	1.5316
32.08	.79516	4	2.657	61	a	67	a	.9104
32.94	.84361	6	3.996	109	a	80	a	1.3625
36.58	.86939	6	4.999	68	a	40	a	1.7000
39.37	.77224	4	2.342	41	a	51	a	.8039

* a) XRF analysis; b) isotope dilution method.

laboratory experience. For $^{87}Sr/^{86}Sr$, precision on single runs varied from $\pm$ 0.0001 to $\pm$ 0.00002, one-sigma error. During the earlier phase analytical results on the SRM 987 strontium standard were 0.71030 (Lambert pers. comm. 1981) and during the later phase 0.71023. All results have been standardized to the latter value. Reproducibility of $^{87}Sr/^{86}Sr$ on the MM30, as seen in duplicates during this and other projects over the same period, was low at $\pm$ 0.0001, because of non-linearity and other problems with the digital voltmeter.

4.3 RESULTS

Each of four isochron plots developed from the data is distinct in age, initial ratio and interpretation. Evidence points to a sequence of geological events, but several problems still exist.

4.3.1 KAM FORMATION

Data scatters widely around an errorchron (n=16) of 2311 Ma, ($^{87}Sr/^{86}Sr$) I.R. = 0.7016 (Figure 21). Six of sixteen analyses, ($^{87}Rb/^{86}Sr$) between 0.7 and 0.8, have extremely variable ($^{87}Sr/^{86}Sr$) ratios, from 0.72425 to 0.73152. This range of strontium isotope ratios indicates the Rb-Sr system to have been open, and as these six points are pivotal to the array any age calculated using them is not valid.

The Brock or Townsite Flow dacite sample (725-6A) plots above the well defined Banting Formation 2490 Ma isochron; it is

considered to be an unaltered or little altered sample. Utilizing this analysis and those Kam Formation samples having $^{87}Rb/^{86}Sr$ less than 0.1 (n=7) an age of 2569 $\pm$ 27 Ma is calculated, $(^{87}Sr/^{86}Sr)$ I.R. = 0.70181 $\pm$ 0.00071. One data point (803-5) is significantly removed from the isochron and has probably been metasomatised. Therefore, with one high and five low $(^{87}Sr/^{86}Sr)$ analyses the isochron calculation yields an age of 2579 $\pm$ 8 Ma, $(^{87}Sr/^{86}Sr)$ I.R. = 0.70154 $\pm$ 0.00021 (Figure 21).

Three samples from this study (725-6A, 620-20 and 710-12AB) and six from Green, Baadsgaard and Cumming (1968) combine to yield a nine point isochron for a suite of Kam Formation rocks principally from the Brock dacitic flow; the age is 2567 $\pm$ 10 Ma, $(^{87}Sr/^{86}Sr)$ I.R. = 0.70182 $\pm$ 0.00028. As data from the earlier study quoted very high error levels, the new low error runs were weighted by a factor of four in the calculation.

Good agreement between the n=7 isochron (2569 Ma) and the n=9 isochron (2567 Ma) indicates a minimum age of 2570 Ma from Kam Formation volcanic rocks.

4.3.2 DUCK FORMATION

Interpretation of eight analyses suggest continual resetting during regional metamorphism and/or episodic resetting during severe shearing. Isochrons have been calculated from the data, however none are considered valid as indicating their primary age:

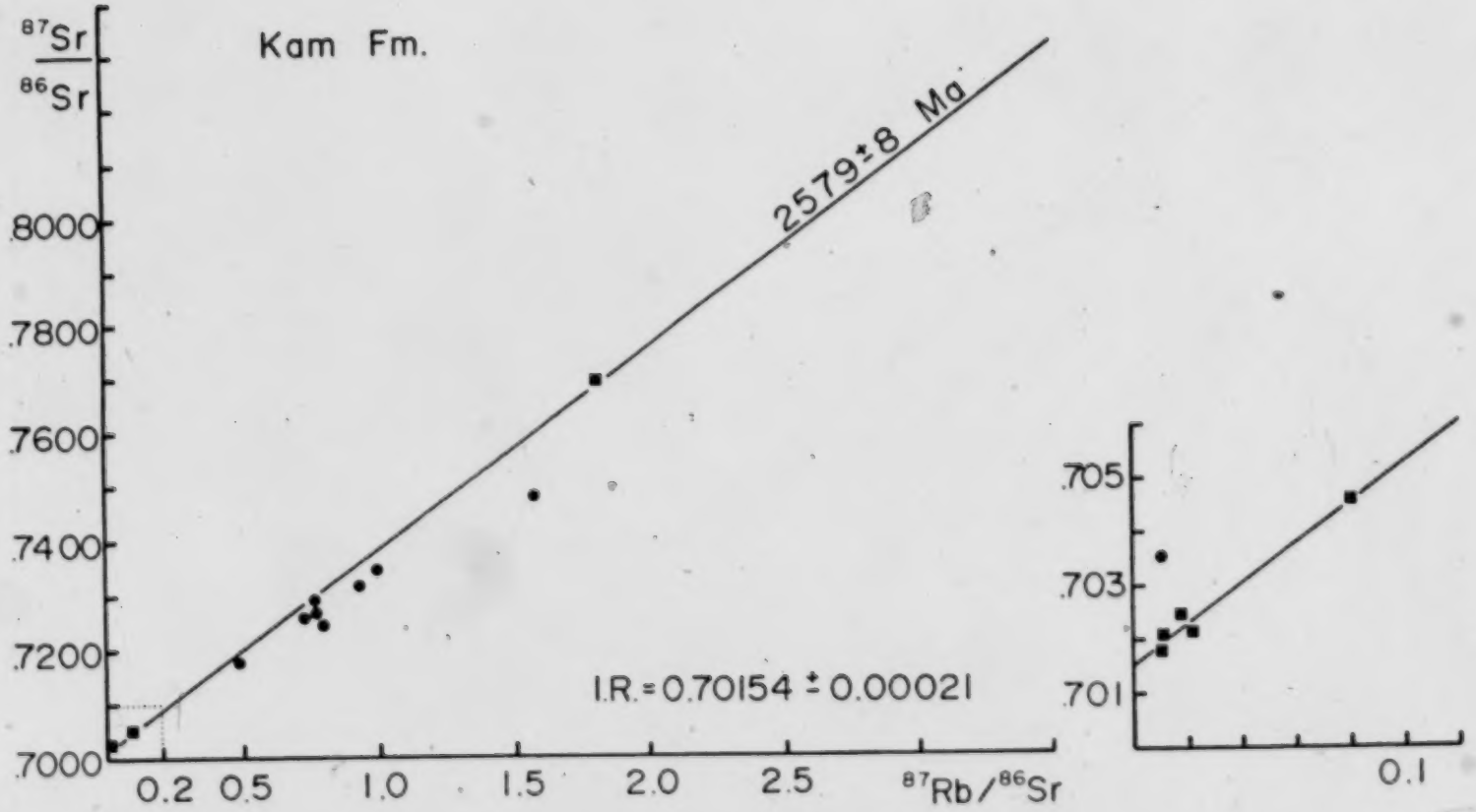

FIGURE 21 - Kam Formation Rb/Sr Best Age Isochron (solid squares only used in calculation).

Figure 22

a) all data (n=8) $t = 2052 \pm 60$ Ma
$(^{87}Sr/^{86}Sr)$ I.R. $= 0.7030 \pm 0.0013$

b) data in Igneous Spectrum (n=3) $t = 2248 \pm$ Ma
$(^{87}Sr/^{86}Sr)$ I.R. $= 0.7016 \pm$

Figure 23

c) high $(^{87}Sr/^{86}Sr)$ data (n=4) $t = 1910 \pm 70$ Ma
$(^{87}Sr/^{86}Sr)$ I.R. $= 0.7048 \pm 0.0014$
$^{87}Sr/^{86}Sr$ greater than 0.7185

d) low $(^{87}Sr/^{86}Sr)$ data (n=4) $t = 2200 \pm 110$ Ma
$(^{87}Sr/^{86}Sr)$ I.R. $= 0.7021 \pm 0.0020$
$(^{87}Sr/^{86}Sr)$ less than 0.7185

-- calculation d), exclude 726-8A $t = 2254 \pm 175$ Ma
$(^{87}Sr/^{86}Sr)$ I.R. $= 0.7018 \pm 0.0031$
726-8A shows probable Rb mobility

Analyses scatter about the all data best fit line, line a of Figure 22, with low correlation and high error suggesting the Rb-Sr system has not remained closed. Isochron ages b to d represent either average values for continual downdating or episodic events (thermal and/or tectonic) at 2200-2250 Ma and 1900 Ma.

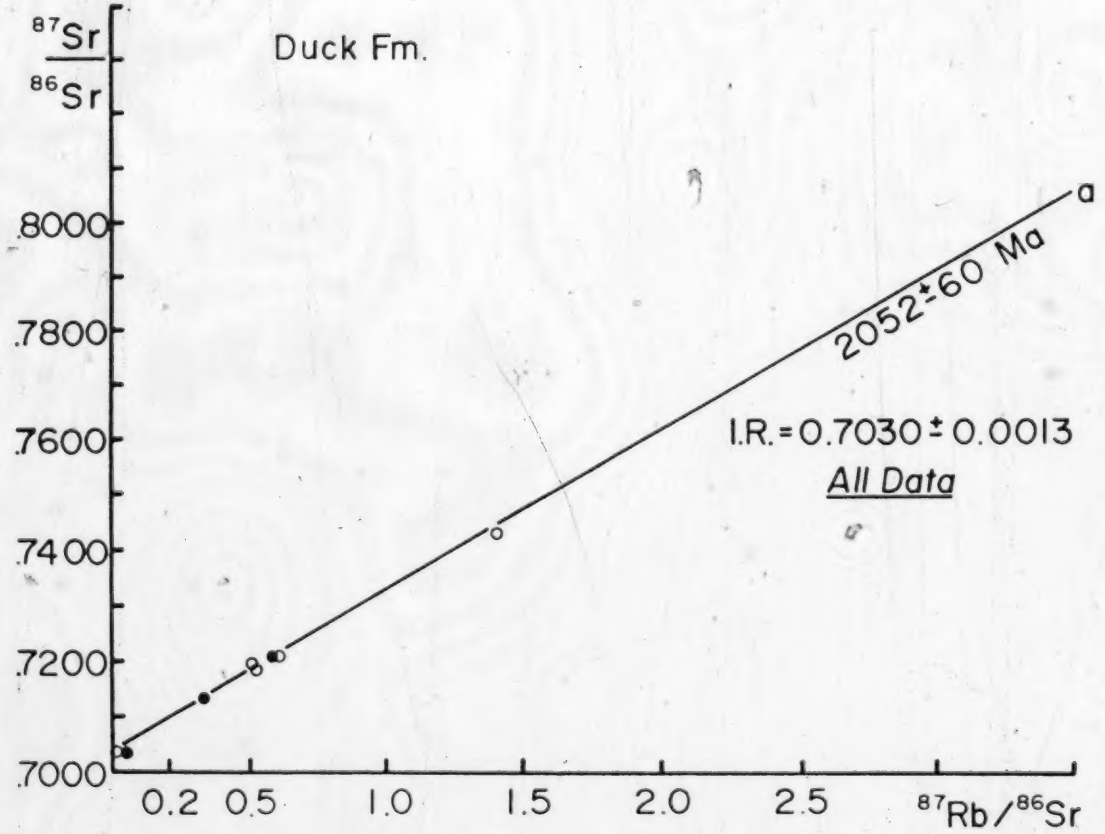

FIGURE 22 - Duck Formation Rb/Sr Isochron a

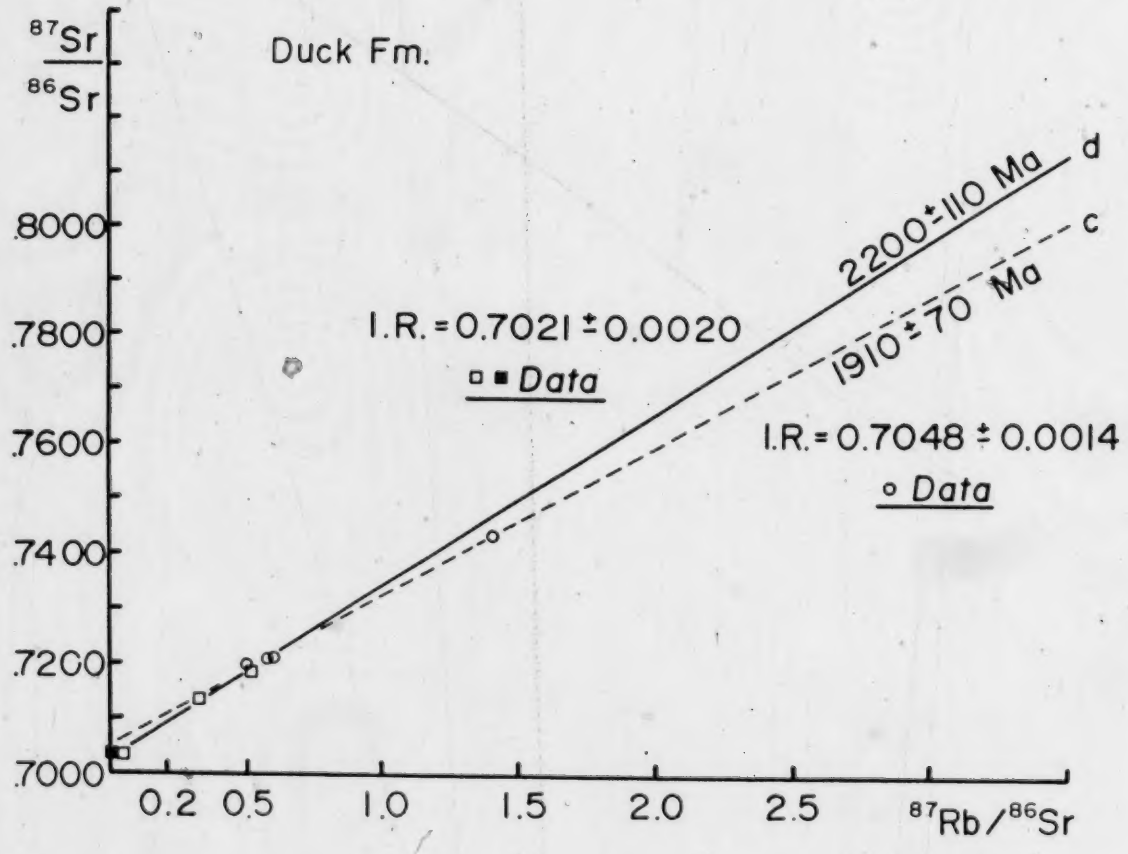

FIGURE 23 - Duck Formation Rb/Sr Isochrons c and d

The lower apparent age for samples with higher Rb/Sr is consistent with the general premise that samples with high Rb/Sr are more likely to be prone to significant alkali mobility than the more refractory lower Rb/Sr samples.

4.3.3 BANTING FORMATION

A five point isochron (Figure 24), calculated from two andesite and four dacitic analyses, yields an age of 2490 ± 40 Ma with the $^{87}Sr/^{86}Sr$ initial ratio being 0.7018 ± 0.0010. One data point (sample 705-1C) plots significantly away from the all data (n=6) isochron, outside acceptable limits, and is not used.

4.3.4 GIANT YELLOWKNIFE SHEAR ZONE

Six drill core samples (Giant Yellowknife Mine, core #12965) through the main ore zone of the Giant Shear were analyzed for Rb-Sr age dating (Table 5). Four values from the main shear plot with good correlation to yield an age of 2512 ± 15 Ma, ($^{87}Sr/^{86}Sr$) I.R. = 0.6991 ± 0.0006 (Figure 25).

As the strontium isotope initial ratio is only slightly above the Basaltic Achondrite Best Initial (BABI = 0.69847 ± 0.00003) or the Juvinas and Sioux County achondrites ratio (JUSI = 0.698976 ± 0.000055) it is too low to represent unaltered Archean greenstone material (Faure 1977). The low initial ratio is probably due to Rb

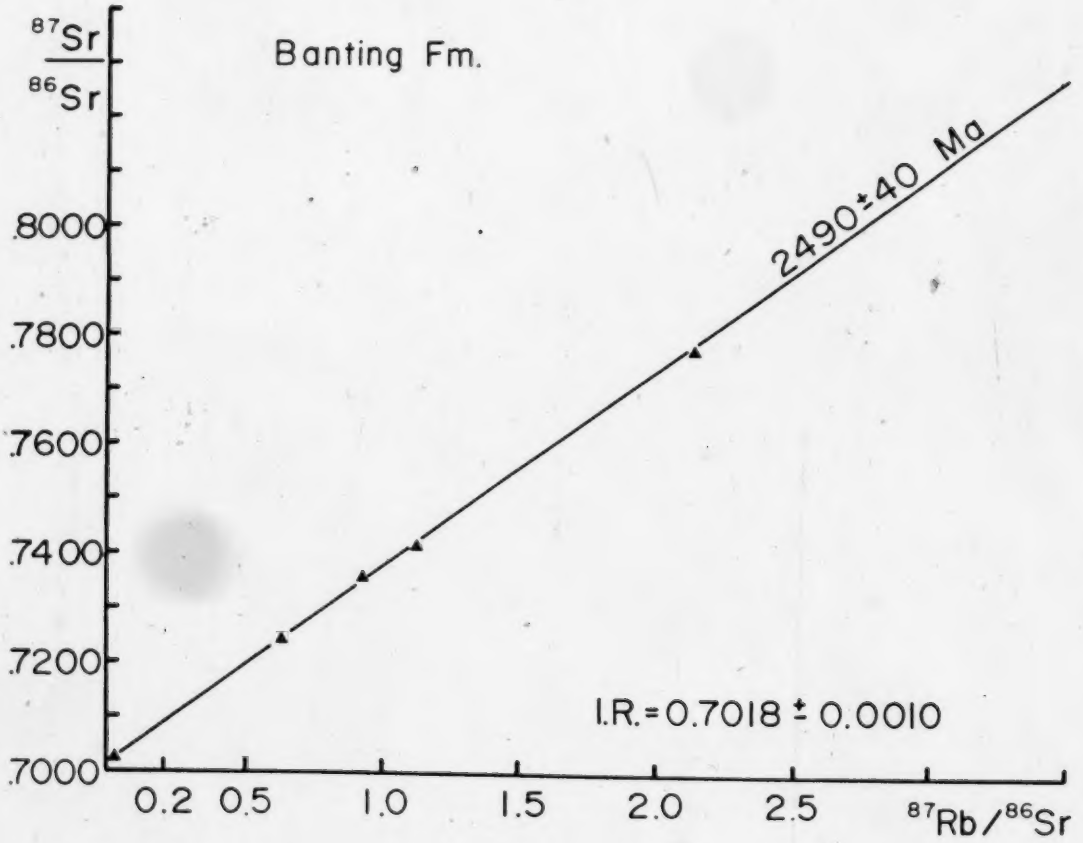

FIGURE 24 - Banting Formation Rb/Sr Isochron

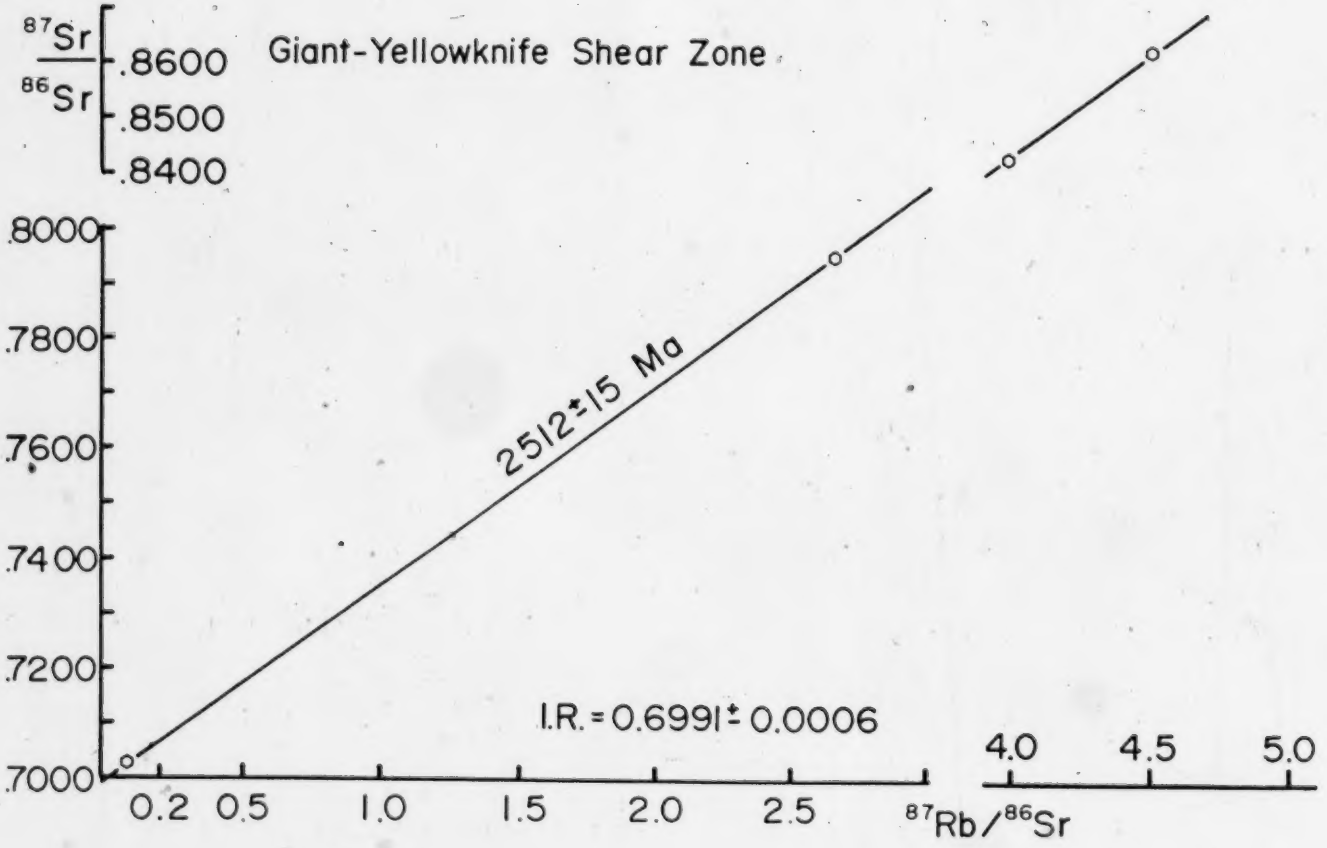

FIGURE 25 - Giant - Yellowknife Shear Zone Isochron

movement affecting the lowest data point, a sheared chlorite schist from the Kam Formation host rock.

On the assumption that the ($^{87}Sr/^{86}Sr$) I.R. of the shear zone was 0.7017, the Shear Zone age calculated to 2490 ± 2 Ma.

4.4 DISCUSSION

Isochrons for the Banting Formation (2490 ± 40 Ma), Kam Formation (Townsite Flow at 2569 ± 27 Ma) and Giant-Campbell shear zone (2512 ± 15 Ma) are close to the K-Ar histogram mean age (2463 Ma) given by Green and Baadsgaard (1971); Banting Formation and shear zone data are within one standard deviation of the mean. A second, much weaker event, is noted on the histogram at 2200 Ma, similar to the Duck Formation 'best' (re-set) date of 2250 Ma.

Data from Green and Baadsgaard (1971) has been re-evaluated using $^{87}Rb\ \lambda = 1.42 \times 10^{-11} yr.^{-1}$:

Western Granodiorite - converted to 2555 ± 58 Ma,
I.R. = 0.7035 ± 0.0027;

Prosperous Lake Granite - converted to 2520 ± 25 Ma
(mineral isochron);

Southeast Granodiorite - converted to 2584 ± 37 Ma,
I.R. = 0.7011 ± 0.0008;

Southeast Granodiorite - recalculated as 2613 ± 19 Ma,
I.R. = 0.70029 ± 0.00107;

Ross Lake Granodiorite - converted to 2457 ± 120 Ma,
I.R. = 0.707 ± 0.005

Ross Lake Granodiorite - recalculated as 2458 ± 44 Ma,
I.R. = 0.7080 ± 0.0026.

Similar re-evaluation of zircon concordia data using Steiger and Jager (1977) decay constants results in an age of 2558 ± 11 Ma for the Western Ganodiorite, and 2585 ± 25 Ma for the Southeast Granodiorite; the respective lower intercept ages, 350 ± 50 Ma (Devonian) and 50 ± 25 Ma (modern), are likely due to episodic lead loss and recent leaching. The Rb-Sr and U-Pb concordia dates are in excellent agreement.

At 2613 ± 19 Ma the recalculated Rb-Sr age for the Southeast Granodiorite is high and the $^{87}Sr/^{86}Sr$ initial ratio is low compared to earlier calculations and other intrusives. A rotated isochron, due to Rb mobility and ^{87}Sr loss, is indicated.

Volcanic rocks in the Yellowknife area yield a minimum Rb-Sr age of 2570 Ma, however re-evaluation of Pb-Pb data from Cumming and Tsong (1975) for the intrusive Western Granodiorite points to volcanism prior to 2636 ± 10 Ma. Preliminary Nd-Sm work yields an age of 2650 ± 26 Ma for Kam Formation volcanics (pers. comm. Lambert 1983).

Mobilization of rubidium and strontium during upper greenschist to amphibolite grade metamorphism, metasomatism and shearing of fine grained mafic to intermediate volcanic rocks has caused resetting of the system, downdating, and confusion over the true $^{87}Sr/^{87}Sr$ initial ratio. Rubidum - strontium and uranium - lead ages for the Western and Southeast Granodiorites indicate them to be essentially synvolcanic, within the defined error limits; agreement

between the two dating methods suggest their Rb-Sr systems have remained closed.

Whole rock Rb-Sr isochrons indicate that Banting Formation rocks are the same age within error (2490 ± 40 Ma) as the Giant-Campbell shear zone (2512 ± 15 Ma), and that both are the same within error as the Prosperous Lake granite mineral isochron age (2520 ± 25 Ma) converted from Green and Baadsgaard (1971). An unpublished zircon date of 2610 Ma has been obtained for the Banting Formation (W. Padgham, pers. comm. 1983). This predates the zircon age of the intrusive Western Granodiorite by 50 Ma.

Recent geological mapping suggests Banting Formation rocks lie on, and are intrusive into the Kam Formation (Easton et al 1981, 1982), as well as being gradational upwards into the Burwash Formation (Helmstaedt et al 1980). The Burwash Formation, youngest member of the Yellowknife Supergroup, was intruded by the Prosperous Lake Granite after major folding. These inter-relationships require that the Banting Formation age be a reset date, possibly a result of regional metamorphism, intrusion of the Prosperous Lake Granite and major shearing all about 2500 Ma.

4.5 SUMMARY OF GEOCHRONOLOGY

Kam Formation data indicates the minimum age of volcanism to be 2570 Ma; Duck Formation analyses scatter about 2200 Ma and 1910 Ma

date lines; Banting Formation samples give an isochron of 2490 Ma; and the Yellowknife Shear Zone data yields an age of 2510 Ma.

Integrating these results with ages recalculated from prior studies suggest the following geochronology:

1) volcanism prior to 2640 Ma, age of the intrusive Western Granodiorite;

2) resetting of the Rb-Sr systems during a phase of South-east Granodiorite remobilization, about 2580 Ma;

3) downdating of the Banting Formation due to intrusion of Prosperous Lake Granite at 2520 Ma and development of the Yellowknife Shear Zone at 2510 Ma.

A satisfactory explanation for the anomalous Duck Formation results must await further studies.

CHAPTER 5

GEOCHEMICAL COMPARISON AND PETROGENETIC MODELS

5.1 INTRODUCTION

Major and trace element analyses have been used to calculate mean composition for each rock type within each volcanic formation. This mean value is considered a valid representation of the chemistry of a particular rock type having had a relatively uniform history. It is necessary to utilize average compositions in order to compare the Yellowknife volcanic belt with analyses available for greenstone belts worldwide.

It will be shown that the Yellowknife data are consistent with derivation of Kam Formation basalts by partial melting of a mantle source, while all other rocks were derived by partial melting of pre-existing basaltic or sialic crust.

Tables 6 and 7 list mean composition by rock type within each formation of the Yellowknife greenstone belt. Eighty samples have been analyzed for 10 major and 12 minor elements; their calculated element ratios are in Table 8. Mean composition of the Kam, Duck and Banting Formations, listed in Table 9, includes 10 major plus 7 minor elements by x-ray fluorescence (n=156), and majors plus 5 minor elements by atomic absorption (n=80).

TABLE 6

MEAN COMPOSITION BY ROCK TYPE FOR YELLOWKNIFE VOLCANIC ROCKS
(having 12 corresponding Minor Element Analyses)
MAJOR ELEMENTS (in weight percent)

	SiO_2	Al_2O_3	FeO_T	MgO	CaO	Na_2O	K_2O	TiO_2	MnO	P_2O_5	Total	N	8.0x
BANTING FM													
DACITE	68.91	15.78	4.18	1.75	3.85	2.54	2.12	0.61	0.12	0.15	100.01	8	9.9
ANDESITE	60.93	15.27	7.41	3.11	8.03	3.36	1.05	0.90	0.15	0.26	100.47	7	18.7
BASALTIC ANDESITE	53.46	17.52	8.69	4.22	7.38	4.75	2.29	1.05	0.13	0.50	99.99	1	20.4
BASALT	52.59	16.15	11.61	6.70	6.58	4.70	0.12	1.15	0.20	0.19	99.99	1	25.1
DUCK FM													
DACITE	65.78	14.42	6.27	3.47	3.79	4.24	0.75	0.96	0.10	0.24	100.02	4	13.6
ANDESITE	58.47	15.60	7.90	4.71	7.15	3.70	0.62	1.35	0.18	0.31	99.99	13	19.9
BASALTIC ANDESITE	54.16	15.00	10.84	5.79	7.71	4.11	0.24	1.56	0.22	0.35	99.98	3	24.5
BASALT	50.41	17.32	11.88	6.21	7.95	3.60	0.47	1.54	0.28	0.33	99.98	3	26.3
UPPER KAM FM													
BASALTIC ANDESITE	54.56	13.09	10.48	8.21	8.94	2.83	0.66	0.95	0.24	0.06	100.02	3	27.8
BASALT	51.02	14.35	12.09	7.78	10.73	2.13	0.48	1.06	0.26	0.09	99.99	15	30.8
LOWER KAM FM													
DACITE	72.15	13.95	3.40	0.85	2.22	3.46	2.94	0.75	0.06	0.22	100.00	1	6.5
ANDESITE	57.72	14.59	10.99	7.25	4.92	2.76	0.27	1.14	0.18	0.18	100.00	2	23.3
BASALT ANDESITE	54.72	14.25	10.71	6.71	10.33	1.56	0.32	1.06	0.24	0.10	100.00	6	27.9
BASALT	51.83	14.68	11.99	6.86	10.40	2.33	0.34	1.21	0.26	0.10	100.00	13	29.5
AVERAGE VALUES													
DACITE	68.20	15.22	4.76	2.21	3.71	3.13	1.76	0.73	0.11	0.18	100.01	13	10.8
ANDESITE	59.18	15.40	8.03	4.43	7.23	3.51	0.73	1.19	0.17	0.28	100.15	22	19.9
BASALTIC ANDESITE	54.46	14.41	10.53	6.65	9.18	2.69	0.53	1.15	0.23	0.18	100.01	13	26.6
BASALT	51.34	14.86	12.01	7.23	10.20	2.43	0.41	1.17	0.26	0.12	100.03	32	29.7

TABLE 7

MEAN COMPOSITION BY ROCK TYPE FOR YELLOWKNIFE VOLCANIC ROCK

MINOR ELEMENTS (in ppm)

	N	Sc	V	Ni	Cu	Zn	Rb	Sr	S(%)	Ba	Zr	Y	Nb
BANTING FM													
DACITE	8	2	95	50	19	68	56	271	0.03	440	173	18	11
ANDESITE	7	7	120	56	48	101	13	223	0.03	136	196	32	12
BASALTIC ANDESITE	1	8	190	22	18	64	46	725	0.08	167	190	32	14
BASALT	1	11	243	95	39	111	1	388	0.03	86	126	26	1
DUCK FM													
DACITE	4	10	126	44	39	90	13	155	0.16	69	183	33	10
ANDESITE	13	12	204	78	61	111	12	150	0.04	60	175	42	10
BASALTIC ANDESITE	3	14	232	66	65	112	3	170	0.03	23	186	44	2
BASALT	3	20	281	123	88	152	7	181	0.07	67	206	37	7
UPPER KAM FM													
BASALTIC ANDESITE	3	18	283	71	102	88	8	108	0.04	84	69	24	3
BASALT	15	21	316	93	100	106	12	124	0.05	19	85	25	1
LOWER KAM FM													
DACITE	1	3	34	7	11	59	64	100	0.04	633	295	48	14
ANDESITE	2	12	227	57	73	99	3	112	0.04	12	148	31	9
BASALTIC ANDESITE	6	21	319	88	80	109	10	122	0.04	15	76	26	2
BASALT	12	18	343	111	120	119	8	124	0.04	24	80	29	2
AVERAGE VALUES													
DACITE	13	5	100	45	25	75	43	220	0.07	341	185	25	11
ANDESITE	22	11	179	69	58	107	11	170	0.03	80	179	38	10
BASALTIC ANDESITE	12	18	278	72	77	101	10	176	0.04	44	108	30	3
BASALT	33	19	315	108	101	114	9	138	0.05	27	96	28	2

TABLE 8

MEAN COMPOSITION BY ROCK TYPE FOR YELLOWKNIFE VOLCANIC ROCKS

	ELEMENT RATIOS												
	Rb/Sr	Ba/Rb	Ba/Sr	K/Rb	K/Ba	CaO/Al_2O_3	Ti/Zr	Nb/Y	V/Ni	Ti/V	Zr/Y	FeO/MgO	Na_2O/K_2O
BANTING FM													
DACITE	0.206	7.85	1.62	314	40	0.243	21.1	0.611	1.90	38.4	9.61	2.38	1.20
ANDESITE	0.058	10.46	0.60	670	64	0.525	27.5	0.375	2.14	44.9	6.12	2.38	3.20
BASALTIC ANDESITE	0.063	3.63	0.23	413	114	0.421	33.1	0.437	8.63	33.1	5.93	2.05	2.07
BASALT	0.025	0.01	0.22	996	11	0.407	54.6	0.038	1.47	29.9	4.84	1.73	39.20
DUCK FM													
DACITE	0.078	5.30	0.41	479	90	0.262	31.4	0.303	2.86	45.6	5.54	1.80	5.65
ANDESITE	0.080	5.00	0.40	429	86	0.458	46.2	0.238	2.61	39.6	4.16	1.67	5.97
BASALTIC ANDESITE	0.017	7.66	0.13	664	87	0.514	50.2	0.045	3.51	40.2	4.22	1.87	17.12
BASALT	0.038	9.57	0.37	557	58	0.459	44.7	0.189	2.28	32.8	5.56	1.91	7.66
UPPER KAM FM													
BASALTIC ANDESITE	0.074	10.50	0.77	684	65	0.682	82.4	0.125	3.98	20.1	2.87	1.27	4.29
BASALT	0.096	1.58	0.15	332	210	0.747	74.6	0.040	3.39	20.0	3.40	1.55	4.44
LOWER KAM FM													
DACITE	0.640	9.89	6.33	381	39	0.159	15.2	0.291	4.85	132.1	6.14	4.00	1.18
ANDESITE	0.026	4.00	0.10	747	187	0.337	46.1	0.290	3.98	30.0	4.77	1.51	10.22
BASALTIC ANDESITE	0.081	1.50	0.12	266	177	0.724	83.5	0.076	3.62	19.9	2.92	1.59	4.87
BASALT	0.064	3.00	0.19	353	118	0.708	90.5	0.068	3.09	21.1	2.75	1.74	6.85
AVERAGE VALUES													
DACITE	0.195	7.93	1.55	340	43	0.243	23.6	0.440	2.22	43.7	7.40	2.15	1.78
ANDESITE	0.064	7.27	0.47	551	76	0.469	39.8	0.263	2.59	39.8	4.71	1.81	4.81
BASALTIC ANDESITE	0.056	4.40	0.25	440	100	0.637	63.7	0.100	3.86	24.7	3.60	1.58	5.07
BASALT	0.065	3.00	0.19	378	126	0.686	73.0	0.071	2.91	22.2	3.42	1.66	5.93

TABLE 5

A: ALL DATA BY X.R.F. (N=155)

	SiO_2	Al_2O_3	Fe_2O_3	FeO	MgO	CaO	Na_2O	K_2O	TiO_2	MnO	P_2O_5	TOTAL*	N
BANTING FM	61.27	15.73	7.81	-	3.54	6.38	3.08	1.06	0.77	0.16	0.20	100.00	29
DUCK FM	56.34	15.34	9.19	-	4.91	7.37	3.55	0.52	1.46	0.18	0.30	99.66	44
Upper KAM FM	51.05	14.18	13.05	-	7.36	10.23	2.10	0.45	1.06	0.25	0.09	99.82	31
Lower KAM FM	53.09	14.16	12.37	-	6.57	10.12	2.40	0.36	1.20	0.23	0.12	100.71	52

B: SAMPLES HAVING BOTH X.R.F.AND A. A. ANALYSES(N=80)

BANTING FM	63.74	15.68	-	6.20	2.74	5.93	3.13	1.50	0.78	0.15	0.22	100.08	17
DUCK FM	57.70	15.54	-	8.52	4.83	6.74	3.84	0.57	1.23	0.18	0.31	99.56	23
Upper KAM FM	51.60	13.99	-	11.70	7.91	10.43	2.24	0.51	1.03	0.25	0.09	99.75	18
Lower KAM FM	54.25	14.45	-	11.09	6.59	9.45	2.28	0.39	1.12	0.24	0.10	99.96	22

* Major element analyses in weight percent.

TABLE 10

A: ALL DATA BY X.R.F. (N=156)

	X.R.F.							A.A.				
	Rb	Sr	S	Ba	Zr	Y	Nb	Sc	V	Ni	Cu	Zn
BANTING	26	309	0.03	294	168	25	10					
DUCK	10	176	0.05	50	175	39	7					
UPPER KAM	11	127	0.05	28	81	31	2					
LOWER KAM	8	134	0.04	28	92	29	3					
B: SAMPLES HAVING BOTH X.R.F. AND A.A. ANALYSES (N=80)												
BANTING	34	291	0.03	363	181	31	11	5	119	53	32	84
DUCK	10	156	0.06	58	182	40	8	13	204	76	62	113
UPPER KAM	11	121	0.05	30	84	25	2	21	310	89	100	102
LOWER KAM	8	121	0.04	25	86	28	2	17	297	90	96	137

* S given in weight percent, all other minor elements in ppm

Inter-formation comparison of similar rock type shows a general trend of decreasing primitive character with higher perceived stratigraphic position within the belt. Iron, magnesium, calcium, manganese, vanadium and chromium decrease in abundance for each rock type, from Kam to Duck to Banting Formation. Inconsistencies exist, however, for Kam Formation dacites, Banting Formation basalts and basaltic andesites resulting from insufficient sample population, alteration or true petrogenetic differences.

Comparative data, for this discussion, has been taken from Goodwin (1977, 1979) for the Abitibi belt and Superior Province; Naldrett et al (1978) for the Abitibi, Wabigoon, Uchi Lake and Ennadai belts; and Condie (1976, 1981) for overall average Archean volcanic rocks and specific greenstone belts.

It has been shown that alkalies (Na, K) were mobile and that the Rb-Sr system did not remain closed. Supposedly immobile elements, such as iron and nickel, are not likely to have moved en masse as seen in the quite reasonable averages, ratios and trends especially for Zr, Ti and Y as well as the standard rare earth element patterns already published. Anomalous results for the Duck Formation may be due to localized CO_2 matasomatism (Easton, pers. comm. 1982), but may also be due to liquid immiscibility or mixing of magmas.

5.2 FORMATION CHARACTERISTICS

5.2.1 KAM FORMATION

Lower Kam Formation basalts (Table 6, n=13) are Ti enriched, 1.21% TiO_2 and Ti/Zr=90, similar to intermediate high Ti basalts of Naldrett et al (1978); Superior Province tholeiitic basalts average 1.16% TiO_2 and Ti/Zr=64. Upper Kam Formation basalts and basaltic andesites are consistently more primitive than lower unit counterparts; SiO_2 51.02 vs 51.83 percent, MgO 7.78 vs 6.86 percent, CaO 10.72 vs 10.40 percent, and FeO_T/MgO 1.55 vs 1.74 respectively. Primitive or fundamental character may be expressed in higher mean contents of mafic elements, the five basic oxides Fe_2O_3, FeO, MgO, CaO and MnO (Goodwin 1979); upper unit basalts have a value of 30.8 versus 29.5 for the lower unit.

The sole analysis of a Kam Formation dacite yields low MgO (0.85%), V (34 ppm), and Ni (7 ppm) resulting in high FeO_T/MgO (4.0) and Ti/V (132), but V/Ni (4.8) is not inconsistent with comparative averages; FeO_T and MnO are lower than might be expected. Similarly the sum of 5 basic oxides (B.Ox.) is 6.5 percent versus 13.6 and 9.9 percent for Duck and Banting Formation dacites respectively. Superior Province tholeiitic dacites average 0.89% MgO, 108 ppm V, 12 ppm Ni, FeO_T/MgO=4.6, Ti/V=30, V/Ni=9, (B.Ox.)=9.5 percent.

5.2.2 DUCK FORMATION

Major and minor element diagrams show the Duck Formation as highly variable in element correlations, trend and composition. The broad scatter of data on SiO_2 vs Zr/TiO_2 (Figure 14) and FeO_T vs Zr/TiO_2 (Figure 15) overlap parts of both the Kam and Banting Formation fields. It also includes intervening and more extreme compositions ranging into the alkali basalt field (Figure 14) or trending from high Ti (LKT) to high Zr (CAB) on Figure 17 (Zr-Ti/100-Yx3), from tholeiitic to calc-alkaline on Figure 10 (A.F.M.), and from low Al_2O_3 (oceanic island) to high Al_2O_3 (orogenic) on Figure 11 (MgO-FeO_T-Al_2O_3). Figures 10 and 15 both demonstrate the Duck Formation iron enrichment and iron depletion trends.

There are a few high Al basalts containing greater than 16.5 percent Al_2O_3, at FeO_T/FeO_T+MgO = 0.65 (Naldrett and Goodwin 1977), and relatively low CaO/Al_2O_3 ratios (0.46) compared to the average Yellowknife basalt (0.69). Samples of high Ti basalts (1.54% TiO_2) and basaltic andesites (1.56% TiO_2) exceed the Yellowknife basalt (1.17% TiO_2) and basaltic andesite (1.15% TiO_2) mean values. These results are anomalous when compared to Abitibi belt and Superior Province averages (Goodwin 1977, 1979).

Duck Formation dacites show a primitive character, (B.Ox.)= 13.6 percent, compared to average Superior Province calc-alkaline (10%) or tholeiitic (9.9%) dacites. They also exceed Kam Formation (6.5%) and Banting Formation (9.9%) dacites. The silica content is

low (65.78%) versus the Yellowknife mean (68.20%), iron and magnesium are high (6.27% and 3.47%) compared to the mean values (4.76% and 2.21%).

5.2.3 BANTING FORMATION

The Banting Formation is andesite-dacite in composition; a basaltic andesite sample is high in Al_2O_3 (17.52%), K_2O (2.29%), Na_2O (4.75%), P_2O_5 (0.50%), and Sr (725 ppm). Andesites have low Na_2O (3.36%) and high CaO (8.03%, CaO/Al_2O_3=0.52). Dacites have high K_2O (2.12%), Na_2O (2.54%), CaO (3.85%) and slightly enriched TiO_2 (0.61%). Comparison is with Kam and Duck Formation averages, data from the Abitibi greenstone belt and mean Superior Province values.

5.3 COMPARISON AND CLASSIFICATION

Basalts, andesites and felsic volcanic rocks from Archean greenstone belts have been classified by, and petrogenetic models developed from, rare earth element patterns and corresponding major/minor element chemistry. Classification of volcanics from the Yellowknife greenstone belt, by comparison of discriminant elements and element ratios (Condie 1981) is given in Table 11.

Kam Formation basalts are considered TH1, previously termed light rare earth element (LREE) depleted Archean tholeiites (DAT). Discriminants yield a somewhat mixed picture as 3 of 11 indicate TH2 rather than TH1, but analyses by Condie and Baragar (1974) show both

TABLE 11: Discriminant Element Classification of Yellowknife Volcanic Rocks

1. DACITES

	Al_2O_3	Na_2O	Zr	Ba	Y	Ti/V	Ti/Zr	Zr/Y
BANTING FM	FI	FII	FI	FI	FI	FI	FI	FII
DUCK FM	FII	FII	FI	FI	FII	FI	FI	FII
UPPER KAM FM	-	-	-	-	-	-	-	-
LOWER KAM FM	FII	FII	FII	FI	FII	FII	FI	FII

2. ANDESITES

	FeO	MgO	Ni	Zn	K_2O	Rb	Ba	Sr	Y
BANTING FM	AII(I)	AII(III)	AII(III)	AI(III)	AI(III)	AI	AI	AI(III)	AII
DUCK FM	AI	AII	AI	AI	AI	AI	AI	AI(III)	AIII
UPPER KAM FM	-	-	-	-	-	-	-	-	-
LOWER KAM FM	AI	AI	AII	AI	AI	AI	AI	AI(III)	AII(I)

3. BASALTS

	TiO_2	CaO	K_2O	P_2O_5	V	Zr	Sr	Y	Ti/Zr	Zr/Y	Ti/V
BANTING FM	TH2	TH2	TH1	TH2	TH1	TH2	TH2	TH2	TH2	TH2	TH2
DUCK FM	TH2	TH2	TH2	TH2	TH1	TH2	TH2	TH2	TH2	TH2	TH2
UPPER KAM FM	TH2	TH1	TH2	TH1	TH2	TH1	TH1	TH2	TH2	TH1	TH1
LOWER KAM FM	TH2	TH1	TH1	TH1	TH2	TH1	TH1	TH2	TH1	TH1	TH1

lower and upper unit tholeiites to have flat REE patterns (TH1), possibly with a slight negative Eu anomaly. Duck and Banting Formation basalts are TH2, or (LREE) enriched Archean tholeiites (EAT).

Andesites from the Kam Formation are AI, Archean Andesites - type 1, according to the discriminants FeO, MgO, Zn, K_2O, Rb, Sr and two slightly enriched light rare earth element patterns (Jenner et al 1981); Ni and Y suggest type AII. Duck Formation andesites are also AI, 7 of 9 discriminants; MgO suggest AII while Y indicates AIII. Banting Formation andesites show type AI, AII and AIII compositions, based upon trace element discriminants. Type AIII is ignored as it has weak support and has been previously reported only from the Abitibi belt; hence the discrimiants favour type AI by a 5 to 4 margin. Also two REE analyses (Jenner et al 1981), show a slight LREE enrichment, i.e. type AI.

The Kam Formation dacite (n=1) is an undepleted siliceous volcanic (USV) or FII, despite low Ba and high Ti. Suggested discriminants (8) for dacites leave the designation for Duck Formation samples undecided:

FI - Zr, Ba, Ti/Y, Ti/Zr

FII - Al_2O_3. Na_2O, Y, Zr/Y

One REE analysis of a Duck Formation dacite gave a generally flat pattern with a slight LREE enrichment and a positive Eu anomaly (FII), however confusion in the discriminants may indicate more than one source rock for these lavas. Dacites from Banting Formation traverses are type FI, depleted siliceous volcanics (DSV), according to 6 of 8

discriminants and three REE patterns (Jenner et al 1981). The statement "FII volcanics only are reported from...the Yellowknife belt in Canada (Condie and Baragar 1974)", (Condie 1981) must now be modified.

Table 12 summarizes results of the comparative analysis for the Yellowknife volcanic belt and relates to Figure 9-16 of Condie (1981, p.295) for possible petrogenetic models.

TABLE 12:

Formation	Basalt	Andesite	Dacite
Banting	TH2	AI	FI
Duck	TH2	AI	FII
Kam	TH1	AI	FII

Comparison and classification of rocks from the Yellowknife greenstone belt indicate variable composition in relatively close proximity, suggesting different source material chemistries and/or modes of magma generation.

5.4 MODELS OF MAGMA GENESIS

5.4.1 OVERVIEW

A summary by Morse (1980) uses a tripartite division of the uppermost mantle into plagioclase, spinel and garnet facies lherzolites. Addition of aluminous phases to lherzolite composition (oli-

vine, orthopyroxene, clinopyroxene) is required to supply sufficient aluminum and alkalies for the plagioclase component of a basaltic magma upon melting. Work by Solomon (1976) and Presnall et al (1979) is used to argue that garnet lherzolite rises adiabatically, recrystallizes to spinel lherzolite (20 kb or 70 km), continues to rise and undergoes partial melting as it hits the spinel lherzolite solidus (12 kb or 42 km). Upon further upwelling the mantle material follows the solidus P-T curve, at least to the plagioclase lherzolite cusp where maximum melting occurs for a given heat input and magma tends to separate from its residual crystal phases prior to eruption.

This general model of magma genesis is similar to those utilized by Jahn et al (1980), Jolly (1980) and Condie (1981) for production of Archean tholeiitic and komatiitic magma from plagioclase and garnet lherzolites (depleted and undepleted), peridotites and pyrolites.

5.4.2 TIPASJARVI, FINLAND

Jahn et al (1980) used rare earth element data to model three Finish greenstone belts. The small Tipasjarvi belt, long dimension 10 kilometres, is discussed as it contains all REE pattern types recognized by the study. Results required a heterogeneous lower crust - upper mantle system having three source materials which, by partial melting, produced either subvolcanic fractionating aliquots or extruded melts (Jahn et al 1980, Fig. 13):

1) theoretical pyroxene pyrolite - undepleted, producing three tholeiitic samples by varying degrees of partial melting, and a komatiite by a 45-50% partial melt with successive fractionation of olivine, clinopyroxene and plagioclase;

2) undefined LREE depleted source rock - possibly pyroxene pyrolite or spinel lherzolite, below the garnet stability pressure (less than 30 kb or 100 km) produces komatiitic magma by a high degree of partial melting (40-60%) followed by progressive fractionation of olivine + clinopyroxene and clinopyroxene + plagioclase;

3) very strongly LREE depleted source rock - mantle peridotite, in the garnet stability field (greater than 30 kb) produces tholeiites and komatiites by varying degrees of partial melting.

The authors emphasized that both partial melting and fractional crystallization were important in production of the Tipasjarvi suite of volcanic rocks and that a single volcanic conduit can access a variety of mantle reservoirs of distinct chemistry and age.

5.4.3 ABITIBI, CANADA

Jolly (1980) has proposed two models for the observed crystallization trends in Abitiba lavas:

1) fusion of an upper mantle (approximately 30 kb) source rock, garnet peridotite, enriched in LREE with elevation of one or more aliquots to less than 9 kilobars, followed by continuous fractionation and the rise of four 'series' of subvolcanic magmas which undergo high level (less than 1.4 kb or 5.3 km) fractionation and extrusion of individual rock types;

2) continuous high level (less than 9 kb or 30 km) fusion of plagioclase peridotite, LREE enriched, at progressively declining temperatures and elevation of four magma 'series' to subvolcanic levels (less than 1.4 kb or 5.3 km) followed by fractionation and extrusion.

The author notes that a shallow depth of fractionation is supported by crystallization sequences deduced from thin section study and as predicted by O'Hara (1968):
Magnesian Suite - olivine, orthopyroxene, clinopyroxene, plagioclase;
Tholeiitic Suite - olivine, plagioclase, clinopyroxene;
Calc-alkaline Suite - clinopyroxene plus plagioclase.

Abitibi lavas of any class may be found adjacent in almost all traverses requiring that many fractionating sources supply magma to eruptive centers. Recent modeling of Archean greenstone belts suggest a heterogeneous mantle undergoing varying degrees of partial melting at varying depths at approximately the same time. Heterogeneity may be due to mantle-only processes, but may also be effected by anatexis or high pressure conversion of crustal material (e.g. basalt to eclogite).

5.5 PETROGENESIS OF YELLOWKNIFE VOLCANIC ROCKS

5.5.1 SOURCE ROCKS AND LIMITATIONS

Magma is generated not only by partial melting of appropriate mantle source material, undepleted and/or depleted pyrolites or

peridotites (lherzolites), but also by anatexis of supracrustal material. Downwarping, subduction in more recent tectonics, of mafic volcanic rocks results in progressive metamorphism through amphibolite, garnet amphibolite and eclogite facies eventually reaching the solidus curve, likely the wet solidus. Composition of an anatectic melt is dependent upon original rock bulk composition, mineralogical phases of the metamorphic rock undergoing anatexis, and the degree of partial melting.

Morse (1980) notes that generation of basaltic magma from basaltic source material requires total melting at the liquidus. However, trace element modeling of Archean greenstones has shown:

1) an eclogite of tholeiitic composition (TH1) will produce tholeiitic magmas of composition TH2 by 50%, or less, partial melting (Condie and Harrison 1976; Arndt 1977); and

2) partial melting of garnet amphibolite or amphibolite (30-40%), or possibly garnet lherzolite (20-30%), may produce the same TH2 rock (Arth et al 1977, Jahn et al 1979).

Transformation from metabasalt, amphibolite and garnet amphibolite, to eclogite will vary over a range of temperature - pressure conditions, depending upon bulk composition, with a transition zone of garnet granolite. Upper amphibolite facies basaltic rocks have a mineral assemblage of hornblende-plagioclase-garnet-quartz-cummingtonite +/- biotite, chlorite, ilmenite, magnetite, sphene, rutile at a pressure/depth range of 2-8 kb/7-30 km. Eclogites (pyrope rich garnet - jadeite rich pyroxene omiphacite (Jd-Di)ss +/-

hypersthene or kyanite, quartz, rutile; +/- hornblende, zoisite;+/- glaucophane, epidote) are stable only under unusual conditions; generally very high pressure (15-20 kb/50-70 km) and low water content. A granolite assemblage (orthopyroxene-garnet-clinopyroxene-plagioclase-quartz +/- hornblende, biotite) is defined by Winkler (1976) to exist in the transition zone, under the condition of P_{H2O} much less than P_{TOTAL}. Granolites and eclogites of slightly different composition can be stable under the same P-T conditions.

Eclogites are of relatively minor occurrence in presently preserved Archean terrain, possibly due to slightly steeper thermal gradients and an early Archean lithosphere of less than 50 km (Condie 1980). The low P_{H2O} condition required for granolite and eclogite stability may not have been met by downwarping wet basaltic material. Hydrous tholeiitic metabasalt likely crossed the wet solidus curve prior to development of granolite or eclogite mineralolgy, hence partial melts were derived from amphibolites or garnet amphibolites. Crustal thickness of the Archean proto-Slave Province is therefore an important factor in determining source material and phases controlling composition of extruding magma.

Tonalitic material has been entrained in a diatreme intersected by deep mine workings within lower Kam Formation mafic lavas. Similar rock has been mapped in various field locations (Point Lake, Benjamin Lake, Ross Lake) as being unconformably overlain by rocks of the Yellowknife Supergroup volcano-sedimentary sequence, indicating an earlier sialic crust. Classification of Duck and Banting Formation

rocks as TH2 type basalts point to pre-existing TH1 tholeiitic basalts. Heterogeneous high and low Al_2O_3 trondhjemite/tonalite rocks, and TH1 tholeiites form the bimodal association utilized by Condie (1981) to generate andesitic granulites by metamorphism, and quartz monzonite-granite-granodiorite intrusives or felsic volcanics (FII) by anatexis.

Petrogenetic indications are derived through comparison of the Yellowknife volcanic rocks with Archean bulk average compositions, specific greenstone belts and more recent volcanism, utilizing trace and rare earth element modelling of magma genesis. Results suggest that mafic lavas of the Kam Formation (TH1) are partial melts of an undepleted (spinel?) lherzolite mantle source material while all other flows are anatectic melts of pre-existing crustal material. Felsic intrusives and some flows are attributed to partial melting of earlier crustal material, either bimodal or andesitic in composition.

Duck and Banting Formation basalts (TH2), all andesites (AI), and Banting Formation dacites (FI) were derived by varying degrees (20-40%) of TH1 basaltic source partial melting: amphibolites, garnet amphibolites or eclogites. Amphibolite and garnet amphibolite are preferred sources, possibly with both contributing magma during development of the Yellowknife greenstone belt.

Kam and Duck Formation dacites (FII) may be due to anatexis of either a bimodal trondhjemite/tonalite - amphibolite association or an andesitic granulite source rock. The Kam Formation dacite sample

population is too small (n=1) to positively characterize dacites of the formation. Discriminants for Duck Formation dacites are split between the amphibolite source (FI) and the more complex bimodal association or andesitic granulite source (FII).

5.5.2 DISCUSSION

The FeO_T vs Zr/TiO_2 plot, Figure 15, shows the Duck Formation having a wide range of Zr/TiO_2 values and a variable 'differentiation trend'. Diverse composition, notably basalts and basaltic andesites, may be due to a complex of lavas from lherzolite, amphibolite and/or garnet amphibolite source rocks extruded almost simultaneously via the same conduit system. Low Zr/TiO_2 samples plot within the OFB field but overlap onto the LKT field. The reason is unclear, but White, Jakes and Christie (1970) and Pearce and Cann (1973) suggest a gradation from LKT through CAB to shoshonites in volcanic arc settings, and that volcanic arc rocks are chemically more variable than OFB. Duck Formation data indicates a primitive volcanic arc setting.

Duck and Banting Formation samples yield J-type, hornblende controlled, differentiation trends on a CaO vs Y diagram, Figure 20. Kam Formation data suggests an L-type, pyroxene controlled, trend but a single high Y dacite analysis defines the curve. These observations agree with suggested amphibolite and lherzolite source rocks, respectively, however they may not be applicable to multi-source greenstone belts.

Dacite values from the Kam and Banting Formations both lie on the high-Y side of the typical calc-alkaline trend (Figure 20) and their magma source may be unrelated to those of adjacent mafic to intermediate lavas; possibly partial melts of an andesitic granulite phase. The Kam Formation dacite, Townsite or Brock flow, may be an extrusive phase of sub-volcanic intrusions which subsequently intruded the lava pile, e.g. Western or Stock Lake Granodiorite.

Figure 17, Zr-Ti-Y, shows a clear separation of basalts from possibly different source rocks. Kam Formation samples are similar to DSDP 37, enclose the average tholeiite value from undepleted lherzolite source rock and have a trend similar to chondritic values. Duck Formation data is distinct from Kam Formation, DSDP 37 and chondritic values; the higher Zr/Y ratio may be due to the amphibolite source rock and the broad range due to greater chemical diversity. Banting Formation rocks group in a high Zr - low Y area, with a few points scattering toward Kam Formation values; they trend similar to Kam Formation data but at greater Zr contents, reflecting a more siliceous or differentiated suite of rocks.

We therefore have a very diverse suite of volcanic rocks in the Yellowknife Supergroup, in accord with the model proposed by Henderson (1981) who discusses the Yellowknife supracrustal rocks in terms of depositional basins. Paleocurrent data from basinal turbidites indicate sediment transport normal to the fault basin margin, defined by orientation of the linear belt of mafic volcanics. Volcanism occurs along basin marginal faults and extends only a short way

into the basin proper, approximately 15 km at Yellowknife. Felsic volcanism occurs either within the basin or just outside the basin margin. This view of the Yellowknife belt is similar to the generalized model for Archean granite - greenstone belt terrain proposed by Lambert (1981).

Stationary hot spots cause initial doming, and then incipient rifting of Slave Province proto-continent, having both sialic (granodoritic) and simatic (tholeiitic) components. Early lavas extruded onto the rift floor are basaltic partial melts from undepleted (spinel?) lherzolite mantle source rocks, i.e. TH1 magmas. Subsequent volcanism is due to partial melting of pre-existing tholeiites, either proto-oceanic floor or very early post-rift lavas, to form TH2 tholeiitic magmas.

Felsic volcanism, associated with the lower and middle stages (Kam and Duck Formation) is ascribed to remelting of both the proto-continent trondhjemite/tonalite and basaltic rocks. Partial melting of this bi-modal source may result in later granodiorite, quartz-monzonite and granite batholitic diapirs. As they intrude the volcano-sedimentary sequence and the proto-continental crust they often mask the supracrustal disconformity with an intrusive contact. Later stage dacites (Banting Formation) were likely due to partial melting of proto-oceanic floor meta-basaltic material.

The Duck Formation LKT-OFB-CAB trend may be the result of interaction between mantle derived TH1 partial melt and basaltic crust

material, possibly in the region of the Moho discontinuity (30 km), to generate a relatively small amount of hyrid magma now identified as LKT composition. Partial melting of proto-oceanic floor TH1 basaltic material generated most of the TH2 mafic and all of the A1 intermediate composition flows of the Duck Formation. Felsic volcanics may have resulted from either, or both, differentiation of the magma from basaltic crust source rocks or/and partial melting of bimodal source rocks near the sialic crust - basaltic crust boundary. Low potassium tholeiite samples were taken from the up plunge core area, the lowermost exposure of Duck Formation rocks. In this position they are located stratigraphically similar to the low potassium tholeiites and spilites of the Solomon Island and Fiji; areas where the seismic zone is vertical or diffuse or virtually absent.

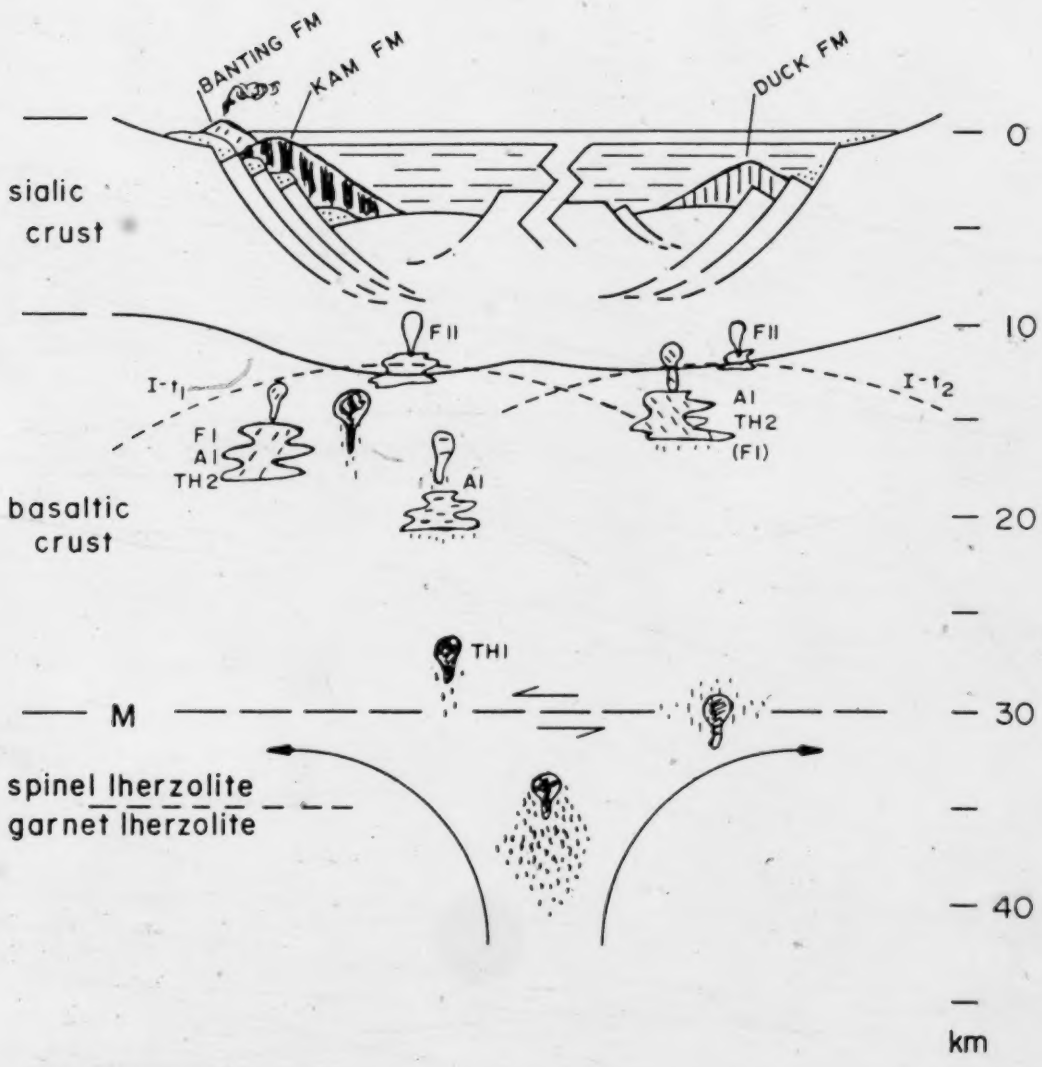

Legend

M - Moho discontinuity
I - Isotherm
t_1, t_2 - time
TH1, TH2, A1, F1, F11 - Magma types (after Condie 1981)

FIGURE 26 - Petrogenetic Model for Yellowknife Area

CHAPTER 6

CONCLUSIONS

1) The Yellowknife greenstone belt developed from magmas of differing petrogenetic histories, extruded contemporaneously through two systems: the Kam-Banting conduit system and the Duck conduit system.

2) The Kam Formation is dominated by ocean floor basalts (OFB); a few samples are low potassium tholeiites (LKT). A limited but definite tholeiitic trend is evident. Partial melting of mantle derived undepleted peridotite, possibly spinel lherzolite, resulted in type TH1 (light rare earth element depleted) mafic volcanism.

3) Crustal and mantle source rocks, varying degrees of partial melting and magma mixing resulted in extrusion of a chemically diverse Duck Formation. Petrogenetic interpretation is hindered by pervasive alteration of many samples (as seen in thin section), scatter on geochemical diagrams, and an open Rb-Sr system. These broad geochemical trends, however, are not due entirely to secondary processes.

4) Banting Formation volcanism followed partial melting of amphibolite, and probable hornblende controlled fractionation. Partial melting of meta-basaltic crustal material, TH1 composition similar to lowermost Kam Formation flows, resulted in primarily andesite-dacite magma composition, with minor basalt. Extrusion was

via part of the Kam conduit system, and overlapped with cessation of Kam Formation volcanism.

5) The rubidium-strontium systems did not remain closed, they have been episodically and/or continually reset at least down to 1900 Ma. 'Best' ages for the Kam Formation (Brock Townsite member) and Banting Formations are 2570 and 2490 Ma, respectively. The former is an age of regional metamorphism age related to the granodiorite batholiths at 2560-2580 Ma. The latter represents episodic downdating related to the Giant-Yellowknift Shear Zone (2510 Ma) and intrusion of the Prosperous Lake Granite (2520 Ma). Rubidium mobility caused an exceedingly low $^{87}Sr/^{86}Sr$ initial ratio (rotated isochron) and the estimated age of the Yellowknife Shear Zone is 2490 Ma. Minimum age of volcanism is 2640 Ma, the Pb-Pb age for the Western Granodiorite. Resetting continued on an irregular basis to 1900 Ma (Kam and Duck Formations), Rb-Sr; K-Ar ages on plutons.

6) The Yellowknife volcanic belt is a greenstone of moderate size and character; volcanic rocks are overwhelmingly subalkaline in character; both tholeiitic and calc-alkaline trends have been shown, no ultramafics and few rhyolites have been identified, mafic to felsic volcanic cycles are few and incomplete, the lateral extent and stratigraphic thickness are less than those of many Archean greenstone belts.

7) A model of ensialic development at a late stage in the evolution of the Slave craton is consistent with all known facts. The

Slave proto-craton was rifted by a mantle hot spot resulting in extrusion of tholeiitic basalts and basaltic andesites, derived from partial melting of mantle material. Partial melting of pre-existing hydrous basaltic crustal material produced intermediate to felsic volcanics of calc-alkaline affinity, with some mafic volcanism. Partial melting of pre-existing sialic crustal material resulted in extrusion of calc-alkaline felsic volcanic rocks.

BIBLIOGRAPHY

Arndt, N. and C. Brooks (1980) Penrose Conference Report on Komatiites. Geology, v.8, pp.155-156, March

Baragar, W.R.A. (1966) Geochemistry of the Yellowknife volcanic rocks. Canadian Journal of Earth Science, v.3, pp.668-702.

Baragar, W.R.A. and J.C. McGlynn (1976) Early Archean Basement in the Canadian Shield: A review of the evidence. Geological Survey of Canada, Paper 76-14, 21 pages.

Brown, I.C. (1949) Structure of the Yellowknife Gold Belt, Northwest Territories. Harvard University, unpublished Ph.D thesis.

(1952) A nomenclature of igneous rocks. Transactions of the Canadian Institute of Mining and Metallurgy, v.55, p.53.

Brown, C.E.G. and A.S. Dadson (1953) Geology of the Giant Yellowknife Mine. Transactions of the Canadian Institute of Mining and Metallurgy, v.56, pp.59-76, also Canadian Mining Bulletin, v.46, no.491, pp.151-168 (1953).

Boyle, R.W. (1961) The Geology, Geochemistry, and Origin of the Gold Deposits of the Yellowknife District. Geological Survey of Canada, Memoir 310, 193 pages.

Boyle, R.W. (1979) The geochemistry of gold and its deposits. Geological Survey of Canada, Bulletin 280, 584 pages.

Canadian Mines Handbook, Northern Miner Press Ltd., Toronto, Canada.

Campbell, N. (1949) The Con-Rycon Mine, Yellowknife, N.W.T. Bulletin of the Canadian Institute of Mining and Metallurgy, v.42, no.446, pp.288-292.

Cann, J.R. (1969) Spilites from the Carlsberg Ridge, Indian Ocean. Journal of Petrology, v.10, pp.1-19.

Chayes, F. (1964) A petrographic distinction between Cenozoic volcanics in and around the open oceans. Journal of Geophysical Research, v.69, p.1573.

Clee, T.E., K.G. Barr and M.J. Berry (1974) Fine structure of the crust near Yellowknife. Canadian Journal of Earth Science, v.11, pp.1534-1549.

Coish, R.A. (1974) Ocean floor metamorphism in the Betts Cove Ophiolite, Newfoundland. Contributions to Mineralogy and Petrology, v.60, pp.255-270.

Condie, Kent C. (1976) Trace element geochemistry of Archean greenstone belts. Earth Science Reviews 12, pp.393-417.

Condie, K.C. (1976) Trace element models for the origin of Archean volcanic rocks, in B.F. Windley (Ed.) The Early History of the Earth.

(1981) Archean Greenstone Belts. Developments in PreCambrian Geology 3, Elsevier Scientific Publishing Company.

Condie, K.C. and W.R.A. Baragar (1974) Rare-earth element distributions in volcanic rocks from Archean greenstone belts. Contributions to Mineralogy and Petrology, v.45, pp.237-246.

Cumming, G.L. and F. Tsong (1975) Variations in the isotopic composition of volitilized lead and the age of the Western Granodiorite, Yellowknife, Northwest Territories. Canadian Journal of Earth Science, v.12, pp.558-573.

Drury, S.A. (1977) Structures induced by granite diapirs in the Archaean greenstone belt at Yellowknife, Canada: Implications for Archaean geotectonics. Journal of Geology, v.85, pp.345-358.

(1979) Rare-earth and other trace element data bearing on the origin of Archaean granitic rocks from Yellowknife, Northwest Territories. Canadian Journal of Earth Science, v.16, pp.809-815.

Easton, R.M. and V. Jackson (1981) Geology of the Walsh Lake Map Area, preliminary map (1:10,000 approx.). E.G.S. 1981-3, D.I.A.N.D., Yellowknife, N.W.T.

Easton, R.M., C. Ellis, H. Helmstaedt, V. Jackson, B. O'Hearn, M. Dean, H.C. Bruneau, and J. Wahlworth (1982) Geology of the east side of Yellowknife Bay (1:10,000 approx.). E.G.S. 1982-5, D.I.A.N.D., Yellowknife, N.W.T.

Ewing, T.E. (1979) Two calc-alkaline volcanic trends in the Archean: Trace Element Evidence. Contributions to Mineralogy and Petrology, v.70, no.1, pp.1-7.

Faure, G. (1977) Principles of Isotope Geology. John Wiley and Sons, Inc.; 464 pages.

Floyd, P.A. and Winchester, J.A. (1975) Magma type and tectonic setting discrimination using immobile elements. Earth and Planetary Science Letters, v.27, pp.211-218.

(1978) Identification and discrimination of altered and metamorphased volcanic rocks using immobile elements. Chemical Geology, v.21, pp.291-306.

Folinsbee, R.E., H. Baadsgaard, G.L. Cumming and D.C. Green (1968) A very ancient island arc. in The Crust and Upper Mantle of the Pacific Area. (Ed.) L. Knopoff, C.L.Drake and P.J.Hart. American Geophysical Union, Geophysics Monograph, v.12, pp.441-448.

Frith, R.A. (1973) The geology of the Bear-Slave boundary in the Indin Lake area, District of Mackenzie. in Report of Activities, Part A. Geological Survey of Canada, Paper 73-1A, pp.146-148.

(1978) Tectonics and metamorphism along the southern boundary between the Bear and Slave Structural Provinces. in Metamorphism in the Canadian Shield. Geological Survey of Canada, Paper 78-10, pp.103-113.

Frith, R.A., R. Frith, H. Helmstaedt, J. Hill, and R. Leatherbarrow (1974) The geology of the Bear-Slave boundary in the Indin Lake area, District of Mackenzie. in Report of Activities, Part A. Geological Survey of Canada, Paper 74-1A, pp.165-171.

Frith, R.A. and J.D. Hill (1975) The geology of the Hackett-Back River greenstone belt - preliminary account. in Report of Activities, Part C. Geological Survey of Canada, Paper 75-1C, pp.367-370.

Frith, R.A. and R. Leatherbarrow (1975) Preliminary report of the geology of the Arseno Lake map-area (86B/12), District of Mackenzie. in Report of Activities, Part A. Geological Survey of Canada, Paper 75-1A, pp.317-321.

Frith, Rosaline, R.A. Frith and R. Doig (1977) The geochronology of the granitic rocks along the Bear-Slave Structural Province boundary, northwest Canadian Shield. Canadian Journal of Earth Science, v.14, pp.1356-1373.

Fraser, J.A. (1978) Metamorphism in the Churchill Province, District of Mackenzie. in Metamorphism in the Canadian Shield. Geological Survey of Canada, Paper 78-10, pp.195-202.

Fraser, J.A., P.F. Hoffman, T.N. Irvine, G. Mursky (1972) The Bear Province. in Variations in Tectonic Styles in Canada. Geological Association of Canada, Special Paper No. 11, pp.453-503.

Fyson, W.F. (1975) Fabrics and deformation of Archaean metasedimentary rocks, Ross Lake - Gordon Lake area, Slave Province, Northwest Territories. Canadian Journal of Earth Science, v.12, pp.765-776.

Goff, S.P. and C.M. Scarfe (1981) Personal communication of unpublished study, "A review of element stability of altered volcanic rocks and the use of immobile element diagrams as petrogenetic and tectonic indicators." University of Alberta, Department of Geology.

Goodwin, A.M. (1972) The Superior Province. in Variations in Tectonic Styles in Canada. Geological Association of Canada, Special Paper No. 11, pp.527-623.

(1977) Archean Volcanism in Superior Province, Canadian Shield. in Volcanic Regimes in Canada. Geological Association of Canada, Special Paper No. 16, pp.205-241.

(1979) Archean volcanic studies in the Timmins - Kirkland Lake - Noranda region of Ontario and Quebec. Geological Survey of Canada, Bulletin 278.

Green, D.C., H. Baadsgaard and G.L. Cumming (1968) Geochronology of the Yellowknife area, Northwest Territories, Canada. Canadian Journal of Earth Science, v.5, pp.725-735.

Green, D.C. and H. Baadsgaard (1971) Temporal evolution and petrogenesis of an Archaean crustal segment at Yellowknife, N.W.T., Canada. Journal of Petrology, v.12, no.1, pp.177-217.

Hauer, L. (1979) Preliminary geological map of the northern end of the Yellowknife greenstone belt. E.G.S. 1979-10, D.I.A.N.D., Yellowknife, N.W.T.

Helmstaedt, H, J. King and R. Boodle (1980) Geology of the Banting and Walsh Lakes Map Area. N.T.S. 85J/9, scale 1:10,000 (approx.). E.G.S. 1980-5, D.I.A.N.D., Yellowknife, N.W.T.

Henderson, J.F. and I.C. Brown (1952) The Yellowknife greenstone belt. Geological Survey of Canada, Paper 52-28.

(1966) Geology and structure of the Yellowknife greenstone belt, District of Mackenzie, N.W.T. Geological Survey of Canada, Bulletin 141, 87 pages.

Henderson, J.B. (1970) Stratigraphy of the Archean Yellowknife Supergroup, Yellowknife Bay - Prosperous Lake Area, District of Mackenzie. Geological Survey of Canada, Paper 70-26, 12 pages.

(1972) Sedimentology of Archean turbidites at Yellowknife, Northwest Territories. Canadian Journal of Earth Science, v.9, p.882.

(1975) Sedimentology of the Archean Yellowknife Supergroup at Yellowknife, District of Mackenzie. Geological Survey of Canada, Bulletin 246.

(1978) Age and origin of the gold-bearing shear zones at Yellowknife, Northwest Territories. in Current Research, Part A. Geological Survey of Canada, Paper 78-1A, pp.259-262.

(1981) Archaean Basin Evolution in the Slave Province, Canada. in Precambrian Plate Tectonics, pp.213-235. (Ed.) A. Kroner, Developments in Precambrian Geology 4. Elsevier Scientific Publishing Company.

Hoffman, P.F. and J.B. Henderson (1972) Archean and Proterozoic sedimentary and volcanic rocks of the Yellowknife - Great Slave Lake area, Northwest Territories. in Guidebook to Field Excursion A28. International Geological Congress, Twenty-fourth Session, Montreal, Canada.

Hughes, C.J. (1973) Spilites, keratophyres and the igneous spectrum. Geology Magazine, v.109(6), pp.513-527.

Humphries, Susan and Geoffrey Thompson (1978) Trace element mobility during hydrothermal alteration of oceanic basalts. Geochimica et Cosmochimica Acta, v.48, pp.127-136.

Jahn, B-M, B. Auvray, S. Blais, R. Capdevila, J. Cornichet, F. Vidal and J. Hameurt (1980) Trace element geochemistry and petrogenesis of Finnish greenstone belts. Journal of Petrology, v.21 pt.2, pp.201-244.

Jenner, G.A., B.J. Fryer and S.M. McLennan (1981) Geochemistry of the Archean Yellowknife Supergroup. Geochimica et Cosmochimica Acta, v.45, pp.1111-1129.

Jensen, L.S. (1976) A new cation plot for classifying subalkalic volcanic rocks. Ontario Division of Mines (Ontario Geological Survey), Miscellaneous Paper 66.

Jolliffe, A.W. (1938) Yellowknife Bay - Prosperous Lake Area, Northwest Territories. Geological Survey of Canada, Paper 38-21.

(1942) Yellowknife Bay, District of Mackenzie, Northwest Territories. Scale - 1 inch: mile or 1:63,360. Geological Survey of Canada, Map 709A.

Jolly, W.T. (1980) Development and degradation of Archean lavas, Abitibi area, Canada, in light of major element geochemistry. Journal of Petrology, v.21 pt.2, pp.323-363.

Kerrich, R., W.S. Fyfe, and I. Allison (1977) Iron reduction around gold-quartz veins, Yellowknife District, N.W.T., Canada. Economic Geology, v.72, pp.657-663.

Kerrich, R. and I. Allison (1978) Vein geometry and hydrostatics during Yellowknife mineralization. Canadian Journal of Earth Science, v.15, pp.1653-1660.

Lambert, M.B. (1977) Anatomy of a greenstone belt - Slave Province, N.W.T. in Volcanic Regimes in Canada. Geological Association of Canada, Special Paper No. 16, pp.331-340.

Lambert, R.St.J. (1981) Earth tectonics and thermal history: Review and hot-spot model for the Archean. in Precambrian Plate Tectonics, pp.453-466, (Ed.) A. Kroner, Developments in Precambrian Geology 4. Elsevier Scientific Publishing Company.

Lambert, R.St.J. (1981) (Personal Communication) Strontium Standard SRM 987 results.

Lambert, R.St.J. and J.G. Holland (1974) Yttrium geochemistry applied to petrogenesis utilizing calcium-yttrium relationships in minerals and rocks. Geochimica et Cosmochimica Acta, v.38, pp.1393-1414.

MacDonald, G.A. and T. Katsura, (1964) Chemical composition of Hawaiian lavas. Journal of Petrology, v.5, p.82.

McGlynn, J.C. and J.B. Henderson (1972) The Slave Province. in Variations in Tectonic Styles in Canada. Geological Association of Canada, Special Paper No. 11, pp.505-526.

Morse, S.A. (1980) Basalts and phase diagrams. Springer-Verlag New York Inc., 493 pages.

Naldrett, A.J., A.M. Goodwin, T.L. Fisher and R.H. Ridler (1978) The sulfur content of Archean volcanic rock and a comparison with ocean floor basalts. Canadian Journal of Earth Science, v.15, pp.715-728.

Nielsen, P.A. (1978) Metamorphism of the Arseno Lake area, Northwest Territories. in Metamorphism in the Canadian Shield. Geological Survey of Canada, Paper 78-10, pp.115-122.

Nikic, Z., H. Baadsgaard, R.E. Folinsbee and A.P. Leech (1975) Diatreme containing boulders of 3030 m.y. old tonalite gneiss, Con Mine, Yellowknife, Slave Craton. Geological Society of America, Abstract in Program, v.7, p.1213.

Nikic, Z., H. Baadsgaard, R.E. Folinsbee, J. Krupicka and A. Leech (1980) Boulders from the basement, the trace of an ancient crust? in Selected studies of Archaean gneisses and Lower Proterozoic rocks, southern Canadian Shield. G.B. Morey and G.Y. Hanson (ed.). Geological Society of America, Special Paper No. 182, pp.169-175.

O'Hara, M.J. (1968) The bearing of phase equilibrium studies in synthetic and natural systems on the origin and evolution of basic and ultrabasic rocks. Earth Science Reviews, v.4, pp.69-133.

Pearce, J.A., and J.R. Cann (1973) Tectonic setting of basic volcanic rocks - Determined using trace element analyses. Earth and Planetary Science Letters, v.19, pp.290-300.

Pearce, T.H., B.E. Gorman, and T.C. Birkett (1977) The relationship between major element chemistry and tectonic environment of basic and intermediate volcanic rocks. Earth and Planetary Science Letters, v.36, pp.121-132.

Presnall, D.C., J.R. Dixon, T.H. O'Donnell and S.A. Dixon (1979) Generation of mid-ocean ridge tholeiites. Journal of Petrology, v.20, pp.3-36.

Price, R.A. and J.W. Douglas (1972) Variations in Tectonic Styles in Canada. Geological Association of Canada, Special Paper No. 11, 688 pages.

Ramsay, C.R. and C. Kamineni (1977) Petrology and evolution of an Archean metamorphic aureole in the Slave Craton, Canada. Journal of Petrology, v.18, no.3, pp.460-486.

Ringwood, A.E. (1982) Phase Transformations and differentiation in subducted Lithosphere: Implications for mantle dynamics, basalt petrogenesis and crustal evolution. Journal of Geology, v.90, pp.611-643.

Robertson, D.K. and G.L. Cumming (1968) Lead and sulfur isotope ratios from the Great Slave Lake area, Canada. Canadian Journal of Earth Science, v.5, pp.1267-1276.

Schwarzer, R.R. and J.J.W. Rogers (1974) A worldwide comparison of alkali olivine basalts and their differentiation trends. Earth and Planetary Science Letters, v.23, pp.286-296.

Steep, N.H. and B.F. Windley (1982) Archean plate tectonics: Constraints and inferences. Journal of Geology, v.90, pp.363-379.

Solomon, S.C. (1976) Geophysical constraints on radial and lateral temperature variations in the upper mantle. American Mineralogist, v.61, pp.788-803.

Steiger, R. and E. Jager (1977) Subcommission on Geochronology: convention on the use of decay constants in geo- and cosmochronology. Earth and Planetary Science Letters, v.36, pp.359-362.

Stockwell, C.H. (1933) Great Slave Lake - Coppermine River Area, Northwest Territories. Geological Survey of Canada, Summary Report 1932, pt.C, pp.37-63.

(1963) Second report on structural provinces, orogenies, and time-classification of rocks of the Canadian Shield. Geological Survey of Canada, Paper 62-17, pp.123-133.

(1964) Fourth report on structural provinces, orogenies, and time-classification of rocks of the Canadian Precambrian Shield; in Age Determinations and Geological Studies. Geological Survey of Canada, Paper 64-17, pt.II, pp.1-24.

(1970) Geology of the Canadian Shield, Chapter IV, in Geology and economic minerals of Canada; (Ed.) R.J.W. Douglas, Geological Survey of Canada, Economic Geology Report No. 1, pp.44-150.

Stockwell, C.H. and D.F. Kidd (1932) Metalliferous mineral possibilities of the mainland part of the North West Territories. Geological Survey of Canada, Summary Report 1931, pt.C, pp.70-85.

Thompson, P.H. (1978) Archean regional metamorphism in the Slave Structural Province - A new perspective on some old rocks. in Metamorphism in the Canadian Shield. Geological Survey of Canada, Paper 78-10, pp.85-102.

Traill, R.J. (1950) Dacites of the Lower Yellowknife Group (unpublished B.Sc. thesis). Queen's University Library, Kingston, Ontario.

Winchester, J.A. and P.A. Floyd (1976) Geochemical magma type discrimination: Application to altered and metamorphosed basic igneous rocks. Earth and Planetary Science Letters, v.28, pp.459-469.

(1977) Geochemical discrimination of different magma series and their differentiation products using immobile elements. Chemical Geology, v.20, pp.325-343.

Windley, B.F. (1977) The Evolving Continents. John Wiley and Sons.

Wright, G.M. (1967) Geology of the southwestern barren grounds, parts of the Districts of Mackenzie and Keewatin. Geological Survey of Canada, Memoir 350.

APPENDIX A

GEOCHEMICAL DATA

		Page
1)	X-RAY FLUOORESCENCE	
	- Procedure and Precision	147
	- Data	148
2)	ATOMIC ABSORPTION SPECTROSCOPY	
	- Procedure	166
	- Standards and Recommended Values	166
	- Data	168

APPENDIX A

1) MAJOR AND MINOR ELEMENTS BY X-RAY FLUORESCENCE

Analyses were performed on a Philips 1450 AHP (Automated Hardeure Programmed) unit at McMaster University, Hamilton, Ontario. Trace element analyses used 3.5 grams of powder, as fine as possible but at least -200 mesh, mixed with 3 drops of Moliwol, an organic compound binder, and pressed in an aluminum cup under 20,000 p.s.i. The pellet was then analyzed directly. All trace element 'raw' count rates were corrected for major element absorption effects using (i) alpha coefficients, (ii) absorption coefficients or (iii) the Mo-compton peak method.

Major element analyses used 0.5 grams of sample with 3.0 grams of flux (a 1:1 mixture of $Li_2 B_4O_7$ and $LiBO_2$). It was fused in a Pt-Au crucible and poured into a Pt-Au mold, the exact size of the XRF sample holder. The glass disc from the mold was run directly. Again, corrections were made for absorption.

For the fusion method, the major elements have a precision better than 1% of the value (one sigma standard deviation). Data given in Table A1 on 2 standards are typical.

TABLE A1: Recommended Values for International Standards

STANDARDS	JBI			DRN		
	X n=13		Rec'd Value	X n=13		R.V.
Major Elements						
SiO_2	52.99	.30	53.14	54.53	.27	54.15
TiO_2	1.30	.01	1.35	1.10	.01	1.13
Al_2O_3	14.63	.08	14.76	17.83	.14	17.98
Fe_2O_3	8.86	.08	9.10	9.93	.09	9.92
MnO	.15	.01	.15	.22	.01	.22
MgO	8.01	.14	7.84	4.45	.09	4.58
CaO	9.29	.10	9.44	7.11	.06	7.26
Na_2O	2.78	.11	2.82	3.01	.09	3.07
K_2O	1.39	.03	1.43	1.70	.03	1.77
P_2O_5	.27	.01	.26	.25	.01	.26

Minor Elements - Precision

Rb - ± 2% of the values down to 30 ppm; ± 10% below that

Sr - ± 1% of the values down to 50 ppm; ± 5% below that

Zr - ± 7% in Yellowknife sample conc. range.

Y - ± 10% in Yellowknife sample conc. range

Nb - ± 20% in Yellowknife sample conc. range.

Trace element results are not as good as the major elements. There are two reasons for this, 1) a much lower level of concentration and 2) the 'real' answer is not known as well in the standards. Recommended values for precision are as on Table A1.

Accuracy is considered good where reliable values in the standard are known.

The raw data for major element analyses performed on glass discs totalled between 97-100%, recalculated to 100% anhydrous. A few samples gave low totals and were checked for suspected high volatile content:

Sample #	Raw Data Total	Loss On Ignition*
740-8b	95.23	4.73
740-9	93.90	8.56
740-10	95.98	5.18
740-11	94.78	4.94
803-4	93.67	8.02

* (1000°C for 30 minutes)

There likely is not a direct correspondence between raw data total and L.O.I. but it is a good guide to total volitile content. The glass fusion process with flux probably does not completely remove all volitile constituents.

Table A2. X-ray fluorescence analyses. (1) Lower Kam Formation

Sample:	620-10	620-20	620-30	620-40	620-50	620-60	620-70	620-50B	703-1A	703-2A
SiO_2	50.07	53.44	50.39	54.37	50.21	51.04	50.13	49.75	52.12	52.45
Al_2O_3	13.68	15.11	13.65	13.27	14.79	14.76	15.41	14.96	13.72	14.56
Fe_2O_3	12.88	10.09	14.99	12.44	13.21	13.32	12.01	12.86	13.97	12.74
MgO	6.56	5.92	6.43	7.38	7.77	7.99	9.84	7.44	6.69	4.27
CaO	13.51	11.97	10.38	9.19	9.82	9.84	9.01	9.33	9.41	10.26
Na_2o	2.14	2.32	1.80	1.80	2.86	1.73	1.97	4.34	2.00	3.30
K_2O	.10	.08	.82	.36	.10	.09	.18	.09	.02	.38
TiO_2	.79	.87	1.17	.90	.93	.94	1.07	.92	1.65	1.61
MnO	.22	.17	.26	.22	.25	.22	.26	.26	.22	.29
S	0.04	0.04	0.05	0.04	0.03	0.05	0.03	0.03	0.04	0.05
P_2O_5	.06	.03	.10	.06	.07	.06	.10	.06	.20	.14
Ba	0	0	97	0	7	0	14	5	39	13
Nb	2	1	2	1	2	0	5	1	2	0
Zr	51	39	71	63	58	57	69	58	107	94
Y	25	19	30	22	23	26	23	25	37	34
Sr	122	187	105	85	151	84	144	158	152	95
Rb	1	0	28	13	2	3	9	1	10	4

Table A2. X-ray fluorescence analyses. (1) Lower Kam Formation (continued)

Sample:	703-2C	703-3A	710-1A	710-2B	710-3B	710-4A	710-5A	710-6A	710-7A	710-8A
SiO_2	52.46	48.90	52.10	52.12	52.43	76.11	52.22	52.21	56.37	54.40
Al_2O_3	16.33	14.49	13.70	13.56	15.44	12.58	14.06	12.16	13.63	14.39
Fe_2O_3	10.44	15.28	13.49	14.73	12.90	2.19	14.19	11.94	10.55	9.08
MgO	1.90	6.74	7.53	4.27	4.77	1.09	6.23	9.51	7.81	8.73
CaO	15.47	9.81	7.90	9.57	11.28	.94	9.74	11.17	8.83	9.58
Na_2O	1.69	2.59	2.49	2.80	1.61	4.97	1.72	1.57	.80	2.55
K_2O	.08	.24	1.39	.40	.23	1.72	.19	.40	.86	.30
TiO_2	1.33	1.52	1.02	2.12	.99	.32	1.24	.75	.80	.73
MnO	.17	.29	.28	.25	.31	.05	.31	.23	.33	.21
S	0.03	0.03	0.04	0.04	0.04	0.02	0.06	0.07	0.04	0.02
P_2O_5	.14	.14	.09	.17	.05	.03	.10	.05	.04	.04
Ba	5	0	140	247	28	132	7	32	55	10
Nb	1	0	3	0	0	0	3	2	2	2
Zr	88	90	77	113	58	92	75	53	55	57
Y	28	32	25	42	21	8	29	17	18	19
Sr	312	125	81	156	174	90	127	159	87	118
Rb	1	1	44	4	2	24	1	13	28	7

Table A2. X-ray fluorescence analyses. (1) Lower Kam Formation (continued)

Sample:	710-9A	710-10A	710-11A	710-12A	710-12C	710-13A	725-6A	803-1	803-2	803-3
SiO_2	54.00	54.31	53.22	53.44	63.63	50.95	71.87	53.64	54.83	53.32
Al_2O_3	14.49	14.79	14.25	13.11	12.79	14.20	13.90	15.07	15.32	12.95
Fe_2O_3	9.89	10.01	11.73	14.43	6.19	14.06	3.76	11.57	10.95	14.70
MgO	8.08	8.12	9.15	4.64	1.87	6.20	.85	6.53	7.98	5.49
CaO	11.03	9.22	7.81	10.05	8.13	10.41	2.21	10.53	7.10	6.65
Na_2O	2.07	1.85	2.26	1.76	5.01	2.11	3.45	1.06	2.20	4.45
K_2O	.26	.24	.39	.06	.85	.08	2.93	.15	.18	.24
TiO_2	.64	1.11	.88	1.93	1.89	1.57	.75	1.10	1.15	1.79
MnO	.28	.24	.25	.32	.28	.26	.06	.23	.19	.20
S	0.03	0.05	0.03	0.03	0.04	0.04	0.04	0.05	0.03	0.05
P_2O_5	.84	.10	.07	.25	.24	.16	.22	.11	.09	.22
Ba	31	6	48	3	18	1	633	0	6	28
Nb	3	0	4	5	3	4	14	2	0	11
Zr	48	74	72	151	159	118	295	75	76	169
Y	17	24	23	52	53	42	48	25	27	52
Sr	83	171	55	103	94	139	101	131	135	385
Rb	7	7	5	0	0	1	64	0	2	3

Table A2. X-ray fluorescence analyses. (1) Lower Kam Formation (continued)

Sample:	803-4	803-5	803-6	803-7	803-8	803-9	815-1	815-2	815-3	815-4
SiO_2	53.48	51.93	52.99	54.02	50.45	52.33	58.87	50.05	57.62	76.28
Al_2O_3	13.98	14.82	12.76	12.67	13.26	12.64	14.14	12.40	15.18	13.61
Fe_2O_3	9.64	12.27	15.04	13.63	15.67	14.69	10.59	18.12	8.18	.77
MgO	1.98	5.01	5.63	4.78	6.48	5.08	5.56	5.72	5.00	.26
CaO	12.81	11.24	7.29	12.04	10.37	10.89	4.34	9.23	4.93	.92
Na_2O	5.61	2.06	3.84	.65	1.78	2.04	4.34	1.89	6.75	3.68
K_2O	.16	.18	.22	.17	.53	.14	.42	.28	.32	4.41
TiO_2	1.85	1.97	1.30	1.63	1.17	1.74	1.31	1.86	1.54	.06
MnO	.22	.30	.21	.20	.20	.23	.15	.28	.17	.03
S	0.05	0.03	0.05	0.04	0.04	0.04	0.04	0.06	0.06	0.02
P_2O_5	.26	.22	.23	.21	.10	.22	.28	.17	.31	0.00
Ba	22	3	15	4	58	0	24	4	19	571
Nb	0	2	3	1	0	0	15	0	18	12
Zr	164	142	163	149	73	137	219	124	223	75
Y	52	42	49	48	30	42	36	41	39	12
Sr	94	87	95	472	101	112	128	113	68	58
Rb	1	0	2	2	14	1	6	2	3	111

Table A2. X-ray fluorescence analyses. (1) Lower Kam Formation (continued)

Sample	815-5	815-6	815-7	815-8AB	815-9	815-10	815-11	815-12	815-13
SiO_2	75.99	51.25	53.15	54.00	49.38	55.15	52.32	52.06	49.76
Al_2O_3	13.80	13.94	14.30	15.73	14.97	14.68	14.13	12.34	17.38
Fe_2O_3	.98	14.57	11.45	13.09	13.22	13.55	11.61	11.71	11.06
MgO	.38	7.01	7.51	8.08	7.32	8.75	7.57	9.23	7.65
CaO	1.01	6.13	10.70	2.54	12.02	5.39	11.62	11.40	7.76
Na_2O	3.52	4.58	1.52	4.29	1.53	1.13	1.41	1.27	2.63
K_2O	4.22	.52	.40	.28	.14	.12	.17	1.02	2.76
TiO_2	.07	1.53	.71	1.44	1.10	.94	.88	.70	.73
MnO	.02	.34	.17	.14	.22	.20	.21	.21	.24
S	0.02	0.05	0.05	0.03	0.07	0.05	0.04	0.03	0.04
P_2O_5	0.00	.12	.08	.41	.10	.08	.08	.06	.05
Ba	828	4	30	100	15	0	0	125	802
Nb	12	0	2	17	3	3	2	1	11
Zr	82	98	73	263	81	77	67	54	47
Y	13	35	20	47	31	26	23	18	17
Sr	73	41	137	95	235	96	147	90	118
Rb	109	10	9	0	0	0	0	21	92

Table A2. X-ray fluorescence analyses. (2) Upper Kam Formation

Sample:	712-1B	712-2A	712-3A	712-4A	712-5A	712-6B	712-7B	714-1B	714-2B	714-3A
SiO_2	49.62	49.09	49.32	48.67	47.13	49.88	48.40	51.58	50.57	52.84
Al_2O_3	15.65	15.09	14.51	15.13	14.76	13.62	14.26	13.80	14.73	13.53
Fe_2O_3	11.63	14.01	13.39	15.63	15.99	16.33	15.75	13.29	13.42	12.70
MgO	9.11	7.11	8.33	6.22	6.27	7.41	7.67	7.26	6.42	6.27
CaO	10.53	10.88	10.89	8.70	11.47	6.66	9.24	9.42	10.80	9.33
Na_2O	1.74	1.82	1.89	2.95	2.03	3.76	2.63	2.48	1.97	3.51
K_2O	.71	.60	.10	.63	.22	.09	.34	.76	.64	.27
TiO_2	.77	1.08	1.16	1.57	1.63	1.85	1.21	1.05	1.09	1.16
MnO	.19	.24	.31	.36	.34	.30	.39	.27	.28	.28
S	0.05	0.10	0.05	0.04	0.03	0.03	0.03	0.04	0.05	0.03
P_2O_5	.05	.10	.10	.14	.16	.17	.10	.10	.10	.12
Ba	29	23	12	89	29	6	23	19	53	5
Nb	1	0	0	1	0	1	0	0	1	3
Zr	50	66	73	100	112	127	73	76	80	89
Y	22	24	27	32	34	39	30	23	25	28
Sr	93	109	113	148	111	80	109	112	160	107
Rb	25	17	3	14	3	1	7	30	14	3

Table A2. X-ray fluorescence analyses. (2) Upper Kam Formation (continued)

Sample:	714-4A	714-5BC	716-1A	716-2B	716-3A	716-4B	725-1A	725-1BC	725-2B	725-3
SiO_2	50.98	54.46	53.77	53.74	53.54	51.76	49.81	50.97	50.93	54.28
Al_2O_3	14.06	11.37	13.66	13.66	13.77	12.42	14.10	13.93	13.87	16.41
Fe_2O_3	13.76	11.16	10.99	11.58	12.38	11.46	13.56	13.57	14.06	8.89
MgO	7.50	8.36	8.64	7.67	7.35	8.32	6.54	6.33	6.81	4.72
CaO	8.62	8.48	8.23	9.57	9.90	12.54	12.05	10.64	10.72	11.05
Na_2O	2.66	4.64	2.14	2.32	1.62	2.04	2.08	2.85	2.11	3.25
K_2O	.88	.23	1.52	.27	.21	.46	.46	.31	.02	.22
TiO_2	1.13	.96	.80	.88	.94	.73	1.09	1.10	1.16	.99
MnO	.29	.28	.19	.25	.23	.21	.20	.20	.20	.16
S	0.03	0.04	0.03	0.03	0.05	0.04	0.03	0.02	0.05	0.06
P_2O_5	.11	.06	.06	.05	.06	.06	.10	.10	.11	.05
Ba	40	0	245	12	7	5	11	11	9	10
Nb	5	2	2	2	4	0	2	0	3	2
Zr	93	69	62	67	75	246	71	69	74	60
Y	27	25	22	21	24	17	26	29	30	24
Sr	101	88	108	99	128	94	179	154	145	146
Rb	35	4	18	5	2	7	5	3	2	3

Table A2. X-ray fluorescence analyses. (2) Upper Kam Formation (continued)

Sample:	725-3C	725-4A	725-5	730-1A	730-2A	730-3A	730-4	730-5A	730-5B	730-6A	730-7
SiO_2	48.72	50.83	49.39	52.88	54.18	49.88	51.04	46.98	50.70	54.67	52.13
Al_2O_3	14.60	14.90	14.39	14.60	14.32	14.20	13.72	14.83	13.41	14.39	14.07
Fe_2O_3	14.80	12.98	14.69	11.01	10.58	11.89	13.68	16.84	12.43	13.79	12.43
MgO	8.25	7.01	7.94	7.96	6.91	9.73	7.35	8.21	6.99	6.58	7.05
CaO	9.38	10.93	9.42	10.50	10.43	11.54	10.31	9.05	13.38	12.23	10.52
Na_2O	2.02	1.73	2.11	1.69	2.21	1.58	1.76	2.08	1.30	-3.54	1.80
K_2O	.75	.36	.67	.33	.25	.10	.63	.54	.54	.47	.64
TiO_2	1.14	1.01	1.08	.76	.81	.79	1.08	1.06	.94	1.03	1.02
MnO	.24	.19	.22	.22	.22	.24	.33	.32	.21	.27	.23
S	0.04	0.05	0.05	0.05	0.03	0.05	0.08	0.21	0.16	0.09	0.04
P_2O_5	.09	.07	.10	.06	.09	.05	.10	.09	.10	.10	.10
Ba	18	0	7	16	22	1	46	42	43	7	25
Nb	0	1	0	1	3	5	3	2	2	2	1
Zr	66	69	67	72	84	53	78	71	69	74	71
Y	24	27	27	22	23	17	25	21	23	23	22
Sr	161	122	153	143	180	132	128	134	116	163	124
Rb	14	5	12	8	5	3	13	15	11	3	9

Table A2. X-ray fluorescence analyses. (3) Duck Formation

Sample:	720-3B	720-4AC	720-5A	720-6A	720-6B	720-7A	720-7D	720-8A	720-8C	720-9B
SiO_2	55.84	57.05	53.96	53.27	53.05	58.98	53.78	55.54	57.34	58.52
Al_2O_3	14.98	14.93	15.41	13.98	15.99	16.16	16.12	15.01	15.28	14.05
Fe_2O_3	10.49	10.46	10.09	11.80	10.34	6.41	10.99	12.24	8.49	8.59
MgO	5.83	4.59	6.34	6.86	6.53	2.60	3.24	6.71	4.17	4.80
CaO	5.24	7.33	8.49	9.13	8.66	13.78	9.28	5.25	7.46	8.28
Na_2O	4.65	3.15	2.63	2.15	2.56	.12	3.11	2.19	4.03	2.85
K_2O	.37	.58	.69	.60	.41	.96	.36	1.15	.80	.95
TiO_2	1.95	1.32	2.02	1.79	2.06	.72	2.45	1.55	2.01	1.34
MnO	.19	.25	.18	.27	.24	.07	.41	.21	.26	.24
S	0.04	0.03	0.05	0.05	0.04	0.04	0.04	0.04	0.05	0.04
P_2O_5	.46	.33	.20	.15	.16	.21	.27	.16	.16	.37
Ba	41	20	95	35	27	29	34	38	36	117
Nb	14	12	6	5	5	6	6	3	3	13
Zr	202	110	91	108	176	129	120	108	188	235
Y	49	45	33	29	33	38	42	26	32	39
Sr	145	144	260	201	282	101	255	146	180	148
Rb	6	8	17	11	8	22	5	26	19	21

Table A2. X-ray fluorescence analyses. (3) Duck Formation (continued)

Sample:	720-10A	720-10B	720-11	721-1A	721-2B	722-1A	722-2B	722-3A	722-4A	722-4B
SiO_2	60.51	55.93	49.84	62.11	56.11	58.58	53.74	61.00	62.06	59.37
Al_2O_3	14.96	16.14	13.88	14.92	15.41	14.23	14.78	15.21	15.66	15.79
Fe_2O_3	7.18	9.60	13.30	9.54	8.91	8.63	10.83	7.81	7.91	8.24
MgO	4.74	6.18	8.52	3.97	5.94	5.15	6.38	4.72	2.74	4.42
CaO	6.24	5.71	11.28	3.16	7.33	7.52	8.49	4.99	4.81	5.51
Na_2O	3.99	3.88	1.79	4.29	3.71	3.53	2.96	3.67	5.45	4.56
K_2O	.40	.42	.28	.90	.67	.32	.58	.50	.11	.76
TiO_2	1.41	1.48	.81	.82	1.55	1.46	1.84	1.56	.86	.91
MnO	.17	.20	.24	.09	.17	.14	.22	.14	.13	.17
S	0.03	0.04	0.05	0.46	0.03	0.07	0.04	0.03	0.03	0.03
P_2O_5	.38	.45	.06	.20	.21	.43	.20	.38	.26	.27
Ba	25	14	0	116	97	25	77	35	3	52
Nb	14	13	0	10	4	4	10	13	10	6
Zr	228	47	190	143	143	230	114	192	229	211
Y	50	52	18	30	32	49	31	45	32	34
Sr	156	164	110	211	257	201	245	70	155	263
Rb	4	8	1	18	16	5	11	12	2	19

Table A2. X-ray fluorescence analyses. (3) Duck Formation (continued)

Sample:	722-5A	722-6	722-7B	722-8A	726-1BC	726-2B	726-3AB	726-4A	726-5	726-6A
SiO_2	68.56	46.62	50.23	55.82	67.29	56.14	55.82	61.78	61.01	54.56
Al_2O_3	13.87	15.99	18.92	15.05	14.97	16.24	16.53	13.34	14.00	16.16
Fe_2O_3	4.85	14.71	12.62	9.00	4.91	9.62	10.44	7.93	8.03	9.24
MgO	2.61	8.17	4.33	5.47	2.40	5.90	5.90	4.29	4.14	4.77
CaO	5.72	10.09	6.54	7.34	.78	6.85	5.14	7.75	7.40	8.13
Na_2O	3.11	1.54	3.56	4.74	6.48	2.36	3.72	3.05	3.33	4.57
K_2O	.11	.63	1.06	.33	1.88	1.53	.29	.26	.38	.63
TiO_2	.82	1.84	1.97	1.65	.98	1.03	1.53	1.13	1.21	1.32
MnO	.10	.22	.34	.15	.10	.14	.20	.15	.18	.23
S	0.03	0.05	0.13	0.04	0.12	0.03	0.03	0.03	0.03	0.03
P_2O_5	.26	.19	.42	.44	.21	.19	.42	.34	.32	.38
Ba	10	19	191	45	141	284	25	17	27	26
Nb	14	4	6	10	10	11	12	13	6	11
Zr	214	107	186	211	190	193	240	192	191	219
Y	37	36	45	44	24	34	51	41	41	49
Sr	176	216	164	191	56	199	189	96	167	221
Rb	6	18	19	6	27	40	3	3	7	2

Table A2. X-ray fluorescence analyses. (3) Duck Formation (continued)

Sample:	726-7A	726-8A	727-1A	727-2A	727-3A	727-4B	727-5B	727-6A	727-7A	727-8A
SiO_2	58.34	63.35	55.07	53.32	57.32	49.17	60.60	51.13	58.11	60.40
Al_2O_3	15.33	13.51	19.04	15.78	14.73	18.48	13.56	14.41	15.09	16.36
Fe_2O_3	9.00	8.35	9.25	9.13	8.20	13.17	9.73	13.51	6.25	5.62
MgO	4.72	4.78	4.67	5.09	4.84	5.53	4.78	4.95	2.10	2.63
CaO	5.27	5.38	4.93	7.15	8.96	5.72	5.11	11.57	16.38	7.13
Na_2O	4.40	2.95	4.49	7.10	3.56	5.34	4.13	1.98	.43	5.38
K_2O	.82	.11	.51	.51	.51	.06	.09	.10	.05	.56
TiO_2	1.53	1.18	1.50	1.40	1.33	1.78	1.42	1.73	1.27	1.55
MnO	.18	.11	.34	.15	.15	.26	.21	.23	.07	.09
S	0.04	0.03	0.03	0.03	0.04	0.03	0.03	0.03	0.12	0.05
P_2O_5	.41	.28	.21	.37	.39	.49	.37	.38	.25	.28
Ba	35	9	27	108	37	9	20	26	0	132
Nb	12	5	3	12	15	16	13	13	10	12
Zr	245	184	135	226	217	243	163	163	122	149
Y	52	41	36	50	48	47	43	37	31	37
Sr	175	146	211	131	263	269	65	178	106	212
Rb	15	1	11	11	15	0	4	2	0	10

Table A2. X-ray fluorescence analyses. (3) Duck Formation (continued)

Samples:	727-9A	727-11A	727-12A	727-13A
SiO_2	59.57	52.73	52.39	55.44
Al_2O_3	16.25	14.68	14.57	15.22
Fe_2O_3	6.39	13.46	12.76	9.48
MgO	2.40	6.05	5.80	5.32
CaO	10.49	7.00	7.58	8.28
Na_2O	2.70	3.24	4.60	4.36
K_2O	.10	.44	.19	.08
TiO_2	1.67	1.86	1.50	1.27
MnO	.10	.21	.23	.20
S	0.09	0.03	0.04	0.04
P_2O_5	.32	.32	.38	.34
Ba	46	28	11	30
Nb	3	2	2	2
Zr	159	173	185	199
Y	39	41	43	48
Sr	101	177	172	162
Rb	2	7	2	0

Table A2. X-ray fluorescence analyses. (4) Banting Formation (continued)

Sample:	707-1A	707-2AB	707-4AB	707-6B	707-7A	708-2AC	708-3A	708-4C	708-6A	718-1AB
SiO_2	60.61	60.62	59.09	61.25	68.31	67.54	71.86	66.99	52.74	46.80
Al_2O_3	15.81	14.16	15.19	15.61	15.25	16.91	12.57	16.84	15.21	16.76
Fe_2O_3	7.17	7.36	8.69	7.05	4.56	3.68	6.33	8.35	13.24	13.76
MgO	2.80	2.55	4.69	3.60	2.07	1.70	1.09	2.02	3.10	9.49
CaO	6.08	9.96	6.85	7.11	3.92	5.18	4.07	1.39	12.79	10.12
Na_2O	5.90	2.95	3.72	4.02	4.11	1.15	1.01	.52	.64	1.66
K_2O	.56	1.13	.29	.16	1.06	2.72	2.07	2.85	.51	.20
TiO_2	.77	.85	.92	.80	.49	.83	.64	.74	.77	.89
MnO	.14	.17	.19	.15	.08	.12	.24	.14	.77	.21
S	0.02	0.02	0.03	0.04	0.02	0.05	0.04	0.05	0.03	0.04
P_2O_5	.17	.25	.27	.23	.15	.17	.13	.17	.21	.10
Ba	216	57	137	32	255	388	474	434	222	8
Nb	12	15	13	10	13	13	12	2	3	1
Zr	170	178	197	205	170	217	200	124	116	45
Y	22	31	29	27	13	23	27	22	27	25
Sr	300	153	211	245	456	257	187	99	351	245
Rb	19	32	6	1	31	83	56	73	8	2

Table A2. X-ray fluorescence analyses. (4) Banting Formation (continued)

Sample:	718-2AB	718-4A	718-5BDC	718-6ABC	718-7CD	718-8A	718-9AB	718-10ABC	718-11
SiO_2	61.45	51.92	63.82	69.14	66.46	50.68	48.84	70.37	68.54
Al_2O_3	12.66	15.94	16.52	17.12	15.24	16.11	20.78	14.49	15.03
Fe_2O_3	13.51	12.74	5.76	1.55	4.74	12.32	11.03	3.75	4.47
MgO	1.26	6.61	2.12	2.64	1.40	6.61	7.89	1.58	1.50
CaO	4.85	6.50	4.94	2.07	6.40	9.95	7.80	2.73	4.68
Na_2O	4.34	4.64	5.54	4.16	1.77	2.97	2.15	5.27	2.92
K_2O	.12	.12	.45	2.46	3.11	.10	.51	1.15	2.12
TiO_2	1.21	1.14	.59	.63	.60	.95	.75	.46	.52
MnO	.21	.20	.11	.06	.11	.19	.16	.08	.07
S	0.04	0.03	0.03	0.02	0.03	0.04	0.03	0.02	0.03
P_2O_5	.39	.19	.16	.17	.17	.11	.06	.11	.14
Ba	0	86	228	341	647	13	0	565	523
Nb	0	1	13	15	11	0	1	14	13
Zr	213	126	200	195	160	58	40	155	167
Y	64	26	18	17	13	22	18	14	13
Sr	193	388	584	213	179	406	283	372	337
Rb	0	0	7	64	70	0	8	29	46

Table A2. X-ray fluorescence analyses. (4) Banting Formation

Sample:	705-1A	705-1C	705-2A	705-2B	705-3AB	705-4B	705-5A	706-1AB	706-2B	706-3A
SiO_2	61.76	60.30	52.95	63.98	58.18	59.81	58.99	64.89	67.92	59.93
Al_2O_3	14.48	14.63	17.35	14.87	15.49	16.63	16.55	15.00	17.22	15.85
Fe_2O_3	7.39	6.24	9.57	6.63	8.76	7.03	8.78	9.50	4.04	8.55
MgO	4.83	2.30	4.18	3.05	4.74	3.57	5.54	3.03	1.47	5.26
CaO	4.87	14.29	7.31	5.08	7.37	8.51	4.98	5.14	4.91	5.26
Na_2O	4.32	1.00	4.70	4.78	3.78	1.72	3.36	.77	2.29	3.38
K_2O	1.20	.24	2.27	.61	.55	1.30	.47	.70	1.43	.48
TiO_2	.80	.72	1.04	.70	.77	.97	.92	.57	.48	.90
MnO	.11	.05	.13	.11	.14	.18	.14	.25	.11	.16
S	0.03	0.03	0.08	0.02	0.03	0.03	0.03	0.03	0.03	0.03
P_2O_5	.24	.23	.50	.20	.22	.27	.26	.15	.14	.24
Ba	240	12	1607	142	239	144	491	126	418	122
Nb	15	14	14	11	13	15	16	165	11	15
Zr	210	184	190	177	212	195	230	20	163	223
Y	31	26	32	25	34	26	31	12	14	30
Sr	236	178	725	537	263	261	330	290	410	278
Rb	34	5	46	10	38	21	12	19	44	14

APPENDIX A

2) MINOR ELEMENTS BY ATOMIC ABSORPTION SPECTROSCOPY

Procedure

Analyses for seven trace elements were attempted, another was attempted by colourimetry outlined below. Satisfactory results were obtained for five: scandium, vanadium, nickel, copper, zinc. Results for chromium and antimony were unacceptable.

Eighty-three samples were selected to augment data obtained by x-ray fluorescence analyses. They were chosen to cover the range of traverses in the study. Rock powder prepared for XRF analyses were weighed into teflon beakers, repeatedly treated with acid and evaporated, filtered and diluted for analyses. Standard dissolution and analytical procedures were followed.

Standards and Recommended Values

International standards were prepared and run with the eighty A.A. samples. Listed below are the name of standard, weight dissolved, final volume, recommended value in ppm (bracketed), and values obtained:

	Wt.(g)	Vol.(ml)	V	Sc	Ni	Cu	Zn	Cr
MRG-1 (MC)	1.0033	50	567 (399)	24 (48)	170 (200)	133 (135)	193 (185)	(410)
BCR-1 (MC)	.4567	50	459 (520)	22 (33)	22 (15.8)	17 (18.4)	155 (120)	(17.6)
BCR-1 (SG)	.5362	25	466 (520)		33 (15.8)		155 (120)	
AGV-1	.278	25	(125)	3 (13.4)	(18.5)	67 (59.7)	121 (84)	(12.2)
BHVO-1 (SG)	.4865	25	-	-	-	-	-	(320)

Standards were tested for internal consistency on a plot of ppm' vs chart response, where ppm' = R.V.(ppm) x weight(g)/volume(ml), and response is the average increase in digital count on the recorder when analyzing each standard.

Results were good for vanadium. Nickel and copper results were also good, with some differences evident for the two concentrations of BCR-1, (MC) and (SG). Zinc yields a linear trend but away from the origin on the ppm' vs response diagram. Chromium analyses yielded inconclusive results as the ppm' vs response plot is non-linear and test runs on Yellowknife volcanic samples show very low and erratic values; this data has not been tabulated.

TABLE A3 - Date for the Yellowknife Volcanic Rocks:
Elements by Atomic Absorption Spectroscopy

KAM FORMATION (Lower Unit)

	Sc	V	Ni	Cu	Zn
620-10	28	307	128	137	133
620-20	33	366	149	134	107
620-30	27	356	65	119	123
620-40	20	298	61	75	80
620-55	20	319	136	164	97
620-60	17	314	123	151	108
620-70	2	263	124	151	108
703-2a	20	403	79	120	138
710-1a	15	430	71	86	756
710-3b	22	323	192	114	136
710-4a	1	45	14	16	8
710-7a	21	315	90	29	136
710-12a	18	364	46	82	135
710-13a	19	369	107	79	127
815-1	6	156	38	48	86
815-6	12	403	72	162	149
815-7	14	253	92	81	89
815-9	22	328	125	134	108
815-10	18	299	77	98	112
815-11	16	301	75	84	91
725-6	3	34	7	11	69

KAM FORMATION (Upper Unit)

725-1a	21	341	99	119	104
725-3c	24	358	90	128	117
725-5	21	337	89	186	117
730-1a	20	261	100	67	75
730-3a	19	269	126	96	91
730-5b	19	281	64	117	103
730-7	20	314	79	65	113
716-4b	21	271	122	97	80
716-3a	18	296	70	90	100
716-1a	18	265	71	138	66

TABLE A3 (cont'd)

KAM FORMATION (Upper Unit) cont'd

	Sc	V	Ni	Cu	Zn
714-1b	23	320	63	33	106
714-3a	26	351	52	71	114
714-4a	24	322	67	87	100
714-5bc	19	289	71	79	99
712-7b	24	352	100	113	145
712-5a	20	356	79	81	131
712-3a	18	334	126	116	104
712-1b	18	269	137	122	84

DUCK FORMATION

727-1a	16	215	166	62	134
727-2a	10	209	83	54	120
727-5b	12	216	52	88	114
727-8a	18	190	156	75	91
727-11a	13	235	65	31	105
727-12a	18	267	64	97	108
727-13a	12	195	69	67	122
727-4b	15	268	100	83	147
720-4ab	18	195	93	62	127
720-7a	5	131	40	38	48
720-8a	11	185	78	78	96
720-10a	15	198	52	44	109
720-10a	26	320	126	92	112
721-1a	5	120	43	39	129
722-1a	11	310	60	52	136
722-3a	15	255	62	101	133
722-5a	18	95	47	31	74
722-7b	20	255	143	89	197
726-2b	8	161	51	32	99
726-4a	14	167	58	59	107
726-6b	10	218	64	55	135
726-8a	10	163	64	55	135
726-1bc	9	126	46	74	58

TABLE A3 (cont'd)

BANTING FORMATION

	Sc	V	Ni	Cu	Zn
707-7a	2	68	24	14	61
707-6b	7	136	58	53	97
705-4b	6	130	60	47	111
705-5a	6	143	68	70	120
707-2ab	8	137	59	55	106
705-2a	8	190	22	18	64
705-1c	6	116	58	67	78
707-1a	8	152	76	33	88
706-2b	-	74	23	5	37
708-2ab	7	125	121	32	71
708-3ab	2	84	56	13	50
708-4c	6	153	105	41	154
718-7cd	-	95	23	33	63
718-6abc	-	96	27	7	43
718-4a	11	243	95	39	111
718-1ab	18	279	183	69	114
718-2ab	9	24	13	8	106
718-9ab	4	169	189	34	78
718-1-ab	-	63	19	9	64

1) analytical data in parts per million (ppm)
2) - denotes 'not detected'
3) KAM FORMATION samples listed in approximate ascending stratigraphic order

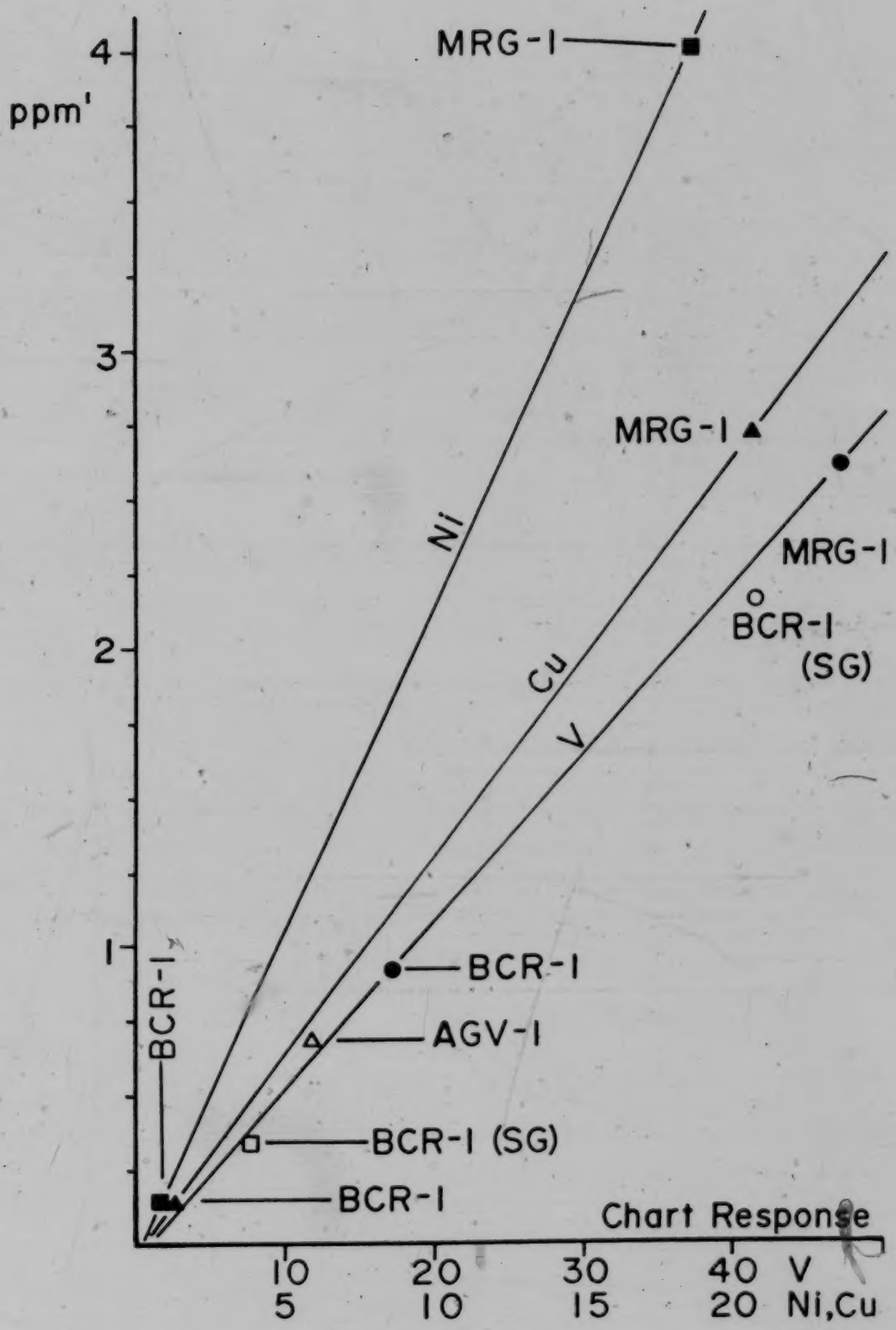

FIGURE A1 - Standards Correlation (ppm' vs response): Ni, Cu, V

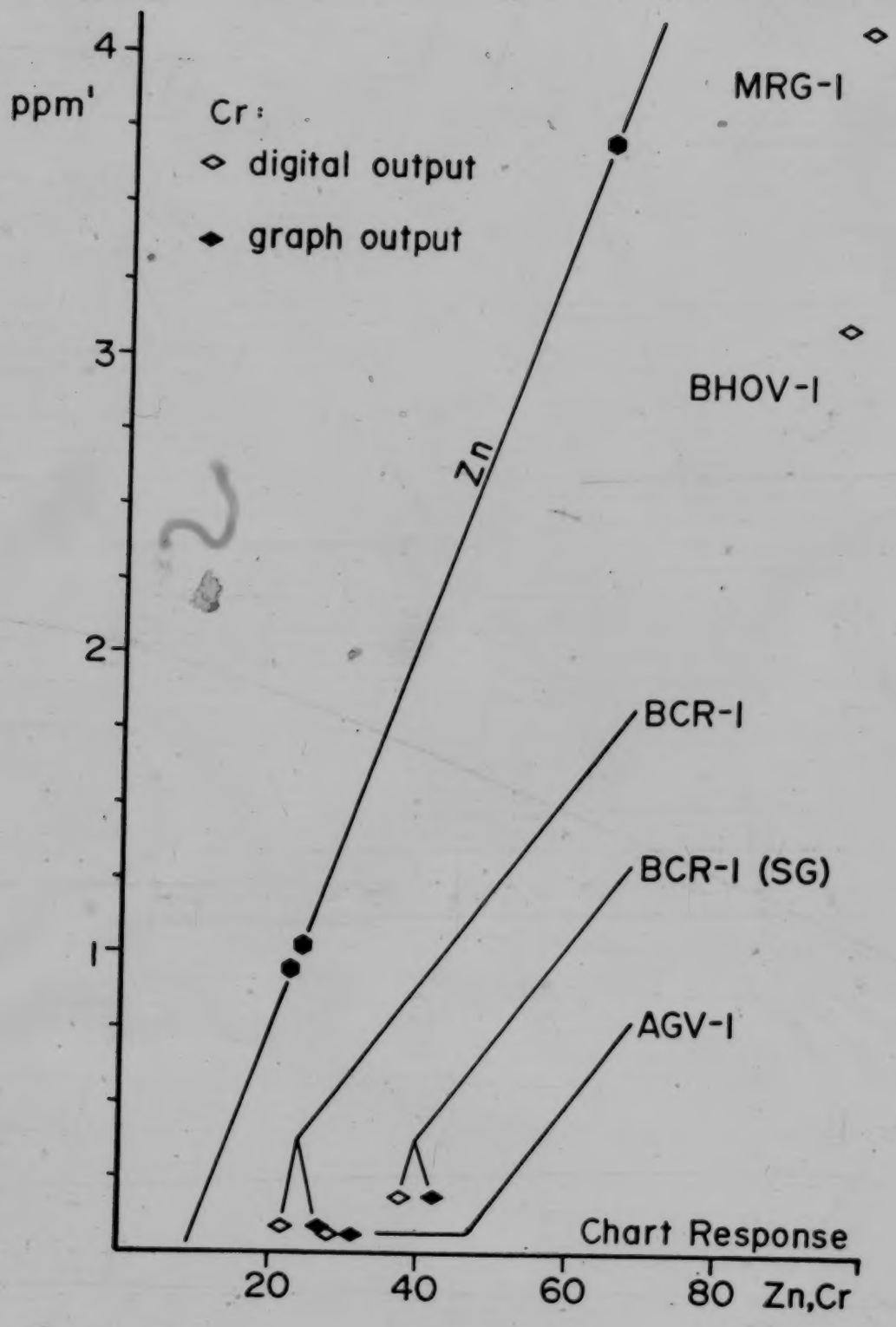

FIGURE A2 - Standards Correlation (ppm' vs response): Zn, Cr

APPENDIX B

COMPARATIVE STUDIES

1) Duplicate Analyses

2) Surface vs Drill Core Samples

3) Variolitic vs Non-variolitic Flows

Duplicate Analyses

Thirteen samples were selected, for comparative x-ray fluorescence analyses, from the three Yellowknife volcanic formations: Kam (6), Duck (4) and Banting (3). Duplicate aliquots for each preselected sample were taken as part of the routine preparation procedure, and assigned a 740 series number. Values obtained for major and minor elements are listed in Tables B1 and B2 respectively. Problems are apparent for sodium and titanium, as 8 of 13 analyses do not overlap within the precision limits. Discrepancies occur for potassium, iron and manganese, where 6 of 13 do not overlap within precision limits.

Given the precision estimates for major elements (Appendix A), the following samples have elements which do not duplicate within the limits:

1) 710-5A, Kam Fm., 5 elements
   SiO_2, Fe_2O_3, CaO, TiO_2, MnO

2) 712-3A, Kam Fm., 5 elements
   SiO_2, CaO, K_2O, TiO_2, MnO

3) 720-6A, Duck Fm., 5 elements
   Fe_2O_3, MgO, Na_2O, TiO_2, MnO

4) 727-5B, Duck Fm., 6 elements

Al_2O_3, Fe_2O_3, Na_2O, K_2O, TiO_2

5) 705-3AB, Banting FM., all 10 elements.

Sample 705-3AB must be a sample mix-up. Sodium (Na_2O) often causes problems due to low count rates. All values less than 0.5% can cause problems as either total counts or count rates are low.

TABLE B1 - Duplicate Analyses: Major Elements (weight percent)

	SiO_2	Al_2O_3	Fe_2O_3	MgO	CaO	Na_2O	K_2O	TiO_2	MnO	P_2O_5	Total
BANTING FM.											
740-13AB	59.65	16.47	6.90	3.84	8.47	1.94	1.29	0.97	0.18	0.28	100.00
705-3AB	58.18	15.49	8.76	4.74	7.37	3.78	0.55	0.77	0.14	0.22	100.00
740-12AB	59.85	14.48	7.38	2.48	10.11	3.26	1.17	0.85	0.15	0.25	100.00
707-2AB	60.62	14.16	7.36	2.55	9.46	2.95	1.13	0.85	0.17	0.25	100.00
740-11	68.37	15.06	4.48	1.69	4.59	3.05	2.03	0.53	0.07	0.14	100.00
718-11	68.54	15.03	4.47	1.50	4.68	2.92	2.12	0.52	0.07	0.14	100.00
DUCK FM.											
740-8B	60.31	13.92	10.13	4.83	5.27	3.49	0.22	1.34	0.19	0.30	100.00
727-5B	60.60	13.65	9.73	4.78	5.11	4.13	0.09	1.42	0.21	0.37	100.00
740-7A	57.75	15.42	9.40	5.02	5.23	4.46	0.80	1.42	0.17	0.34	100.00
726-7A	58.34	15.33	9.00	4.72	5.27	4.40	0.82	1.53	0.18	0.41	100.00
740-5A	60.97	15.43	8.17	4.78	4.94	3.25	0.54	1.46	0.14	0.32	100.00
722-3A	61.00	15.21	7.81	4.72	4.99	3.67	0.50	1.56	0.14	0.38	100.00
740-4A	53.01	13.93	12.30	6.51	9.20	2.41	0.63	1.65	0.22	0.15	100.00
720-6A	53.27	13.98	11.80	6.86	9.13	2.15	0.60	1.79	0.27	0.15	100.00
KAM FM.											
740-10	54.59	15.81	13.14	8.12	2.42	3.64	0.26	1.45	0.14	0.43	100.00
815-8AB	54.00	15.73	13.09	8.08	2.54	4.29	0.28	1.44	0.14	0.41	100.00
740-9	51.74	12.67	14.86	4.89	10.75	2.65	0.20	1.73	0.28	0.23	100.00
803-9	52.33	12.64	14.69	5.08	10.89	2.04	0.14	1.74	0.23	0.22	100.00
740-6	54.45	16.19	9.11	4.88	11.43	2.47	0.31	0.93	0.15	0.07	100.00
725-3	54.28	16.41	8.89	4.72	11.05	3.25	0.22	0.99	0.16	0.05	100.00
740-3A	48.24	14.82	13.40	8.25	11.61	1.99	0.22	1.09	0.26	0.09	100.00
712-3A	49.32	14.51	13.39	8.33	10.89	1.89	0.10	1.16	0.31	0.10	100.00
740-2A	50.65	14.32	14.92	6.20	10.26	1.88	0.23	1.15	0.28	0.10	100.00
710-5A	52.22	14.06	14.19	6.23	9.74	1.72	0.19	1.24	0.31	0.10	100.00
740-1A	49.64	13.81	13.23	8.13	11.75	2.12	0.29	0.78	0.21	0.06	100.00
620-11	50.01	13.89	13.38	8.11	11.30	2.01	0.21	0.79	0.25	0.05	100.00

TABLE B2 - Duplicate Analyses: Minor Elements (ppm)

	Rb	Sr	S	Ba	Zr	Y	Nb
BANTING FM.							
740-13AB	37.6	278.4	.03	235	202	28	13
705-3AB	37.8	262.8	.03	239	212	34	13
740-12AB	32.5	150.8	.03	59	179	31	11
707-2AB	31.6	153.1	.02	57	178	31	15
740-11	44.0	340.0	.02	548	161	14	12
718-11	46.3	336.5	.03	523	167	13	13
DUCK FM.							
740-8B	4.0	63.7	.04	11	182	40	13
727-5B	4.2	84.5	.03	20	163	43	13
740-7A	15.5	172.1	.04	30	244	47	16
726-7A	14.9	175.2	.04	35	245	52	12
740-5A	11.4	70.6	.03	34	195	39	17
722-3A	11.7	69.8	.03	35	192	45	13
740-4A	12.3	198.2	.05	35	93	27	12
720-6A	11.3	200.9	.05	35	108	29	5
KAM FM.							
740-10	0.0	93.9	.03	83	258	44	17
815-8AB	0.4	95.0	.03	100	263	47	17
740-9	0.4	109.7	.05	6	138	42	1
803-9	0.7	112.2	.04	0	137	42	0
740-6	2.4	143.1	.04	0	55	25	0
725-3	2.5	146.3	.06	10	60	13	2
740-3A	2.4	110.6	.05	80	75	27	1
712-3A	2.8	112.9	.05	12	73	27	0
740-2A	0.6	126.5	.06	0	73	30	0
710-5A	0.7	126.8	.06	7	75	29	3
740-1A	2.3	109.8	.05	0	51	24	1
620-11	1.4	112.2	.05	4	50	19	2

Surface vs Pack-sack Drill Core Samples

The 620 series of samples were taken as surface and drill core duplicates; surface grab samples marked 10, 20, 30 etc. and drill samples by 11, 22, 33 etc. (Tables B3 and B4).

Samples were taken of massive flows, sometimes sheared, to look at possible weathering patterns without the effects of pillow lava rim vs core changes. Comparison of their XRF analyses shows only minor variations between the possibly weathered surface samples and the hopefully unweathered drill samples.

All other analyses in this study are surface samples, therefore the surface analyses are considered the norm and changes taken from that base. Seven duplicate samples have been analyzed.

Five of seven samples indicate greater levels of SiO_2 and CaO in the surface grab samples; four of seven similarly indicate enrichment in Al_2O_3 and K_2O. The surface samples seem depleted in Na_2O relative to the drill samples, five of seven samples. Of the minor elements, Y appears more abundant in the surface samples, five of seven analyses. All other elements are erratic in their relationship. The variation shown is not much greater, sometimes less, than in the duplicate section earlier.

TABLE B3 - Surface vs. Drill Core Samples: Major Elements (weight percent)

	SiO_2	Al_2O_3	Fe_2O_3	MgO	CaO	Na_2O	K_2O	TiO_2	MnO	P_2O_5	Total
620-10	50.07	13.68	12.88	6.56	13.51	2.14	.10	.79	.22	.06	100.00
11	50.01	13.89	13.38	8.11	11.30	2.01	.21	.79	.25	.05	100.00
20	53.44	15.11	10.09	5.92	11.97	2.32	.08	.87	.17	.03	100.00
22	50.97	14.67	13.14	6.42	11.47	1.98	.19	.89	.23	.03	100.00
30	50.39	13.15	14.99	6.43	10.38	1.80	.82	1.17	.26	.10	100.00
33	49.59	13.63	14.99	6.95	9.95	2.48	.79	1.25	.27	.11	100.00
40	54.37	13.27	12.49	7.38	9.19	1.80	.36	.90	.22	.06	100.00
44	52.41	14.03	12.75	7.28	10.10	2.05	.22	.89	.21	.07	100.00
50	50.21	14.79	13.21	7.77	9.82	2.86	.10	.93	.25	.07	100.00
55	50.28	14.93	12.85	7.57	9.86	3.22	.07	.92	.24	.06	100.00
60	51.04	14.76	13.32	7.99	9.84	1.73	.09	.94	.22	.06	100.00
66	51.03	14.57	13.28	8.24	9.58	2.00	.10	.93	.21	.06	100.00
70	50.13	15.41	12.01	9.84	9.01	1.97	.18	1.07	.26	.10	100.00
620-77	51.37	15.02	11.41	9.35	8.08	3.21	.11	1.13	.22	.09	100.00

Percentage Variance from Surface Sample Value

620-10										
11	- .12	1.54	3.88	23.63	-16.36	-6.07	110.0	0	13.64	-16.67
20										
22	-4.62	-2.19	30.23	8.45	- 4.18	-14.66	137.50	2.30	32.59	0
30										
33	-1.59	11.25	0	8.07	- 4.14	37.78	- 3.66	6.84	3.85	10.00
40										
44	-3.60	5.73	2.49	-1.36	9.90	13.89	-38.89	-1.11	-4.55	16.67
50										
55	.14	.95	-2.73	-2.57	.41	12.59	-30.00	-1.08	-4/00	-14.29
60										
66	- .02	-1.29	- .30	3.13	- 2.64	25.61	11.11	-1.06	-4.55	0
70										
77	2.47	-2.53	-5.00	-4.98	-10.32	62.94	-38.89	5.61	-15.38	-10.00

TABLE B4 - Surface vs Drill Core Samples: Minor Elements (ppm)

	* Ba	Zr	Y	Nb	Rb	Sr	S
620-10	0	51	25	2	1.1	122.2	.04
620-11	4	50	19	2	1.4	112.2	.05
620-20	0	39	19	1	.0	187.3	.04
620-22	0	42	16	2	.9	204.3	.04
620-30	97	71	30	2	28.1	104.7	.05
620-33	49	69	28	1	24.4	97.9	.06
620-40	0	63	22	1	12.8	85.3	.04
620-44	2	68	24	2	6.5	99.0	.04
620-50	7	58	23	2	1.8	150.3	.03
620-55	0	59	23	0	.3	159.6	.03
620-60	0	57	26	0	3.3	84.2	.05
620-66	0	56	23	1	5.4	80.2	.05
620-70	14	69	23	5	8.8	143.6	.03
620-77	0	71	21	4	6.2	112.8	.04

Percentage Variance from Surface Sample Value

620-10							
620-11	300.00	-1.96	-24.00	0	27.27	-8.18	25.00
620-20							
620-22	0	7.69	-15.79	100.00	800.00	9.08	0
620-30							
620-33	-49.48	-2.82	- 6.67	-50.00	-13.17	-6.49	20.00
620-40							
620-44	100.00	7.94	9.09	100.00	-49.22	16.06	0
620-50							
620-55	-85.71	1.72	0	-50.00	-83.33	6.19	0
620-60							
620-66	0	-1.75	-11.54	0	63.64	-4.75	0
620-70							
620-77	-92.86	2.90	- 8.70	-20.00	-29.55	-21.45	33.33

* if Ba = 0 then assume 1 ppm, if Rb = 0 then assume 0.1 ppm
if Nb = 0 then assume 1 ppm.

Variolitic and Enclosing Non-Variolitic Flows

All samples are from a lower Kam Formation traverse sampling the same variolitic flow, also above and below the variolitic flow, in three locations along strike.

Geochemical comparison of the variolitic flow with underlying and overlying lavas (Tables B5 and B6) shows the variolitic flows to consistently have the highest CaO content, and the highest CaO/Al_2O_3 ratio. The underlying non-variolitic flows consistently have the lowest CaO/Al_2O_3 ratio. On various discrimination diagrams the variolitic lavas are basaltic andesites, almost andesites, however, the non-variolitic flows are mostly basalts (4 of 6) or quite mafic basaltic andesites. The high CaO content is evident on the CaO vs Y plot (Lambert and Holland 1974), although no other consistent patterns are seen.

TABLE B5 - Variolitic vs Non-variolitic Flows: Major Elements (weight percent)*

	SiO_2	Al_2O_3	Fe_2O_3	MgO	CaO	Na_2O	K_2O	TiO_2	MnO	P_2O_5	B.Ox	CaO/ Al_2O_3
803 - 3	53.32	12.95	14.70	5.49	6.65	4.45	0.24	1.79	0.20	0.22	27.04	.513
803 - 1	53.64	15.07	11.57	6.53	10.53	1.06	0.15	1.10	0.23	0.11	28.86	.698
803 - 2	54.83	15.32	10.95	7.98	7.10	2.20	0.18	1.15	0.19	0.09	26.22	.463
803 - 5	51.93	14.82	12.27	5.01	11.24	2.06	0.18	1.97	0.30	0.22	28.82	.758
803 - 4	53.48	13.98	9.64	1.98	12.81	5.61	0.16	1.85	0.22	0.26	24.65	.916
803 - 6	52.99	12.75	15.03	5.63	7.29	3.84	0.22	1.80	0.21	0.23	28.17	.571
803 - 9	52.33	12.64	14.69	5.08	10.89	2.04	0.14	1.74	0.23	0.22	30.89	.861
803 - 7	54.02	12.67	13.63	4.78	12.04	0.65	0.17	1.63	0.20	0.21	30.65	.950
803 - 8	50.45	13.26	15.67	6.46	10.37	1.78	0.53	1.17	0.20	0.10	32.72	.782

* Samples listed: overlying unit (non-variolitic), variolitic unit, underlying unit (non-variolitic).

TABLE B6 - Variolitic vs Non-variolitic Flows: Minor Elements (ppm)

	Ba	Zr	Y	Nb	Rb	Sr	S	Zr/TiO_2	Y/Nb	Zr/P_2O_5	FeO_T/MgO
803 - 3	28	169	52	11	3.0	384.8	.05	.009	4.7	.077	2.41
803 - 1	0	75	25	2	.1	130.5	.05	.007	12.5	.072	1.59
803 - 2	6	76	27	0	1.9	135.2	.03	.007	27	.084	1.23
803 - 5	3	142	42	2	.1	86.7	.03	.007	21.0	.065	2.20
803 - 4	22	164	52	0	1.2	94.1	.05	.009	52	.063	4.38
803 - 6	15	163	49	3	1.7	95.0	.05	.009	16.3	.071	2.40
803 - 9	0	137	42	0	.7	112.2	.04	.008	42	.063	2.60
803 - 7	4	149	48	1	2.2	472.3	.04	.009	48.0	.071	2.40
803 - 8	58	73	30	0	14.1	101.4	.04	.006	30	.073	2.57

* Where Nb = 0 (ppm), assume Nb = 1 (ppm) for Y/Nb ratio calculation.

APPENDIX C

COMPARATIVE ELEMENT PLOTS

Average Archean Rocks (Condie 1981)

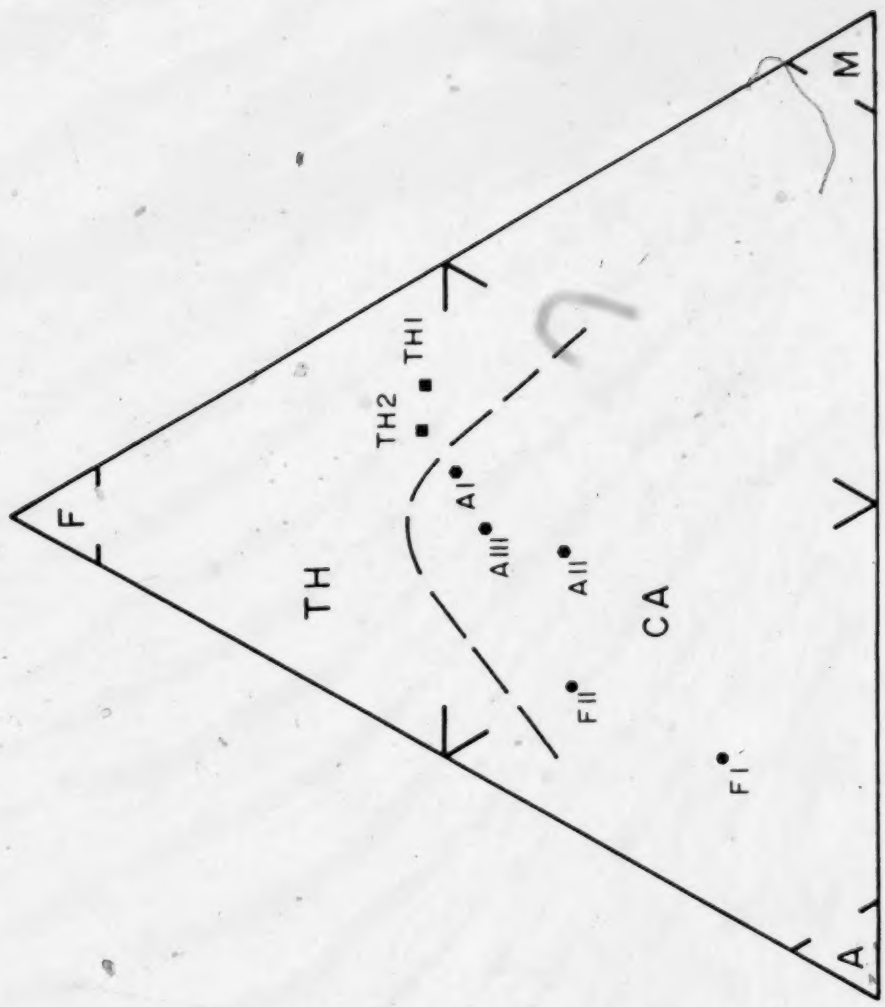

FIGURE C1 - AFM (Archean Average Rock Values)

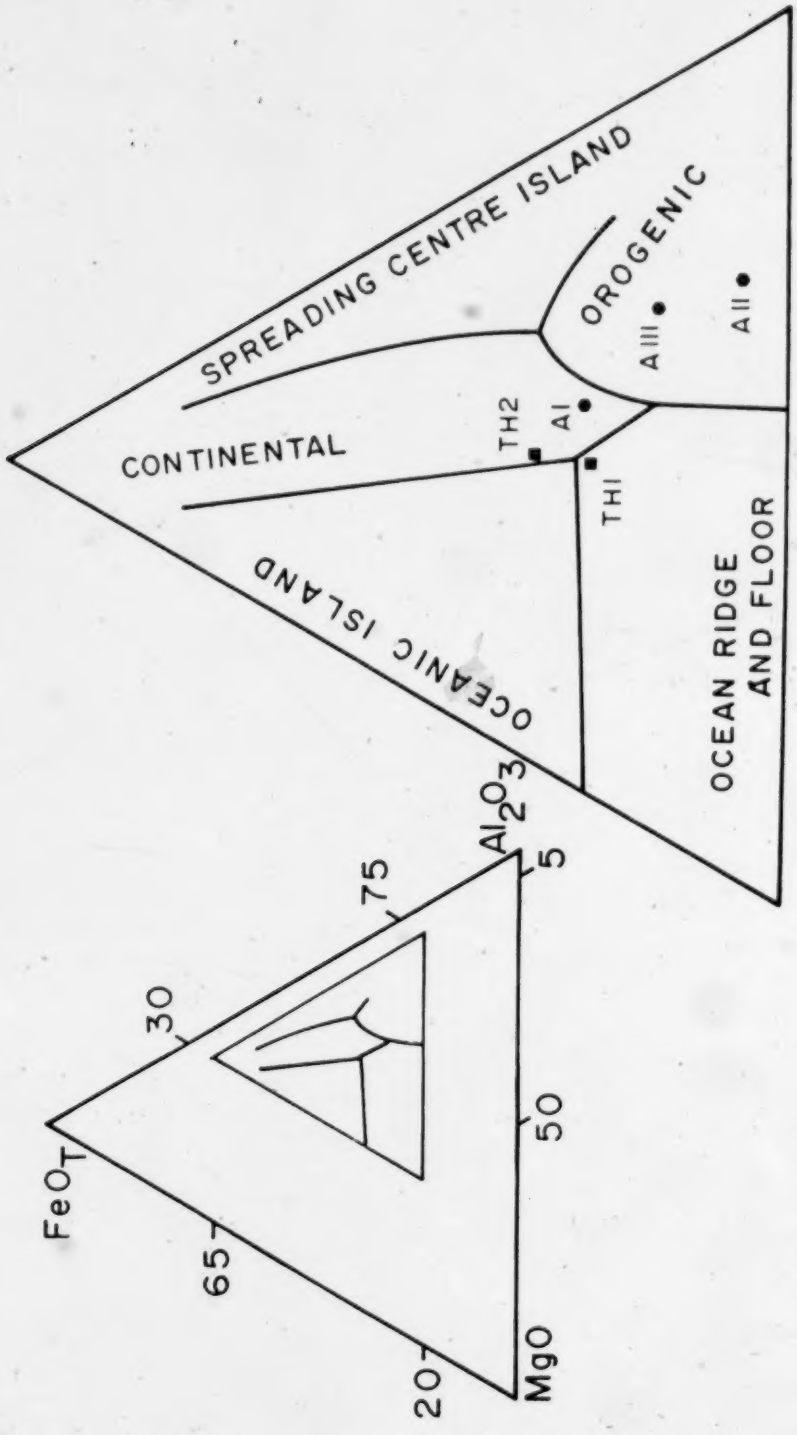

FIGURE C2 - $MgO - FeO_T - Al_2O_3$ (Archean Average Rock Values)

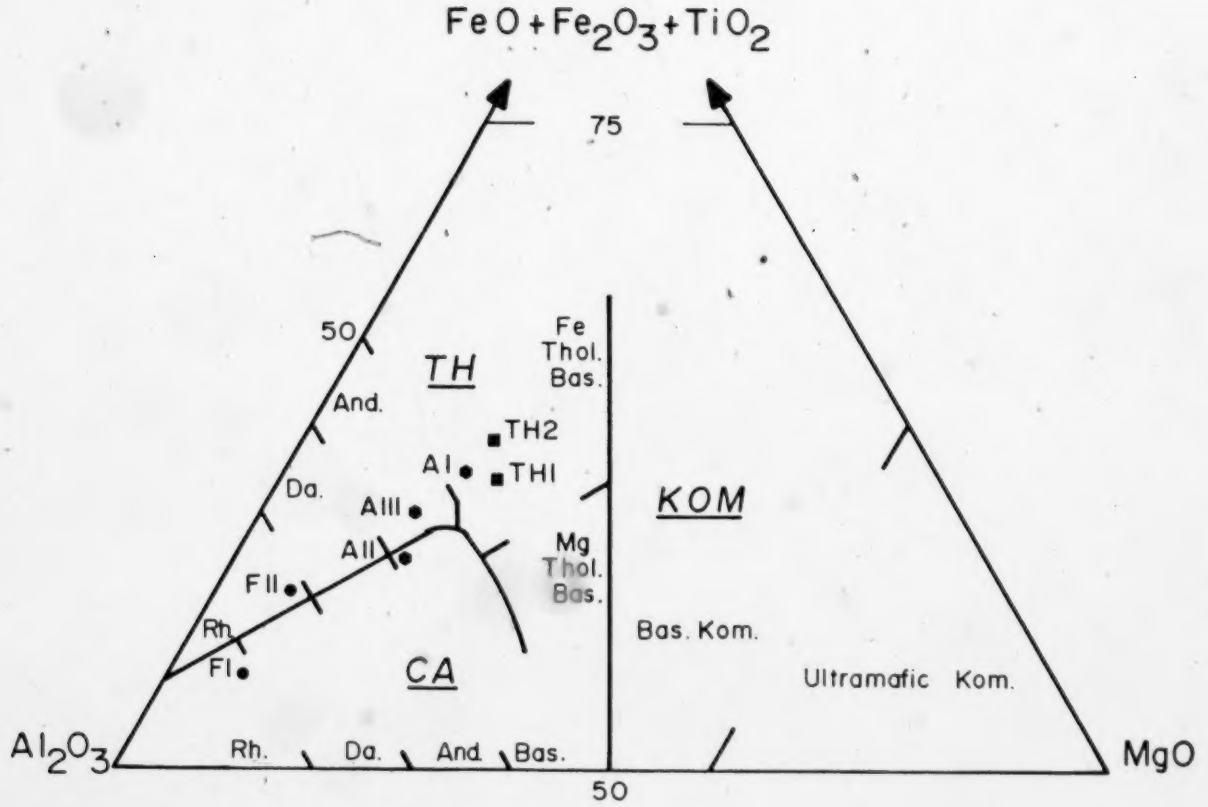

FIGURE C3 - Al_2O_3-($FeO+Fe_2O_3+TiO_2$)-MgO (Archean Average Rock Values)

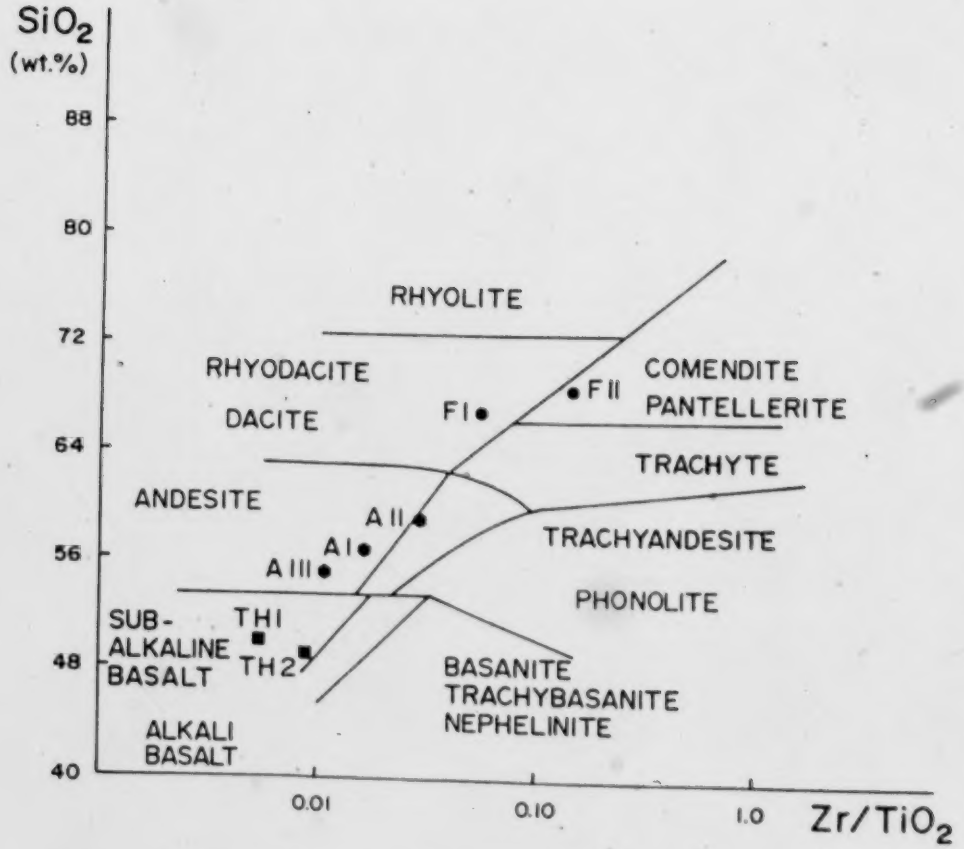

FIGURE C4 - SiO_2 - Zr/TiO_2 (Archean Average Rock Values)

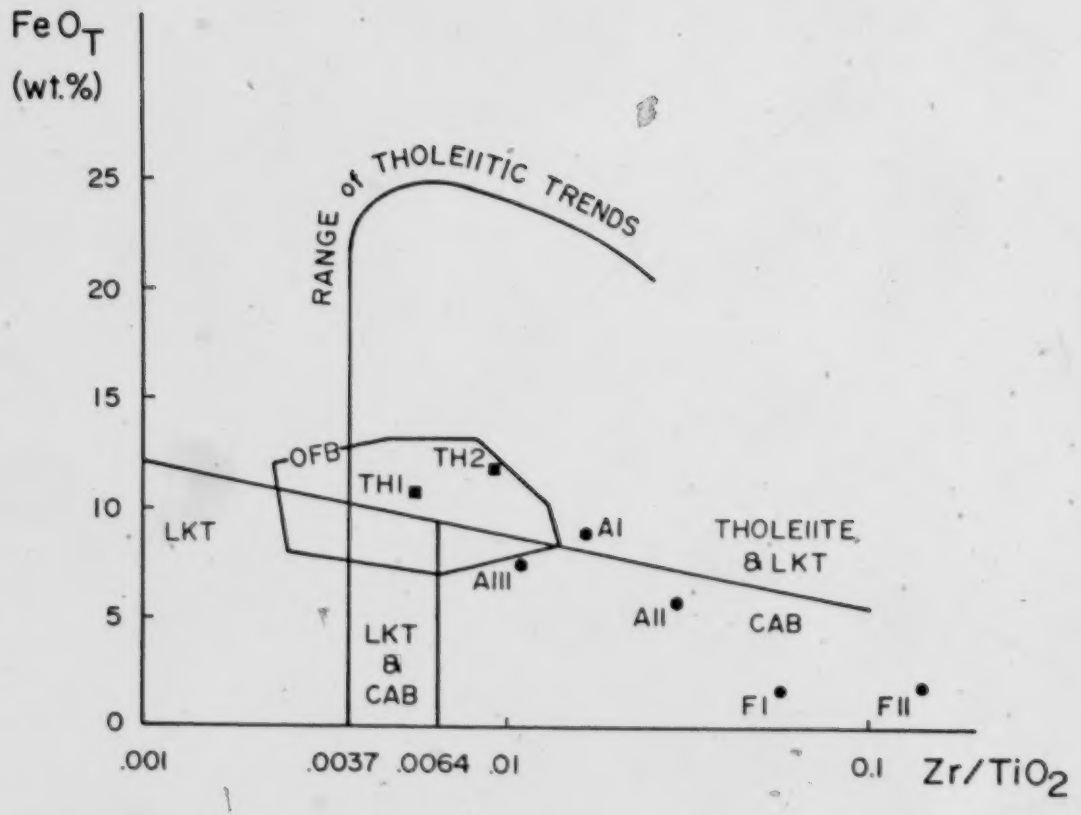

FIGURE C5 - FeO_T - Zr/TiO_2 (Archean Average Rock Values)

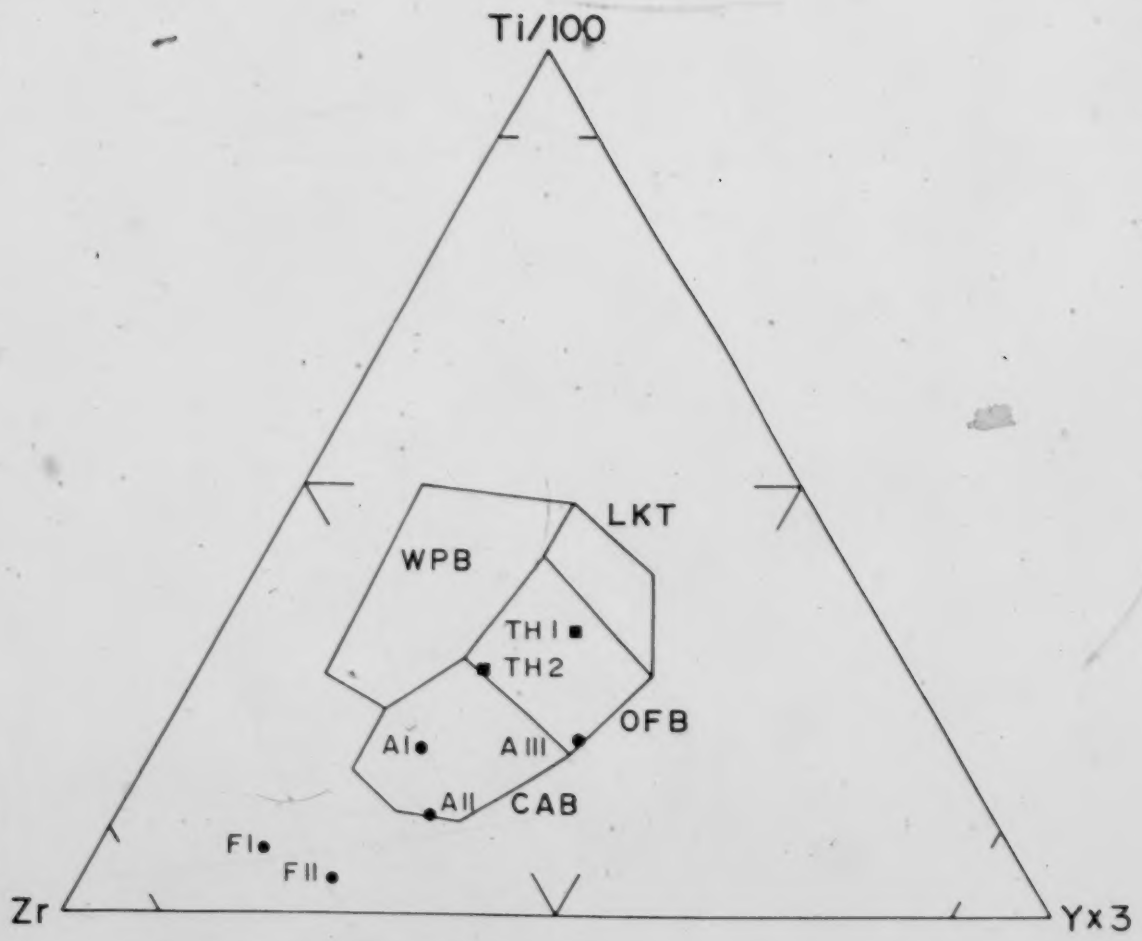

FIGURE C6 - Zr - Ti/100 - Yx3 (Archean Average Rock Values)

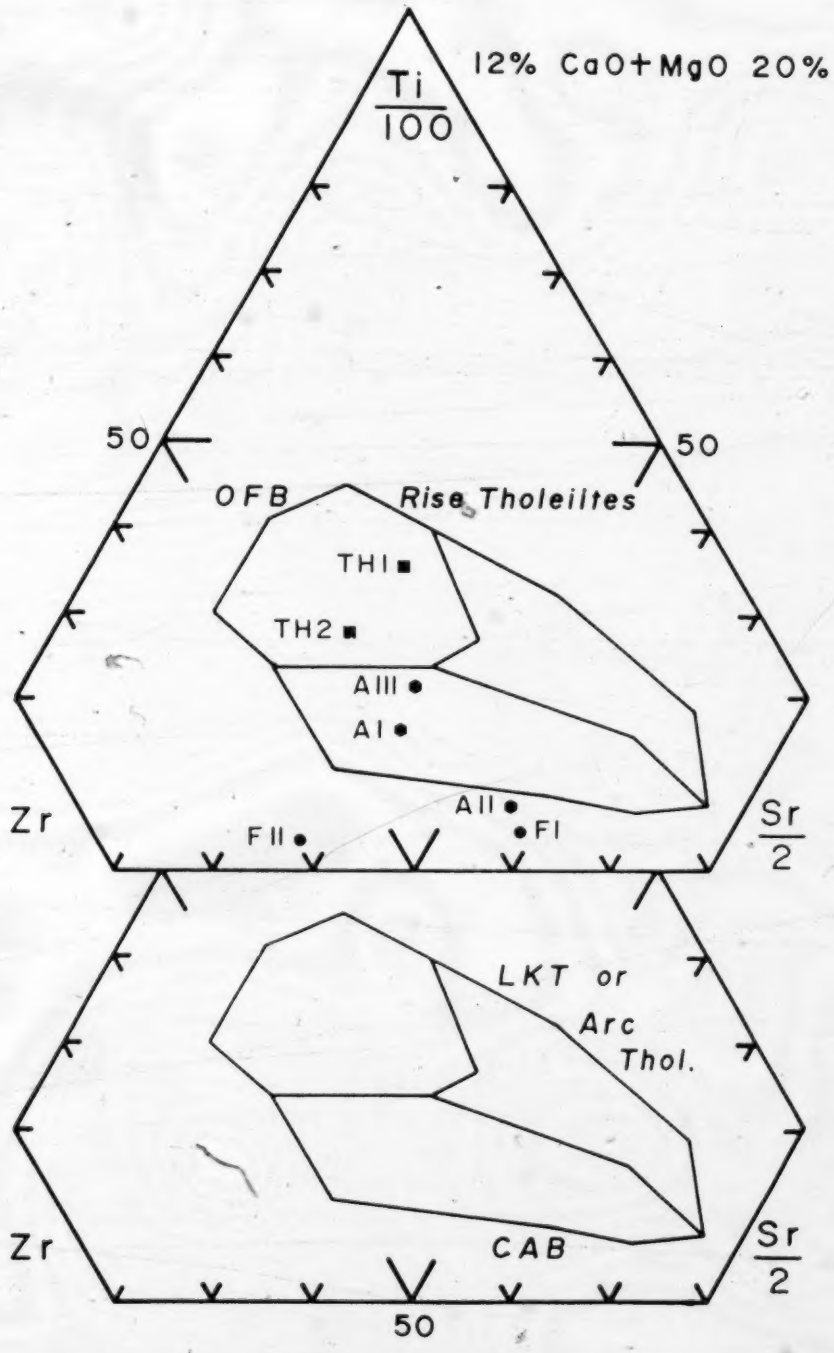

FIGURE C7 - Zr - Ti/100 - Sr/2 (Archean Average Rock Values)

*Note - (CaO+MgO) requirement not applied.

VITA

NAME: MICHAEL PATRICK CUNNINGHAM

PLACE OF BIRTH: Port Arthur, Ontario, Canada

YEAR OF BIRTH: 1952

POST SECONDARY EDUCATION AND DEGREES:

University of Western Ontario
London, Ontario

1972 - 1975 B.Sc.
1975 - 1977 B.Sc. (Honours Standing - Geology)

Department of Geology
University of Alberta
Edmonton, Alberta

1978 - 1983 M.Sc. (Candidate)

RELATED WORK EXPERIENCE:

Consulting Geologist
Westsun Petroleums and Minerals Ltd., Calgary, Alberta
1983

Project Geologist
Zelon Enterprises Ltd., Vancouver, British Columbia
1978 - 1982

Research and Teaching Assistant
University of Alberta, Edmonton, Alberta
1978 - 1979

Geologist
Essex Minerals Company, Toronto, Ontario
Summer 1977

PUBLICATIONS:

Lambert, R.St.J. and M.P. Cunningham (1983) Rb-Sr Geochronology of the Yellowknife Archean, N.W.T.; G.A.C./M.A.C./C.G.U. Joint Annual Meeting, Program with Abstracts, v.8.